UC San Diego

UC San Diego Electronic Theses and Dissertations

Title

Kinetics and mechanism of the interaction of the C1 domain of protein kinase C with lipid membranes

Permalink

https://escholarship.org/uc/item/1vw5x6bm

Author

Dries, Daniel Robert

Publication Date

2007

Peer reviewed|Thesis/dissertation

eScholarship.org Powered by the California Digital Library
University of California

UNIVERSITY OF CALIFORNIA, SAN DIEGO

KINETICS AND MECHANISM OF THE INTERACTION OF THE C1 DOMAIN OF PROTEIN KINASE C WITH LIPID MEMBRANES

A Dissertation submitted in partial satisfaction of the requirements for the degree

Doctor of Philosophy

in

Biomedical Sciences

by

Daniel Robert Dries

Committee in charge:

Professor Alexandra C. Newton, Chair
Professor Joseph A. Adams
Professor Edward A. Dennis
Professor Elizabeth A. Komives
Professor Palmer W. Taylor

2007

The Dissertation of Daniel Robert Dries is approved, and it is acceptable in quality and form for publication on microfilm.

_____

_____

_____

_____

_____
Chair

University of California, San Diego

2007

Dedicated to

Bob and Lisa

TABLE OF CONTENTS

Page

SIGNATURE PAGE iii

DEDICATION iv

TABLE OF CONTENTS v

LIST OF ABBREVIATIONS x

LIST OF FIGURES xi

LIST OF TABLES xiv

ACKNOWLEDGMENTS xv

CURRICULUM VITA xviii

ABSTRACT xxii

CHAPTER 1: INTRODUCTION 1

Protein Kinase C: The Early Years 1

The Structure of Protein Kinase C 2

Translocation to Membranes and PKC's Membrane-Targeting Modules 6

The Structure of the C1 Domain 7

Binding of Phospholipids to the C1 Domain 8

Binding of DG and Phorbol Esters to the C1 Domain 10

Inequality Among C1 Domains 11

Atypical, Non-DG/Phorbol Ester-Binding C1 Domains 12

Questions Addressed in the Following Chapters 14

CHAPTER 2: KINETICS AND MECHANISM OF THE INTERACTION OF THE C1B DOMAIN OF PROTEIN KINASE C WITH LIPID MEMBRANES 16

Questions Addressed in Chapter 2 19

Design of a Fluorescence-Based Probe for the Interaction of the C1b Domain of PKCβI/II with Lipid Membranes 19

Binding of C1bβ-Y123W to Vesicles Containing Increasing Mole Percent Phosphatidylserine 23

Sensitivity to Ionic Strength of the Interaction of C1bβ-Y123W with Lipid Vesicles 27

Interaction of C1bβ-Y123W with Phosphatidylserine (PS) and Phosphatidylglycerol (PG) 29

Interaction of C1bβ-Y123W with Phorbol Ester *versus* Diacylglycerol 38

Conclusions 41

Acknowledgement 55

CHAPTER 3: A SINGLE RESIDUE IN THE C1 DOMAIN SENSITIZES NOVEL PROTEIN KINASE C ISOFORMS TO CELLULAR DIACYLGLYCEROL PRODUCTION 56

Questions addressed in Chapter 3 57

Sequence alignment of various C1 domains 57

Binding of C1bβ and C1bδ Domains to Lipid Vesicles *in vitro* 58

Binding of C1bβ and C1bδ Domains to Lipid Vesicles Containing Phosphatidylserine *versus* Phosphatidylglycerol 61
Translocation of C1bβ and C1bδ Domains to Membranes in Response to Natural Agonist *in vivo* 62
Ca^{2+}-Independent Protein Kinase C Activity for Wild-Type and Mutant PKCβ and Wild-Type PKCδ 64
Basal Localization of Wild-Type and Mutant C1bβ and C1bδ Domains and Full-Length Proteins *in vivo* 66
Structure and Surface Properties of Representative C1 Domains 67
Conclusions 71
Acknowledgement 74

CHAPTER 4: THE INCREASED ELECTROSTATIC POTENTIAL OF THE ATYPICAL C1 DOMAIN OF PROTEIN KINASE C ζ DOES NOT INCREASE ITS AFFINITY FOR ANIONIC LIPIDS RELATIVE TO TYPICAL C1 DOMAINS 75
Regulation of Atypical PKCs by Phospholipids 75
Structures of Typical and Atypical C1 domains 77
Molecular Modeling and Electrostatic Potential Maps of the C1b Domain of PKCγ and the C1 Domain of PKCζ 79
Binding of C1bβ and C1ζ to Phosphatidylserine-Containing Membranes 81
Binding of C1ζ to a Panel of Phosphoinositides and Phospholipids 83

Conclusions 85

Acknowledgement 90

CHAPTER 5: SUMMARY AND CONCLUSIONS 91

Significance 93

APPENDIX: EXPERIMENTAL 98

I. Materials 98

II. Methods 99

Cloning of Protein Kinase C and C1 Domains 99

Mutagenesis 99

Bacterial Production of Recombinant Protein and Bacterial Cell Lysis 99

Purification of C1 Domains 100

Lipids 101

Preparation of Lipid Vesicles for Stopped-Flow Spectroscopy 102

Preparation of Sucrose-Loaded Lipid Vesicles (SLVs) 103

Incorporation of PMA into Vesicles 104

Steady-State Fluorimetry 104

Sucrose-Loaded Vesicle (SLV) Assay 105

Silver Staining of SDS-PAGE Gels 106

Data Analysis for Sucrose-Loaded Vesicle Assay 107

Stopped-Flow Fluorescence Spectroscopy 107

Cell Culture 109

Protein Kinase C Activity Assay 110

Cell Imaging 110

Phospholipid Dot Blot 111

Sequence Alignment and Phylogenetic Analysis 112

Modeling 112

REFERENCES 114

LIST OF ABBREVIATIONS

BSA	bovine serum albumin
CKAR	C kinase activity reporter
DG	sn-1,2,-dioleoylglycerol
DTT	dithiothreitol
EDTA	ethylenediaminetetraacetic acid
GST	glutathione-*S*-transferase
HEPES	N-[2-hydroxethyl]piperazine-N'-[2-ethanesulfonic acid]
PAGE	polyacrylamide gel electrophoresis
PC	phosphatidylcholine
PE	phosphatidylethanolamine
PG	phosphatidylglycerol
PI	phosphatidylinositol/phosphoinositide
PI3K	phosphoinositide-3-kinase
PKC	protein kinase C
PMSF	phenylmethylsulfonylfluoride
PS	phosphatidylserine
SDS	sodium dodecylsulfate
SLV	sucrose-loaded vesicle
TEMED	N,N,N',N'-tetramethylethylenediamine
Tris	tris(hydroxymethyl)aminomethane

LIST OF FIGURES

Page

Figure 1. G-protein coupled receptor (GPCR)-mediated hydrolysis of phosphoinositide-4,5-bisphosphate (PI-4,5-P_2) activates protein kinase C (PKC) 3

Figure 2. Domain structure and regulators of protein kinase C family members 4

Figure 3. Tyrosine at position 22 is in the C1b domains of conventional protein kinase C isoforms is a conserved branch of C1 domains in multicellular animals 13

Figure 4. Sites of tryptophan mutations in the design of a fluorescent probe for the C1 domain 21

Figure 5. C1bβ-Y123W can be used as a fluorescence-based readout for binding to lipid vesicles 22

Figure 6. The mutant C1bβ-Y123W binds with similar affinity as wild-type domain to PMA-containing vesicles 24

Figure 7. PS increases the affinity of C1bβ-Y123W for PMA-containing lipid vesicles tenfold 24

Figure 8. Dissociation experiments using competition and dilution yield similar rate constants 28

Figure 9. The association of C1bβ-Y123W with lipid vesicles containing 5 or 0.1 mol% PMA and 20 mol% PS is not sensitive to ionic strength above 150 mM KCl 30

Figure 10. C1bβ-Y123W has selectivity for PS over PG only in the context of DG-containing membranes 33

Figure 11. C1bβ-Y123W does not show selectivity for PS over PG in the context of PMA-containing membranes even under low-affinity conditions 33

Figure 12. Sample traces for the association of C1bβ-Y123W with lipid vesicles containing 5 mol% PMA or 5 mol% DG and 30 mol% PS or PG 36

Figure 13. Sample traces for the association of C1bβ-Y123W with lipid vesicles containing 5 mol DG and either 30 mol% or 40 mol% PS or PG 37

Figure 14. Binding of wild-type C1bβ, C1bβ-Y123W, and C1bδ to lipid vesicles containing 5 mol% DG and 30 mol% PS 39

Figure 15. C1bβ-Y123W binds PMA-containing vesicles with fivefold higher affinity than DG-containing vesicles containing 30 mol% PS 42

Figure 16. C1bβ-Y123W binds PMA-containing vesicles with tenfold higher affinity than DG-containing vesicles containing 40 mol% PS 42

Figure 17. Chemical structures of dioleoylglycerol (DG) and phorbol-12-myristate-13-acetate (PMA) 48

Figure 18. Chemical structures of the anionic phospholipids 1-palmitoyl-2-oleolyl-*sn*-glycero-3-[phospho-L-serine] (PS) and -[phospho-racemic-(1-glycerol)] (PG) 48

Figure 19. Model for the interaction of the C1 domain with lipid membranes 51

Figure 20. Sequence alignment of the C1 domains of representative conventional and novel PKC isoforms and other C1 domain-containing proteins across species 59

Figure 21. Mutation of Tyr22 to Trp in the C1b domain of PKCβ increases its affinity for DG-containing membranes and reduces selectivity for PMA over DG similar to the C1b domain of C1bδ 60

Figure 22. Trp at position 22 of the C1 domain is responsible for efficient translocation to membranes in response to natural agonist 65

Figure 23. Trp at position 22 increases calcium-independent PKC activity 65

Figure 24. Residue 22 affects localization of the C1b domain and full-length PKC 68

Figure 25. The C1 domain's ability to bind DG arises from modulation of the width and surface properties of the loops surrounding the hydrophobic DG-binding cleft 70

Figure 26. Homology modeling of the C1 domain of PKCζ (C1ζ) and comparison with the C1b domain from PKCδ (C1bδ) 80

Figure 27. C1ζ has a greater electrostatic potential than C1bδ due to a cluster of basic residues occluding the ligand-binding cavity 82

Figure 28. C1bβ and C1bβδ have similar electrostatic potential maps 84

Figure 29. C1ζ does not bind to a panel of phospholipids 86

Figure 30. Summary of the results from Chapters 2 through 4 96-97

LIST OF TABLES

Page

Table 1. Apparent equilibrium and kinetic parameters for the association of C1bβ-Y123W with lipid vesicles of increasing mol% PS 26

Table 2. Comparison of values of k_{off} from association and dissociation experiments..... 28

Table 3. Binding of C1bβ-Y123W to lipid vesicles composed of 20 mol% PS and 5 *versus* 0.1 mol% PMA 31

Table 4. C1bβ-Y123W has selectivity for PS over PG only in the context of DG-containing membranes..... 34

Table 5. Apparent equilibrium and kinetic parameters for the association of C1bβ-Y123W with lipid vesicles of 5 mol% PMA and 30 mol% PS or PG 34

Table 6. Apparent equilibrium and kinetic parameters for the association of C1bβ-Y123W with lipid vesicles of 40 mol% PS and either 5 mol% PMA or DG 43

Table 7. Apparent binding constants (K_d) for the interaction of the C1b domain with membranes..... 63

Table 8. Binding affinity for the interaction of the C1bβ and C1ζ with PS-containing membranes..... 84

Table 9. Dependence of k_{off} on the ratio of [C1bβ-WT] : [C1bβ-Y123W] 109

ACKNOWLEDGEMENTS

I am particularly grateful to Dr. Alexandra C. Newton, who has been an inspiration and a role model. Thank you for enthusiastically encouraging independence and exploration, and thank you even more for providing guidance and focus when it was critical.

I would also like to thank the other members of my committee for their assistance and thoughtful discussions; these include Drs. Joe Adams, Ed Dennis, Betsy Komives, and Palmer W. Taylor.

Thank you to the Pharmacology and Molecular Biophysics Training Grants at the University of California, San Diego; the National Institutes of Health; and the Honor Societies of Phi Kappa Phi and Alpha Lambda Delta Honors Society for financial support.

I would like to thank the many members of the Newton lab who offered guidance and fruitful conversations. In particular, I would like to thank Dr. Jon Violin for help with fluorescent work; Drs. Maya Kunkel, C.C. King, Tianyan Gao, and Hilde Abrahamson for general assistance; and most especially Mrs. Lisa Gallegos for a wonderful collaboration. Thank you also to Ms. Shelly Barnes for the preparation of the construct for the purification of the C1 domain of PKCζ.

Thank you to Dr. Susan Taylor for use of the Jobin (Edison, NJ) Yvon-SPEX FluoroMax-2 fluorescent spectrometer, Dr. Patricia Jennings for use of the Applied Photophysics Π*-180 stopped-flow fluorescence spectrometer, Dr. Lynn Ten Eyck for modeling assistance provided through the Biomedical Sciences course number

BIOM205, and Dr. Roger Tsien for use of the Tecan Safire fluorescent plate reader. I would also like to thank Dr. Zoran Radic in Dr. Palmer Taylor's laboratory for much assistance with stopped-flow spectroscopy and kinetic analysis. Thank you also to Dr. Seth Field, who performed the phospholipid dot blot described in Chapter 4.

Thank you to all of the students, faculty and staff of the Biomedical Sciences Program at the University of California, San Diego, for a unique and immensely enjoyable experience in my doctoral training. Thank you to all of the very special friends I made throughout the years, in particular Matt, Gerald, Alison and Sandy.

Thank you especially to Dr. Hal White, III, whose enthusiasm, encouragement, and commitment to education will forever be an inspiration.

I would also like to thank Sara from the bottom of my heart – the successful completion of this thesis is due in large part to her patience, understanding, and encouragement throughout my final year of training.

Finally, I would like to thank my entire family for providing such a loving and supportive environment in which to grow up. I would especially like to thank my parents, Bob and Lisa, who have been selfless and supportive in all I have done. Thank you for providing me with every opportunity to succeed and for making my future limitless.

Published Material and Material in Preparation

Chapter 2, in part, is a reprint of the material as it will appear in Dries, D. R., Newton, A.C. (2007) *Journal of Biological Chemistry*. The dissertation author will be the author of this paper; A. C. Newton is the principal investigator on the supporting

grant. Chapter 3, in part, is a reprint of the material as it appears in Ref. (55). The dissertation author and L. L. Gallegos contributed equally to the work and co-authored this paper; A. C. Newton was the principal investigator on the supporting grant.

CURRICULUM VITAE

EDUCATION

Ph.D.:	2007, Biomedical Sciences University of California, San Diego
B.S.:	2000, Biochemistry (with Honors, Magna Cum Laude) University of Delaware

RESEARCH AND PROFESSIONAL EXPERIENCE

2000-2006	Graduate Research Assistant *Kinetics and Mechanism of the Interaction of PKC's C1 Domain with Lipid Membranes* University of California, San Diego (with A. C. Newton, Pharmacology)
1998-2000	Undergraduate Research Assistant, Honors Thesis *BVES: A Novel Protein in Heart Development* University of Delaware (with M. K. Duncan, Biology)
1998	Undergraduate Research Assistant *Development of a Novel Organometallic Cyclization Reaction in the Chemical Synthesis of a Natural Product, Ptilocaulin* University of Delaware (with D. F. Tabor, Chemistry & Biochemistry)

RESEARCH INTERESTS

Protein:lipid interactions
Enzyme kinetics
Molecular modeling
Fluorescence spectroscopy

AWARDS & FELLOWSHIPS

2004	American Society of Biochemistry and Molecular Biology Travel Award
2002-2004	Molecular Biophysics Training Grant (2T32 GM-08326)
2000-2002	Pharmacology Training Grant (2T32 GM-07752)

2000	Phi Kappa Phi Graduate Research Fellowship Alpha Lambda Delta Graduate Research Fellowship Phi Beta Kappa Membership Bachelor of Sciences Degree with Honors Magna cum laude graduate
1999-2000	Howard Hughes Undergraduate Research Fellowship

AFFILIATIONS

2003-2005	American Society of Biochemistry and Molecular Biology (ASBMB)
2002-2003	Biophysical Society

SERVICE

2003	Graduate Admissions, Graduate student representative
2003-2004	Biomedical Sciences Program Student Advisory Group
2003-present	Volunteer instructor, Salk Science Mobile Laboratory
2004	First annual ASBMB Student Hill Day; Washington, D.C., Oct. 13-15, 2004; organized by Mr. Peter Farnham, Public Affairs Officer, American Society of Biochemistry and Molecular Biology (ASBMB)
2006	Manuscript reviewer, *Journal of Medicinal Chemistry*
2006	Consultant, Bio-Rad Laboratories

TEACHING & MENTORING EXPERIENCE

Teaching:

2001	Teaching Assistant, University of California, San Diego BIBC103 – Biochemical Techniques (Biology) Course Instructor: Mrs. Lara Soowal
2004	Teaching Assistant, University of California, San Diego SPPS223 – Kinetics and Metabolism (School of Pharmacy) Course Instructor: Dr. Palmer Taylor

Mentoring:

1999-2000	Justin DiAngelo, undergraduate researcher, Univ. of Delaware *Currently:* Graduate student at Univ. of Pennsylvania (Cell and Molecular Biology, Advisor: Dr. Morris Birnbaum)

2002 Svetlana Pavlovic, summer undergraduate researcher, Univ. of California, San Diego (SURF program, UCSD)
Currently: Graduate student at Cornell Univ. (Dept. of Pathology and Laboratory Medicine, Advisor: Dr. Domenick Falcone)

2004 Shelly Barnes, undergraduate researcher, Univ. of California, San Diego
Currently: Medical student at Univ. of Chicago

PUBLICATIONS

Daniel R. Dries, Lisa L. Gallegos, Alexandra C. Newton. "A single residue in the C1 domain sensitizes novel protein kinase C isoforms to cellular diacylglycerol production." *Journal of Biological Chemistry*. In press.

Daniel R. Dries, Alexandra C. Newton. "The contributions of electrostatic and hydrophobic interactions to the association of PKCβII's C1b domain with lipid membranes by equilibrium and kinetic analyses." In preparation.

ABSTRACTS

Daniel R. Dries, Alexandra C. Newton. "The contribution of electrostatic and hydrophobic interactions in the binding of the C1 domain of protein kinase C to lipid membranes." Poster, American Society of Biochemistry and Molecular Biology (ASBMB), San Diego, June 2005.

Daniel R. Dries, Alexandra C. Newton. "The contribution of electrostatic and hydrophobic interactions in the binding of the C1 domain of protein kinase C to lipid membranes." Poster, American Society of Biochemistry and Molecular Biology (ASBMB), Boston, June 2004.

Daniel R. Dries, Alexandra C. Newton. "Kinetics and mechanism of the membrane-targeting C1 domain of protein kinase C as analyzed by stopped-flow kinetics." Poster, American Society of Biochemistry and Molecular Biology (ASBMB), San Diego, April 2003.

Daniel R. Dries, Alexandra C. Newton. "Kinetics and mechanism of the membrane-targeting C1 domain of protein kinase C." Poster, Biophysical Society, San Antonio, February 2003.

GRADUATE LEVEL COURSEWORK

Course ID	Course Name: [Instructor(s), Department in parentheses]
BIOM205	Modeling Biological Macromolecules (Dr. Lynn Ten Eyck, Pharmacology)
BIOM207	Internet Resources for Molecular Biology (Dr. Philip Bourne, San Diego Supercomputer Center)
BIOM208A	Topics in Medical Therapeutics (Dr. Paul Insel, Pharmacology and School of Medicine)
BIOM210	Cellular Biology (Dr. Don Cleveland, Cellular and Molecular Medicine)
BIOM211	Molecular Biology (Dr. Xiang-Dong Fu, Biomedical Sciences)
BIOM212	Cellular and Molecular Pharmacology (Drs. Alexandra Newton & Palmer Taylor, Pharmacology)
BIOM213	Systemic Physiology (Dr. Kim Barrett, School of Medicine)
BIOM219	Ethics in Scientific Research (Dr. Palmer Taylor, Pharmacology)
BIOM230	Receptors/Signal Transduction (Dr. Palmer Taylor, Pharmacology and School of Pharmacy)
BIOM285	Statistical Inference in Medicine (Dr. Harvey Motulsky, Pharmacology)
CHEM209	Macromolecular Recognition (Dr. Gouri Ghosh, Biochemistry)
CHEM216	Chemistry of Enzyme-Catalyzed Reactions (Dr. Elizabeth Komives, Biochemistry)
CHEM219A	Special Topics in Biochemistry (Dr. Patricia Jennings, Biochemistry)
PHAR231	Contemporary Topics in Pharmacology: Fluorescence Spectroscopy (Drs. Palmer Taylor & Roger Tsien, Pharmacology)
PHAR294	Pharm & Molecular Biology Journal Club (Dr. Rik Bundey, Pharmacology)
PHAR295	Pharmacology Research Discussions (Drs. Palmer Taylor & Joan Heller Brown, Pharmacology)
PHYS239	Special Topics: Single Molecule Biophysics (Dr. Doug Smith, Physics)

ABSTRACT OF THE DISSERTATION

KINETICS AND MECHANISM OF THE INTERACTION OF
THE C1 DOMAIN OF PROTEIN KINASE C WITH LIPID MEMBRANES

by

Daniel Robert Dries

Doctor of Philosophy in Biomedical Sciences

University of California, San Diego, 2007

Professor Alexandra C. Newton, Chair

Protein kinase C (PKC) is a critical component of many signaling pathways. As such, PKC regulates such diverse phenomena as memory and learning, immune system responses, and cancer. Binding to membranes regulates the activity of PKC, and the C1 domain of PKC binds to membranes in response to the lipid second messenger, diacylglycerol (DG). This dissertation describes the molecular nature by which the C1 domain of PKC interacts with membranes. First, a fluorescent reporter

is used with stopped-flow fluorescent spectroscopy to analyze the binding kinetics between the C1 domain and lipid vesicles. Kinetic data reveal that both specific and non-specific interactions guide the association of the C1 domain with membranes, whereas hydrophobic contacts between the C1 domain and its ligand determine the rate of dissociation. The data provide evidence for a model that describes the mechanism by which the C1 domain binds to membranes and explain how the DG-mimicking, tumor-promoting phorbol esters (i.e., PMA) exert their potency. Second, an evolutionarily-conserved residue that regulates the C1 domain's affinity for DG has been identified. This residue, which is a conservative change from tryptophan to tyrosine, lies at the apex of the ligand-binding pocket and lowers the affinity for DG 30-fold without affecting the affinity for PMA; tryptophan at this position also localizes the isolated domain to internal membranes. Molecular modeling suggests that this amino acid regulates the width of the ligand-binding pocket, and the identity of this residue explains the Golgi localization of novel PKC isoforms and why novel PKC isoforms rely solely on their C1 domains for activation. Finally, modeling of the atypical C1 domain of PKCζ reveals that the C1 domain cannot bind DG or PMA due to a cluster of basic residues occluding the binding pocket. Moreover, this domain does not have a higher intrinsic affinity for a variety of phospholipids than does a typical C1 domain, despite having a more positive electrostatic potential. The data presented in this dissertation redefine the molecular nature of the interaction of the C1 domain with lipid membranes and offer insights into this unique class of lipid-targeting domains.

CHAPTER 1: INTRODUCTION

Protein kinase C (PKC) is a critical component of many signaling pathways (1). On a cellular level, PKC has long been known to regulate metabolic pathways, smooth muscle contraction, cellular proliferation and growth, differentiation, membrane conductance, exocytosis, synaptic plasticity, long-term potentiation, gene expression, and the down-regulation of receptors (2). On an organismal level, the list of outputs in which PKC plays a role is similarly long and varied. PKC levels are highest in the brain, and as a result, PKC was first purified in large quantities from brain preparations (3). Indeed, PKC is involved in memory and learning, in addition to visual and immune responses (4,5). However, PKC is best known for its role in tumor progression, as PKC was first cloned as the "receptor" for the potent tumor-promoting phorbol esters (6,7). PKC signaling is typically rapid and transient (8), but phorbol ester treatment results in chronic activation of PKC, thus promoting cancer (6). Insights into the molecular origins for the activation of PKC, by both natural ligands and phorbol esters, are critical to the understanding of signal transduction pathways and to the design of discrete modulators of PKC activity

Protein Kinase C: The Early Years

Nishizuka and coworkers first identified PKC as protein kinase M, a constitutively activated kinase in bovine brain that required only Mg^{2+} for its activity (3,9). Drawing upon their earlier experience with protein kinase G, they recognized

protein kinase M as a proteolytic fragment whose regulatory region was liberated from the kinase core by the Ca^{2+} -dependent protease calpain, hence the "*C*" in PKC's name (9). Two years later, the pro-enzyme PKC was shown to be reversibly activated by Ca^{2+} and the phospholipids phosphatidylserine and phosphatidylinositol, although a crude lipid preparation was necessary for maximal activation (10,11). Only one year later, the missing activator was identified as diacylglycerol (DG) (12), for which phorbol esters were soon found to substitute (13). The discovery that phospholipases metabolize phosphoinositides to generate DG, which activates PKC directly, and inositol-3,4,5-trisphosphate, which indirectly activates PKC by causing the release of intracellular Ca^{2+}, poised PKC to be a critical transducer of intracellular signaling events (Figure 1, and (14,15)).

The Structure of Protein Kinase C

PKC (~80 kDa) can be cleaved into an N-terminal regulatory domain (~35 kDa) and a C-terminal catalytic domain (~45 kDa) by proteolysis at a flexible "hinge" region (16). The catalytic domain itself is constitutively active (see above, (3)), but remains in an inactive state through autoinhibition by its regulatory domain, which contains the phospholipid, Ca^{2+}, and DG/phorbol ester binding sites (17). The discovery that PKC is, in fact, a family of several isoforms (18,19) has led to the subclassification of the PKC family into conventional (cPKCs: α, βI/II, γ), novel (nPKCs: δ, ε, η, and θ), and atypical (aPKCs: ι/λ and ζ) isoforms, grouped according to their regulatory domains (Figure 2 and (20)).

PKC undergoes a series of phosphorylations that prime the enzyme for

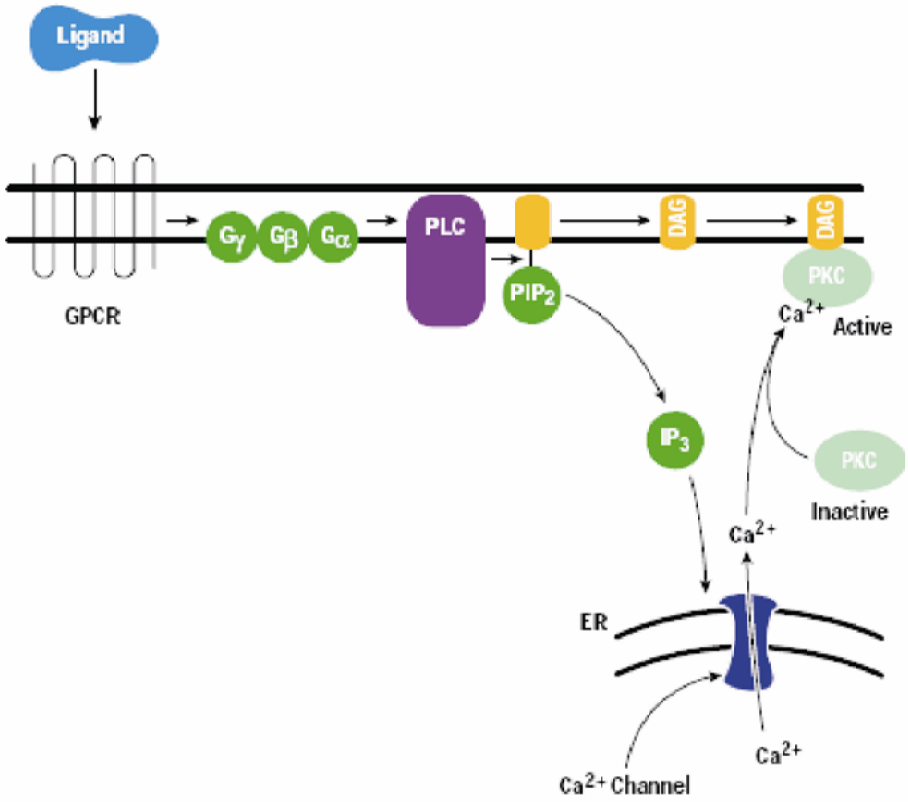


Figure 1. G-protein coupled receptor (GPCR)-mediated hydrolysis of phosphoinositide-4,5-bisphosphate (PI-4,5-P_2) activates protein kinase C (PKC). One mechanism for the activation of PKC. Ligand binds to a seven transmembrane-spanning receptor (GPCR), which couples to the $G\alpha_q$ subunit. Upon ligand binding to the receptor (e.g. UTP binding to the P2Y receptor, Ref. (78)), GDP is exchanged for GTP, which activates the $G\alpha_q$ subunit. GTP-bound $G\alpha_q$ activates phospholipase C, which cleaves PIP_2 into the membrane-bound diacylglycerol (DAG) and the soluble inositol-1,4,5-trisphosphate (IP_3). IP_3 then activates the IP_3-sensitive ryanodine receptor at the endoplasmic reticulum (ER) to release calcium (Ca^{2+}) from internal stores. Ca2+ can then directly activate conventional PKC isoforms via the C2 domain. PKC translocates to the plasma membrane, where it can be fully activated by binding to DAG. It should also be noted that DAG can also be generated from PIP_2 and/or phosphatidylcholine through a receptor tyrosine kinase (RTK) coupling to $G\alpha_{11}$. Taken from http://www.promega.com.

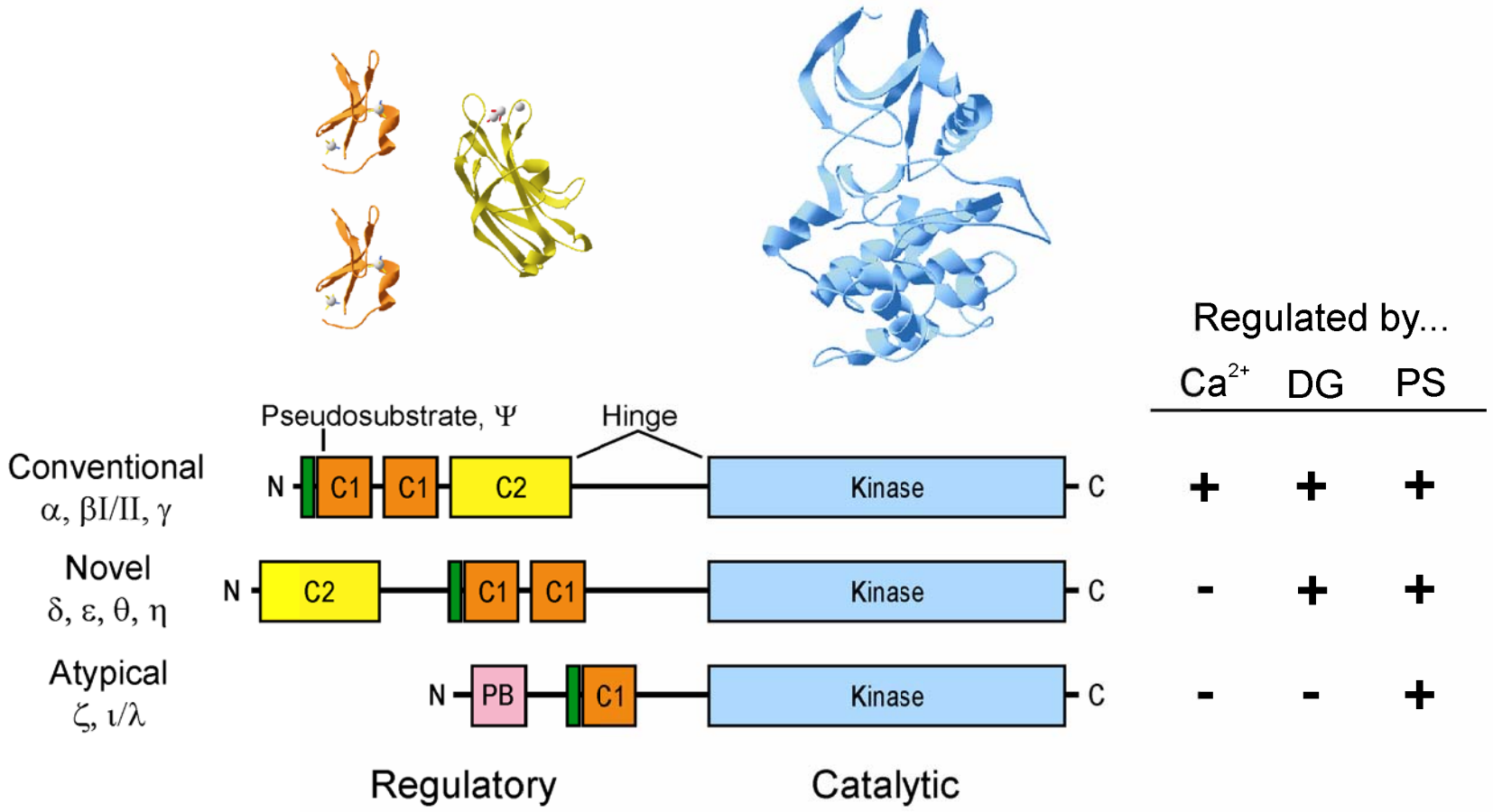


Figure 2. Domain structure and regulators of protein kinase C family members. The protein kinase C family is subgrouped into three categories according to regulatory domain structure and modes of regulation. Domains pictured are the pseudosubstrate domain (ψ) in *green;* the C1 domain, which binds DG, in *orange;* the C2 domain, which binds Ca^{2+} in conventional isoforms only, in *yellow;* and the kinase domain in *blue*. Also shown is the PB domain of atypical kinases in *pink*, which is responsible for protein-protein interactions. Table at right indicates whether each subfamily is (+) or is not (-) regulated by the indicated cofactor.

catalysis (21). However, fully phosphorylated PKC remains in an inactive state in the cytosol, due to a pseudosubstrate that sits in the active site and blocks catalysis (Chapter 1 and (20)). All PKC isoforms contain this autoinhibitory intramolecular pseudosubstrate, which must be removed from the active site for catalysis to occur (Figure 2). This pseudosubstrate is a basic peptide and "looks" like a PKC substrate, with the exception of a non-phosphorylatable alanine in the pseudosubstrate in place of a phospho-acceptor Ser/Thr in a phosphorylatable substrate (22). The removal of the pseudosubstrate from the active site is achieved through the binding of its regulatory domain to lipid membranes (23).

Three types of regulatory subdomains exist in the N-terminus of PKC: the C1, C2, and PB domains (Figure 2). The C1 domain is the binding site for DG and the phorbol esters and contains determinants for the stereospecific binding of phosphatidylserine (PS) (24). The C2 domain is the binding site for Ca^{2+}, which is proposed to facilitate the binding of the C2 domain to lipid by a variety of mechanisms (25). Finally, the PB domain is unique to the atypical subfamily of PKCs and serves as a protein-protein interaction module, rather than as a lipid-targeting module (26). Conventional PKC isoforms contain two tandem C1 domains and one conventional C2 domain; consequently, cPKCs are regulated both by DG and Ca^{2+} (Figure 2). The novel isoforms contain two tandem C1 domains and a non-Ca^{2+}/membrane binding novel C2 domain; consequently, nPKCs are regulated only by DG. The atypical isoforms contain a single, non-DG/phorbol ester-binding C1 domain and no C2 domain; consequently, aPKCs are regulated neither by DG nor Ca^{2+}, although several studies have shown regulation of aPKCs by a variety of anionic lipids (27).

Translocation to Membranes and PKC's Membrane-Targeting Modules

The observation that phorbol esters cause the chronic activation of PKC by redistribution of PKC to the plasma membrane led to the long-standing idea that this "translocation" to the membrane was critical for PKC's activity (28,29). Indeed, the critical regulator for activity is the affinity with which PKC binds to membranes – the net energy that is released in the binding of the regulatory domain to membranes is used to remove the pseudosubstrate from the active site and allow the catalytic transfer of phosphate to substrates (24). Therefore, it is critical to study the mechanism by which PKC's C1 and C2 bind membranes in order to gain an understanding of PKC's signaling.

Many different types of membrane-targeting domains can be found throughout the human genome, including C1, C2, PH, FYVE, PX, ENTH, ANTH, BAR, FERM, and tubby domains (25). These domains are often regulated by lipids and molecules that undergo transient increases during cellular signaling events, such as phosphoinositides, DG, and Ca^{2+}, as mentioned above. Many of these domains use the same mechanism for the reversible binding to membranes: recruitment by electrostatic interactions, followed by membrane penetration due to hydrophobic interactions. However, such mechanisms are only qualitatively similar, as domains even within a certain class vary in the extent to which they use electrostatic interactions and membrane penetration to achieve a reasonable affinity. In fact, weak affinity with high cooperativity across multiple membrane-targeting domains allows the regulatory region of lipid-bound proteins to serve as a "coincidence detector" for small changes in several different soluble or membrane-embedded ligands; such regulation allows

the sensitive regulation of the parent protein, which often results in small changes in protein conformation (25).

Over the years, many groups have studied the interaction of PKC's C1 domain with lipid membranes. Most of these studies have relied on equilibrium or monolayer penetration experiments to describe the nature of this interaction (25). The few kinetic experiments that do exist for the C1 domain use full-length PKC (30,31), which makes it difficult to extract the contribution of individual domains to the interaction with membranes. Moreover, *in vitro* kinetics correlate well with *in vivo* translocation rates and activity (25), thereby emphasizing the suitability and need for simple *in vitro* kinetic studies to describe the interaction of these individual domains with membranes.

The Structure of the C1 Domain

The C1 domain can be found in many signaling enzymes, including kinases, small G-protein GTPase activating proteins and exchange factors, and lipid metabolizing enzymes (32,33). The 50 amino acid domain is small (~8 kDa) and globular and rich in β-sheet with a small C-terminal α-helix (see Figure 4 in Chapter 2). The proper folding of the domain requires two structural zinc ions; these ions are coordinated by two histidines and six cysteines, thereby giving the C1 domain its alternate name, the cysteine-rich domain (CRD) (33). The DG/phorbol ester-binding site is formed by an "unzipped" β-sheet that is held open by a conserved proline and several water molecules (34). Interestingly, a structure with phorbol revealed that the binding of the ligand is achieved through the backbone amides and carbonyls of

Thr12, Leu21, and Gly23 (consensus residue numbering), rather than specific contacts with amino acid sidechains; however, hydrophobic contacts between phorbol and C1 domain reinforce the high-affinity binding (34). Despite being largely hydrophobic, the C1 domain has a ring of basic residues around the middle third of the domain, which may facilitate its interaction with anionic membranes (25,34,35). Due to its hydrophobic nature, one would expect that the ligand-binding pocket of the C1 domain is blocked via intramolecular interactions with its host protein, thereby requiring a conformational change for exposure of the C1 domain's ligand-binding pocket to the membrane-embedded ligand (25). Indeed, this is the case for β2-chimaerin, where the C1 domain is buried by contacts with several regions of the entire protein (36). Similarly, Oancea and Meyer found that the C1 domain of PKCγ is blocked by a pseudosubstrate clamp that needs to be removed in order for ligand to bind (37). Further experiments with PKCβII, however, showed that PMA bound with similar affinity to the C1 domain by itself and to the full-length protein, indicating that the ligand-binding pocket of the C1 domain of PKCβ is not occluded (24). Thus, without structural information for full-length PKC, the positioning of the C1 domain with respect to the rest of the kinase is unclear.

Binding of Phospholipids to the C1 Domain

The original researchers who identified PKC found that phosphatidylserine (PS) and phosphoinositides served as specific activators of the kinase (10,11). PS, however, has been found to be a specific activator of PKC, and the interaction between PS and PKC has been extensively investigated (38). Several reports describe

that anionic phospholipids, in particular PS, participate in the optimal presentation of substrate to the kinase (39-41). Later reports, however, identified PS as a specific allosteric regulator of PKC activity, with Hill coefficients as high as 12 for the full-length enzyme in a mixed-micelle assay and 4 with lipid bilayers (42-46). Another study revealed that the high cooperativity is only *apparent*, as the multivalent PKC binds to multiple lipid-bound ligands independent of one another (47). Further clarification was provided in a study that showed that PKC's apparent cooperativity with PS was in part due to true cooperativity, but also to a "reduction in dimensionality", where the effective concentration of PS is higher for the binding of a second PS molecule to micelle-bound PKC than the binding of the first PS molecular to soluble PKC (43). Moreover, experiments with enantiomeric membranes revealed that PKC stereospecifically recognizes *sn*-1,2-diphosphatidyl-L-serine (and not its enantiomer *sn*-2,3-diphosphatidyl-D-serine) rather than the structure of the membrane itself, with no discrimination for the stereochemistry of the zwitterionic lipid phosphatidylcholine (PC) (48). The specific site for regulation by PS, however, remained a controversy until the publication of a study that pinned the C1 domain, and not the C2 domain, as the site for stereospecific regulation of PKC by PS (24).

Despite the identification of the C1 domain as the site for PS binding, a specific site for this anionic lipid has not been found. Several basic residues provide a positively-charged ring around the middle third of the domain, but biochemical and mutagenesis experiments show that these residues are important for non-specific interactions with anionic lipid (30,49). The observation that DG can cluster PS (50) offers the possibility that the binding of PS is concomitant with binding to DG, thus

giving apparent specificity in the context of DG-containing membranes. An alternate explanation has been proposed whereby non-specific interactions can, in fact, contribute to stereospecific interactions at the membrane, as domains pre-targeted to the membrane by a single contact point only need to find two specific contact points at the membrane surface for stereospecificity, as opposed to the three needed for soluble ligands (35). Indeed, kinetic experiments can offer a unique insight into the mechanism of this binding interaction.

Binding of DG and Phorbol Esters to the C1 Domain

Phorbol esters, such as phorbol-12-myristate-13-acetate (PMA), have long been known to be potent activators of PKC (32). PMA binds to the C1 domain in a similar qualitative manner to DG (51), but PKC binds to PMA-containing membranes with two orders of magnitude higher affinity than to DG-containing membranes (20). Phorbol esters are extensively used in the literature as potent, direct activators of PKC, although many reports caution against the substitution of DG with phorbol esters (see Chapter 3). For example, the affinities of C1 domains for DG do not always correlate well with the extent to which the domains bind phorbol esters (49). However, the manner by which the C1 domain has a higher affinity for PMA- over DG-containing membranes has not been elucidated.

The structure of the C1b domain of PKCδ with and without phorbol revealed that rather than cause a gross conformational change in the domain, phorbol changes the surface properties (34). The polar groups on phorbol bind to the carbonyl and amide functions of Thr12, Leu21, and Gly23 and cap the domain with a hydrophobic

patch, thereby facilitating its penetration into the membrane. But interactions with phorbol are not the same as interactions with DG, as the two often have opposite affinities for any given C1 domain (49). Rather, phorbol is much larger and can form many more hydrophobic contacts with the C1 domain than can the smaller DG (Figure 17, Chapter 1). Indeed, the structure of the C1b of PKCδ reveals many hydrophobic interactions that are important for the interaction between domain and ligand (34). However, the molecular determinants for the specific recognition of PMA *versus* DG have not been elucidated.

Inequality Among C1 Domains

Not all C1 domains were created equal. Many studies have shown the inequality of C1 domains even within the same protein (see Refs. (25,32,35,49) for excellent reviews). Many C1-domain containing proteins contain a tandem repeat of the domain, thereby requiring the designation "C1a" and "C1b" (see cPKCs, nPKCs in Figure 2). However, the C1a and C1b domains of such proteins often exhibit different and opposing affinities for DG and phorbol ester. Therefore, there has been much debate over which C1 domain is critical for activity, with different C1 domains being important for different PKC isoforms (49). Each C1 domain can bind phorbol ester independently, suggesting a potential 2:1 stoichiometry of phorbol ester to PKC (52). Later experiments, however, showed that full-length PKC prefers to bind only one molecule of ligand for activation (53). Therefore, the reason for two tandem C1 domains has remained a mystery and a debate.

Several hypotheses have been proposed for the differences between C1a and

C1b domains. In the case of PKC, the pseudosubstrate is linked to the C1a domain (Figure 2), and, given the importance of the removal of pseudosubstrate from the active site (see above), it is interesting to hypothesize that the C1a domain is the critical determinant for activity. The varying affinity for DG and phorbol ester also suggest that the C1a and C1b domains have evolved for different purposes (49). Finally, different C1 domains have been shown to localize differently within the cell. Some C1 domains display cytosolic localization, some are pre-targeted to the plasma membrane, some are pre-targeted to endomembranes, and some localize to the nucleus (49,54,55). Variation in the loops of the domain may explain the inequalities of C1 domains, with sidechain substitutions altering ligand affinity, membrane penetration, or even intra- or intermolecular protein-protein interactions (49).

Phylogenetic analysis reveals that the variability in C1 domains clusters according to whole-protein function, further suggesting the tight relationship between the binding of C1 domain and the activation of its cognate protein (Figure 3). Indeed, the C1a and C1b domains cluster together, as do the atypical C1 domains. Moreover, an ancestral split formed a subset of C1b domains that contain Tyr at position 22. Interestingly, this subset tracks well with conventional PKC isoforms across species, implicating this residue in a functional role for PKC signaling.

Atypical, Non-DG/Phorbol Ester-Binding C1 Domains

While much is known about the biochemistry and structure of typical C1 domains, studies on atypical C1 domains have lagged. Many atypical C1 domains appear as a single copy, as opposed to the tandem repeat seen for typical domains

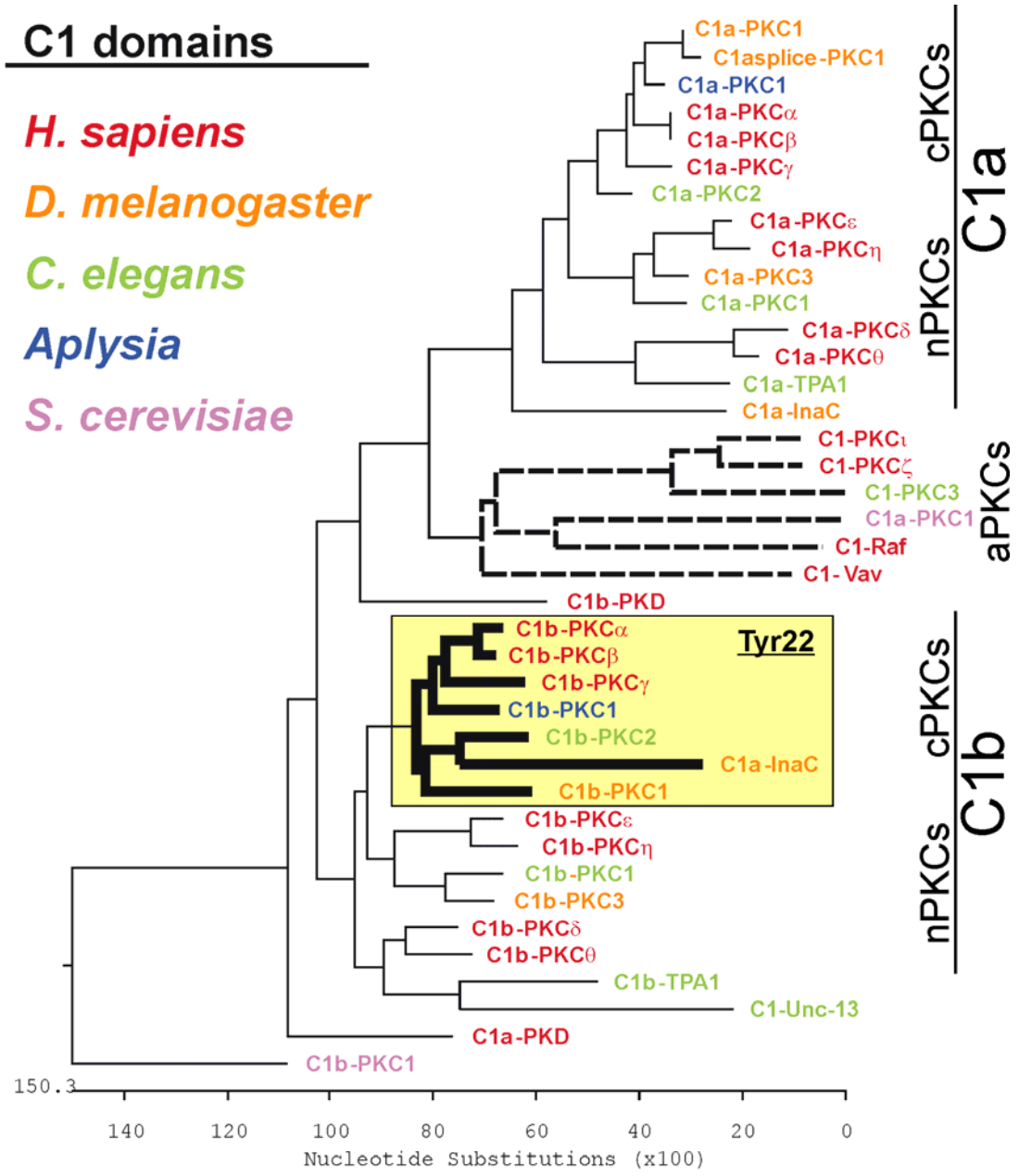


Figure 3. Tyrosine at position 22 is in the C1b domains of conventional protein kinase C isoforms is a conserved branch of C1 domains in multicellular animals. Phylogenetic tree of select C1 domains from PKC isoforms across species and other C1-domain-containing proteins. C1 domains are colored according to species, as indicated in the legend. In bold lines and boxed in *yellow* is the branch of C1 domains that contain Tyr at position 22. In dashed lines is the branch of C1 domains that contain deletions or basic substitutions in the loop in which position 22 is found; these domains do not bind DG. All other domains, excluding the yeast domains, contain Trp at position 22.

(Figure 2). Yet the single C1 domain can bind phorbol ester on its own (52). Several structural studies have elucidated the structural basis for the inability of atypical C1 domains to bind DG. For example, the C1 domain of Raf has a deletion in one of the two walls that form the ligand-binding groove (56). The importance of this loop was confirmed with the structure of the C1 domain of *k*inase *s*uppressor of *R*as (KSR) (57).

The C1 domains of the aPKCs ι and ζ, however, contain an intact binding site, indicating a different mechanism by which these domains cannot bind DG or phorbol esters. Moreover, several studies have shown that atypical PKCs can be regulated *in vitro* and *in vivo* by a variety of anionic lipids (27). During the course of the work presented here, Blumberg and coworkers confirmed the modeling studies presented here; the question of direct binding to negatively-charged lipids, however, was not addressed (54). To date, no direct structural or biochemical evidence supports the direct binding of anionic lipids to the C1 domain of PKCζ.

Questions Addressed in the Following Chapters

This thesis addresses the kinetics and mechanism by which the C1 domain of protein kinase C binds to lipid membranes. Chapter 2 describes the nature and mechanism of the interaction of PKCβII's C1b domain with lipid membranes, the experiments for which provide a model for the binding of the individual domain to membranes. The experiments presented in Chapter 2 analyze the kinetics of the interaction between the C1 domain and both PS and another anionic phospholipid, phosphatidylglycerol (PG). Specificity in the context of DG versus PMA-containing membranes is described, and kinetic parameters for the binding of each are discussed.

Moreover, quenching experiments provide evidence for the positioning of the C1 domain within the lipid/water interface, a topic that has yielded a variety of results from shallow to deep penetration into the membrane (58,59). The results support a model for both the specific and non-specific interactions with lipid membranes and highlight the balance between electrostatic and hydrophobic forces in this interaction.

Chapter 3 identifies a single residue that allows for discrete binding to DG-containing membranes, without disturbing the affinity for phorbol esters. The experiments in Chapter 3 identify the residue at position 22 as critically conserved among conventional *versus* novel PKCs and provide evidence that this residue modulates the affinity of the C1 domain for DG and alters the C1 domain's subcellular localization. This chapter helps to explain why nPKCs have lost the function of their C2 domain for pre-targeting to membranes, thereby allowing nPKCs to respond to agonists that trigger diacylglycerol production alone (60).

Chapter 4 explores the structure and function of an atypical C1 domain, that of PKCζ. Experiments using molecular modeling help to explain why the C1 domains of aPKCs ι and ζ cannot bind DG or phorbol ester. Moreover, *in vitro* binding experiments show that despite the formation of a basic patch that might explain regulation by anionic lipids, the C1 domain of PKCζ does not directly bind a variety of phospholipids. This chapter refutes evidence that suggests that PKCζ's C1 domain directly binds to phospholipids, specifically phosphoinositides. Rather, this chapter suggests that regulation by such lipids occurs through a separate, indirect mechanism.

CHAPTER 2: KINETICS AND MECHANISM OF THE INTERACTION OF THE C1B DOMAIN OF PROTEIN KINASE C WITH LIPID MEMBRANES

Protein kinase C (PKC) is an integral component of many signaling pathways (1). PKC undergoes a series of phosphorylations that prime the enzyme for catalysis (21). However, fully phosphorylated PKC remains in an inactive state in the cytosol, due to a pseudosubstrate that sits in the active site and blocks catalysis (Figure 2 in Chapter 1 and (20)). The removal of the pseudosubstrate is achieved through the binding of PKC's regulatory domains to membranes. One of these domains, the C2 domain, binds Ca^{2+} to pre-localize conventional PKCs to the membrane. A separate subfamily of PKCs, the novel isoforms, contains a "non-functional" C2 domain; therefore, the activity of nPKCs is Ca^{2+}-independent. However, both conventional and novel isoforms are regulated by diacylglycerol (DG), to which a second lipid-targeting module, the C1 domain, binds (20). The critical regulator for activity is the affinity with which PKC binds to membranes – the net energy that is released in the binding of the regulatory domain to membranes is used to remove the pseudosubstrate from the active site and allow the catalytic transfer of phosphate to substrates (24).

The C1 and C2 domains are just two of several membrane-targeting domains (25). These domains are often regulated by lipids and molecules that undergo transient increases during cellular signaling events, including phosphoinositides, in addition to Ca^{2+} and DG, as mentioned above. These domains interact reversibly with lipid membranes in a manner that is dependent on both electrostatic and hydrophobic interactions. Despite similar gross properties for this interaction, these domains vary

widely in the amount to which they rely on electrostatic and hydrophobic interactions, particularly as they vary widely in the degree to which they penetrate into the lipid bilayer. Several studies – both direct and indirect – support a mechanism through which lipid-targeting domains are guided to the membrane by non-specific electrostatic interactions, after which they can find their specific lipid-bound ligand (25). However, kinetic constants for the association and dissociation steps in this process have been lacking.

The interaction of PKC's C1 domain with membranes has been extensively studied over the years. Many equilibrium experiments with the isolated domain have provided details for this interaction (25). However, the few kinetic experiments that do exist for this interaction use full-length PKC (30,31). In order to gain insight into the mechanism of activation of PKC by DG, simple experiments to look at the kinetics of the isolated C1 domain are necessary.

The C1 domain is a small, globular domain of 50 amino acids and is found in many signaling enzymes, including kinases, small G-protein GTPase activating proteins and exchange factors, and lipid metabolizing enzymes (32,33). The domain is mainly β-sheet in character, and two zinc ions, which are required for proper folding of the domain, are coordinated by two histidines and six cysteines, thereby giving the C1 domain its alternate name, the cysteine-rich domain (CRD) (33). The ligand-binding site is formed by an "unzipped" β-sheet that is held open by several water molecules and a conserved proline residue (34). The domain is unusual in that much of the surface is hydrophobic, although a ring of positively-charged residues lines the middle third of the domain and facilitates its interaction with anionic membranes

(25,34,35). Due to the hydrophobic nature of the C1 domain, the ligand-binding pocket is sometimes blocked via intramolecular interactions with its host protein, and a conformational change is necessary for exposure of the C1 domain to ligand (25,35). However, this is not true for all C1 domain-containing proteins (see Chapter 1), as the C1 domain has the same affinity for phorbol esters in both the isolated domain and the full-length protein (24).

As indicated above, the C1 domain's interaction with membranes is also mediated by anionic lipids, specifically PS (20,25). While the site of PS specificity in PKC has remained controversial, experiments with isolated domains identify the C1 domain as the site of PS specificity (24). Other anionic membranes, however, activate PKC and facilitate binding of the C1 domain, but the origin of PS specificity – i.e., a specific recognition site on the C1 domain or properties within the membrane – has remained elusive (61).

Finally, phorbol esters, such as phorbol-12-myristate-13-acetate (PMA), have long been known to be potent activators of PKC (32). PMA binds to the C1 domain in a similar qualitative manner to DG, as the two molecules can compete with one another for the binding site in the C1 domain (51). However, PKC binds to PMA-containing membranes with two orders of magnitude higher affinity than to DG-containing membranes (20). Phorbol esters are extensively used in the literature as potent, direct activators of PKC, although many reports caution against the substitution of DG with phorbol esters (see Chapter 3). Yet, the manner by which the C1 domain has a higher affinity for PMA- than for DG-containing membranes has not been elucidated.

Questions Addressed in Chapter 2

The experiments in Figures 4-19 and Tables 1-6 detail the kinetics and molecular mechanism for the interaction of C1bβ-Y123W with lipid vesicles of varying composition. The results support a model in which the interaction is mediated by a balance between electrostatic and hydrophobic interactions between the domain and lipid. The association of the C1 domain with membranes is guided by electrostatic interactions that appear to be at least partially specific for PS over PG. The dissociation from membranes, however, is determined by hydrophobic interactions with the ligand – DG or phorbol ester. The results suggest that hydrophobic interactions predominate in the binding to PMA membranes, whereas binding to DG membranes is a balance between electrostatic and hydrophobic contributions.

Design of a Fluorescence-Based Probe for the Interaction of the C1b Domain of PKCβI/II with Lipid Membranes

In order to study the kinetics of the association of the C1 domain with lipid vesicles using stopped-flow fluorescence spectroscopy, it was necessary to design a fluorescence-based probe. The C1b domain of the conventional isoform PKCβI/II (C1bβ - the domain is the same for both splice forms) was chosen for the following reasons: a) this domain is very stable and particularly amenable to biochemical studies (24,48,53,60), b) the conventional isoforms serve as the typical PKC isoforms in that they are regulated by DG and Ca^{2+} (20), and c) the PKCβII isoform has often been used for biochemical and biophysical studies (20,23,24,43,44,47,48,53,58,60,62-64).

The kinetics for the association of the C2 domain with lipid vesicles has been studied using fluorescence resonance energy transfer (FRET), in which endogenous tryptophan (Trp) residues transfer their energy to a dansyl-labeled lipid (65). However, the C1bβ does not contain any endogenous Trp residues (see Figure 20 in Chapter 3,). Therefore, Trp was strategically placed at several specific positions within the C1bβ domain (Figure 4). In order to decrease the possibility of making non-functional domains, these mutants were designed to replace specific, unconserved residues with amino acids of similar properties. Despite being highly soluble and able to bind ligand, thereby indicating proper folding, the mutants F114W, H117W, Y123W and L150W did not show the ability to FRET to dansyl-labeled lipid (data not shown). However, one of the mutants, Y123W, did show a decrease in Trp fluorescence emission under conditions in which ~75% of the domain was bound to lipid vesicles (Figure 5A). Importantly, Trp emission could be partially recovered by diluting the vesicles to a concentration in which ~67% of the domain was bound. Moreover, emission could be fully restored upon complete dissociation of C1bβ-Y123W from lipid vesicles by the addition of detergent. Finally, none of the other three Trp mutants displayed this property, indicating that the decrease in Trp emission is a specific property of this mutant and not a non-specific effect of the experimental conditions, e.g. light-scattering by lipid (data not shown).

The mutant C1bβ-Y123W was next tested in stopped-flow fluorescence spectroscopy (Figure 5B). Indeed, initial experiments with vesicles containing 5 mol% PMA and 40 mol% PS confirmed that this domain could be used to study the time-dependent association of C1bβ-Y123W with lipid vesicles. Traces for the

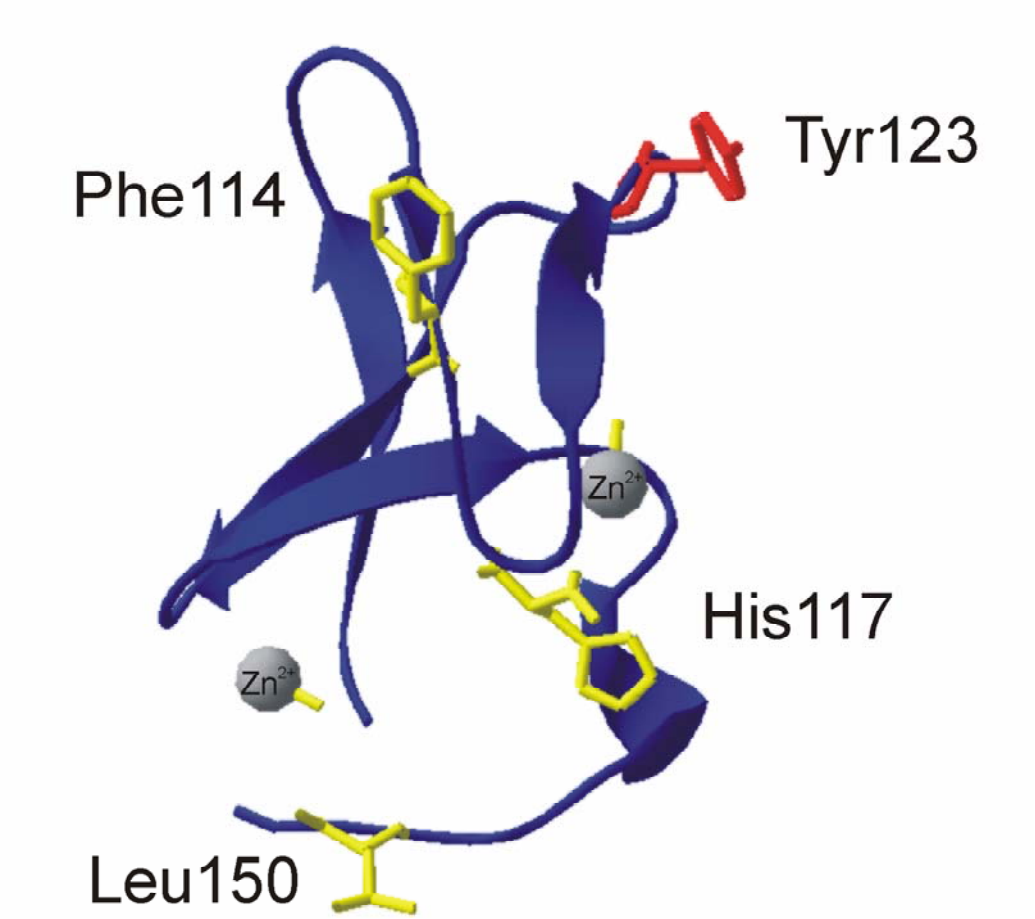


Figure 4. Sites of tryptophan mutations in the design of a fluorescent probe for the C1 domain. The ribbon diagram of the C1 domain is shown, with the mutated residues in stick representation. The environmentally-sensitive Tyr123Trp mutation is highlighted in *red*, the remainder are colored in *yellow*. The two Zn^{2+} ions required for proper folding are shown in *grey*.

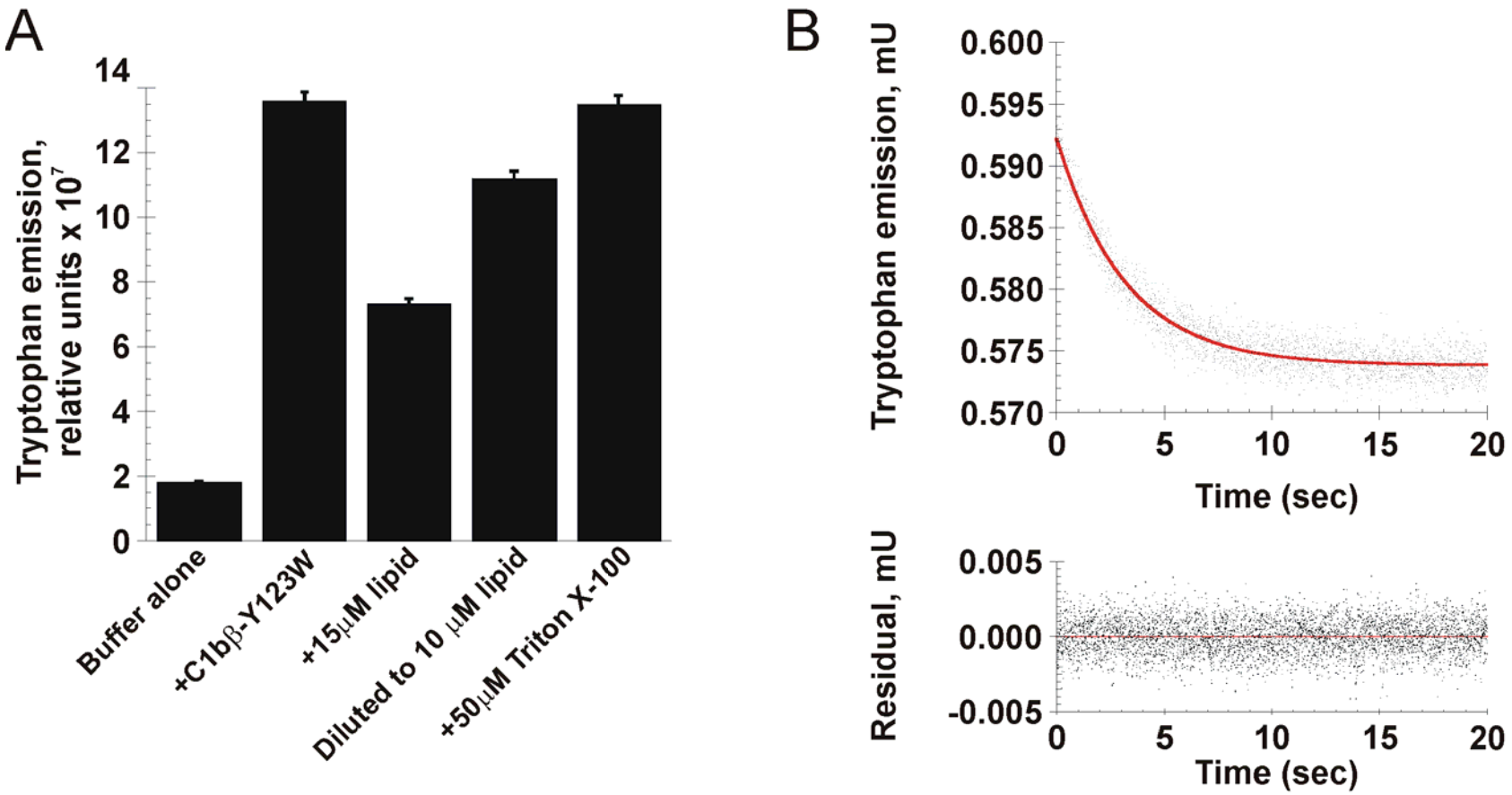


Figure 5. C1bβ-Y123W can be used as a fluorescenct probe for binding to lipid vesicles. *A*. 0.2 μM C1bβ-Y123W was added to a Chelex-treated buffer containing 150 mM NaCl, 200 μM $CaCl_2$, 1 mM DTT, and 20 mM HEPES, pH 7.4, and tryptophan fluorescence was monitored by emission at 320 nm. The indicated solutions were added successively, and fluorescence was read after an incubation time of at least 2 minutes between additions to allow equilibrium to be reached. Vesicles were composed of 5 mol% PMA and 30 mol% PS. *B*, sample kinetic curve for the association of C1bβ-Y123W with lipid vesicles containing 5 mol% PMA and 40 mol% PS. Fluorescence > 320 nm was monitored through a 320 nm high-pass filter. The data is fitted to a monoexponential decay curve describing the quenching of tryptophan fluorescence in this binding reaction. Residuals are plotted below the kinetic trace.

association of the domain with lipid were fit to a monoexponential fit, with residuals indicating simple, monophasic kinetics (Figure 5B, *bottom*). Control experiments in which protein or lipid alone was rapidly mixed with buffer showed no change in fluorescence up to 40 seconds (data not shown). Finally, initial experiments with the mutants C1bβ-F114W, -H117W, and -L150W did not show any time-dependent change in Trp emission (data not shown), further justifying the use of the Y123W mutant for kinetic studies.

Next, the mutation of Tyr123 to Trp was tested for differences in the ability to bind PMA relative to wild-type C1bβ. Figure 6 shows that the wild-type and mutant domains bind to lipid vesicles containing 5 mol% PMA with similar affinity (apparent K_d = 5.3 ± 0.5 and 11.5 ± 0.5, respectively). Moreover, the domains bound identically under moderate-affinity (1 mol% PMA) conditions (apparent K_d = 35 ± 3 and 35 ± 2, respectively). Thus, C1bβ-Y123W can be used a suitable surrogate for wild-type domain in the context of PMA-containing vesicles.

Binding of C1bβ-Y123W to Vesicles Containing Increasing Mole Percent Phosphatidylserine

Previous studies showed that the determinants for the stereospecific interaction of PKC with phosphatidylserine (PS) reside within the C1 domain (24,47,48). Therefore, the kinetics of the interaction of C1bβ-Y123W with lipid vesicles of increasing PS content was analyzed (Figure 7 and Table 1, *left*). Sucrose-loaded vesicle (SLV) equilibrium assays showed that the presence of 10 mol% PS increases

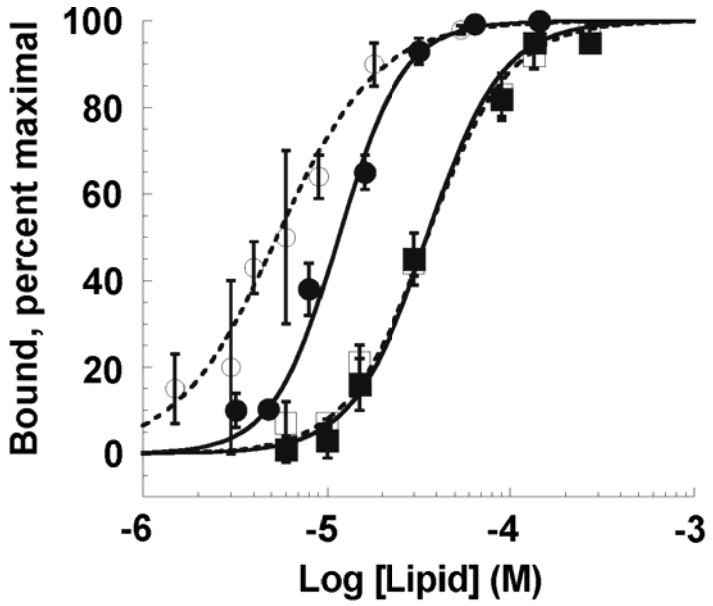


Figure 6. The mutant C1bβ-Y123W binds with similar affinity as wild-type domain to PMA-containing lipid vesicles. Binding of wild-type (C1bβ-WT, ■ and ●) and mutant (C1bβ -Y123W, □ and ○) to lipid vesicles containing 30 mol% PS and either 1 (*squares*) or 5 (*circles*) mol% PMA. Each data point represents the mean of triplicate experiments ± *S.E.*

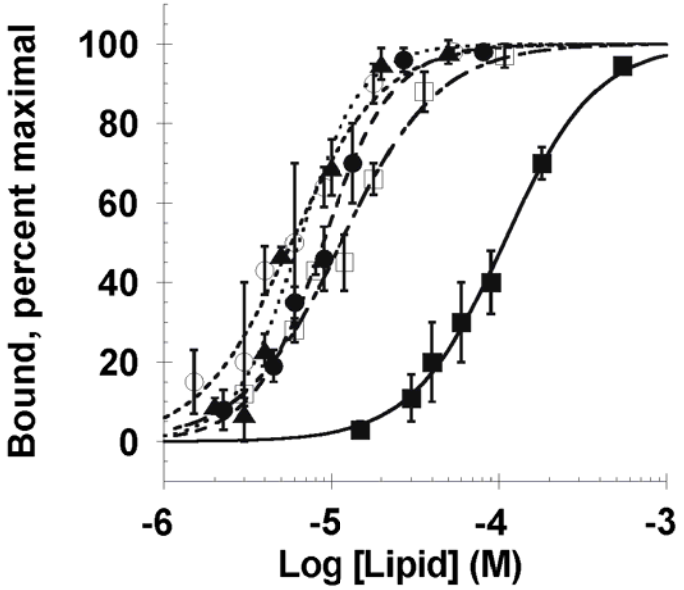


Figure 7. PS increases the affinity of C1bβ-Y123W for PMA-containing lipid vesicles tenfold. Binding of C1bβ-Y123W to lipid vesicles containing 5 mol% PMA and increasing mol% PS as follows (remainder PC): 0 (■), 10 (□), 20 (●), 30 (○), and 40 (▲). Each data point represents the mean of triplicate experiments ± *S.E.*

the affinity of C1bβ-Y123W for lipid vesicles 10-fold over vesicles without PS (apparent K_d = 9.8 ± 0.3 for 10% PS versus 107 ± 8 μM for 0% PS). Interestingly, while going from 0 to 10% increased affinity 10-fold, further increase in mol% PS only increased affinity 1.8-fold at most (apparent K_d = 9.8 ± 0.3 μM for 10% PS and 5.3 ± 0.5 for 30% PS). Finally, Hill coefficients were quite similar throughout, with a value of 1.7 ± 0.1 for 0% PS and ranging from 1.6 to 2.3 for 10-40% PS (Table 1).

We next analyzed the kinetics of the interaction of C1bβ-Y123W with membranes containing increasing mol% PS by stopped-flow fluorescence spectroscopy (Table 1). Association rate constants (k_{on}) increased with increasing mol% PS and varied 30-fold from 0.05 ± 0.02 x 10^9 $M^{-1}s^{-1}$ for 0% PS to 1.62 ± 0.09 x 10^9 $M^{-1}s^{-1}$ for 30 mol% PS. Dissociation rates (k_{off}) decreased with mol% PS, but only varied three-fold at most, with the lowest being 0.04 s^{-1} for 20% PS and the highest being 0.13 ± 0.02 s^{-1} for 0% PS (Table 1). Thus, the association of C1bβ-Y123W with PS-containing vesicles is guided by electrostatic interactions with PS.

Interestingly, the K_d values calculated as the ratio of k_{on}/k_{off} deviated from those seen in the SLV assay at low mol% PS but approached apparent SLV-determined K_d values at high mol% PS (Table 1). One possible explanation for this is that at low mol% PS another microscopic rate constant has been left out from the simple binding mechanism:

$$\text{C1b}\beta + \text{Lipid} \leftrightarrow \text{C1b}\beta\bullet\text{Lipid}$$

Since the observed kinetic traces in association experiments showed reasonable fit to a monoexponential decay, dissociation rate constants were re-analyzed. The

Table 1. Apparent equilibrium and kinetic parameters for the association of C1bβ-Y123W with lipid vesicles of increasing mol% PS. Vesicles were composed of 5 mol% PMA and the indicated mol% PS, with the remainder composed of PC. Apparent K_d^{SLV} and Hill coefficients were taken from the weighted, least-squares fit of the data in Figure 7. k_{on} and k_{off} were taken as the slope and y-intercepts, respectively, of the weighted, least-squares fit of plots of k_{obs} *versus* vesicle concentration in association experiments. k_{on} values are in terms of $(M \text{ vesicles})^{-1}s^{-1}$. K_d^{calc} was calculated as the ratio of k_{off}/k_{on} and converted to μM lipid, assuming 90,000 lipids per vesicle. Also shown is the residence time, τ, which describes the half-life for the dissociation of C1bβ-Y123W from lipid vesicles. Values are presented as the average of at least three

mol% PS	Apparent K_d^{SLV} (μM lipid)	Hill coeff	k_{on} x 10^9 ($M^{-1}s^{-1}$)	k_{off} (s^{-1})	τ (s)	K_d^{calc} (μM lipid)
0	107 ± 8	1.7 ± 0.1	0.05 ± 0.02	0.13 ± 0.02	5.3 ± 0.8	200 ± 100
10	9.8 ± 0.3	1.62 ± 0.08	0.22 ± 0.03	0.11 ± 0.01	6.3 ± 0.6	45 ± 7
20	8.4 ± 0.5	2.1 ± 0.2	0.22 ± 0.03	0.04 ± 0.02	17 ± 9	16 ± 8
30	5.3 ± 0.5	1.6 ± 0.2	1.05 ± 0.06	0.090 ± 0.003	7.7 ± 0.3	7.7 ± 0.5
40	6.3 ± 0.5	2.3 ± 0.4	1.62 ± 0.09	0.063 ± 0.004	11.0 ± 0.7	3.5 ± 0.3

dissociation rate constants in Table 1 were taken from the *y*-intercepts of the linear plots of k_{obs} *versus* lipid concentration from association experiments. To confirm these data, the dissociation of C1bβ-Y123W from lipid vesicles was directly measured by two different methods: competition and dilution. The binding of C1bβ-Y123W to lipid vesicles was allowed to reach equilibrium, after which C1bβ-Y123W was competed off of lipid with a molar excess of the non-fluorescent wild-type C1bβ domain or diluted 10-fold in buffer. Kinetic traces for both types of dissociation experiments at 5 mol% PMA and 0 mol% PS displayed monophasic kinetics with rates similar to each other (Figure 8). Dissociation rates (k_{off}) for 5 mol% PMA and 0 mol% PS were 0.095 ± 0.007 s^{-1} for the competition experiment and 0.128 ± 0.003 s^{-1} for the dilution experiment (Table 2). Moreover, these rates, particularly that of the dilution experiment, are similar to those obtained from association experiments (k_{off} = 0.13 ± 0.02 s^{-1}). Finally, dilution experiments at 40 mol% PS (5 mol% PMA) also produced a dissociation rate constant similar to that derived from association data (k_{off} = 0.063 ± 0.004 and 0.07 ± 0.02 s^{-1}, respectively, Table 2). Thus, kinetic experiments do not provide evidence for a more complicated mechanism than the simple binding equation above.

Sensitivity to Ionic Strength of the Interaction of C1bβ-Y123W with Lipid Vesicles

Since the association of C1bβ-Y123W with lipid vesicles showed a strong dependence on mol% PS, the sensitivity of this interaction to ionic strength was tested. The interaction of C1bβ-Y123W with vesicles containing 5 mol% PMA and 20 mol%

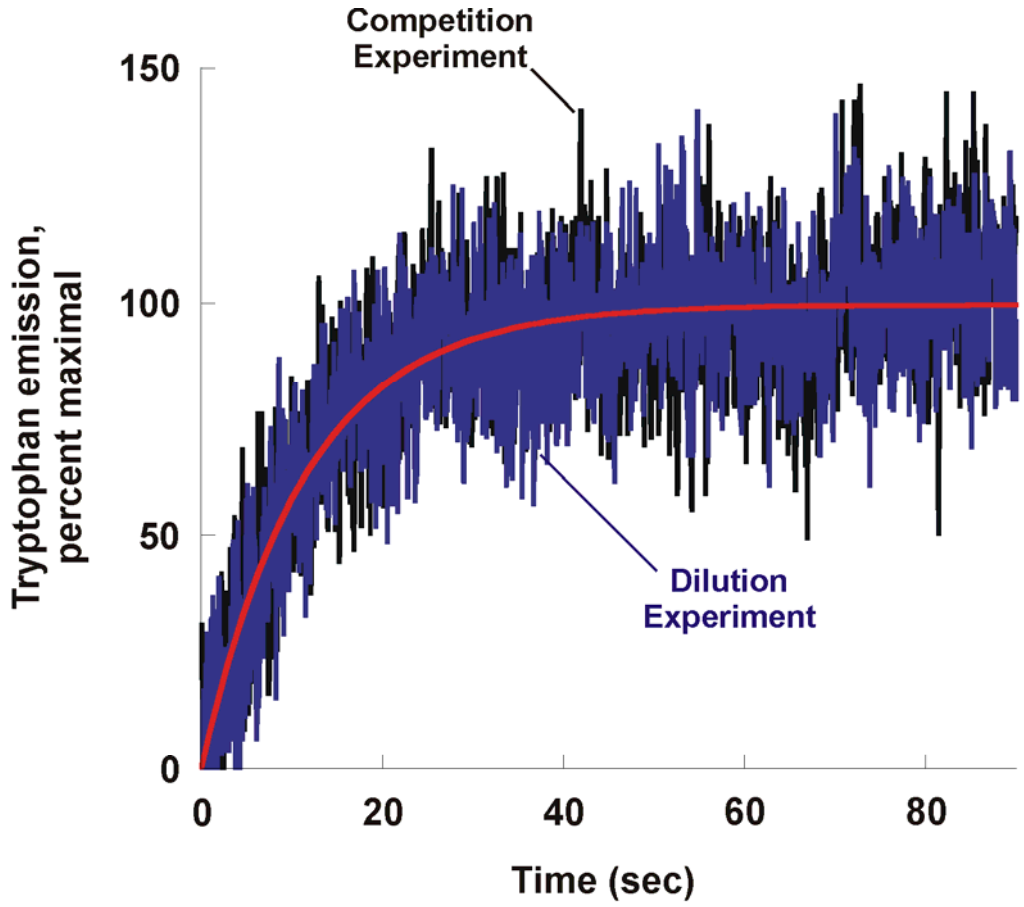


Figure 8. Dissociation experiments using competition and dilution yield similar rate constants. Dissociation rates of the C1bβ-Y123W•Lipid complex were determined by tenfold dilution with buffer (*blue*) or by competition of C1bβ-Y123W with the non-fluorescent C1bβ-WT protein (*black*) in 100-fold molar excess. Shown in *red* is a monoexponential fit for the dilution experiment. The lipid vesicles in the protein•lipid complex for both experiments contained 5 mol% PMA and 95 mol% PC.

Table 2. Comparison of values of k_{off} from association and dissociation experiments. Data are from association and dissociation experiments as described in "Materials and Methods." Values are presented as the average of three experiments ± *S.E.* *N.D.*, not determined.

		Dissociation	
Lipid composition	Association	Competition	Dilution
5%PMA:95%PC	0.13 ± 0.2	0.095 ± 0.007	0.128 ± 0.003
5%PMA:40%PS:55%PC	0.063 ± 0.004	*N.D.*	0.07 ± 0.02

PS was insensitive to KCl concentrations between 150 and 300 mM (Figure 9, *left*). One possible interpretation of these data is that the affinity is extremely high so as to be insensitive to salt; therefore, the same interaction was tested under low affinity conditions (0.1 mol% PMA). Despite the 20-fold lower affinity of C1bβ-Y123W for 0.1 mol% PMA/20 mol% PS vesicles (Table 3), this interaction, too, remained insensitive to ionic strength (Figure 9, *right*). Moreover, initial kinetic experiments showed no effect of ionic strength on the association or dissociation rates of C1bβ-Y123W with lipid vesicles (data not shown).

It is possible that lower salt concentrations would reveal sensitivity of this interaction to ionic strength. In fact, initial kinetic experiments revealed 50-fold higher rates of association when the ionic strength was dropped to 50 mM from 150 mM (data not shown). However, this effect was suspected to be due to aggregation, as gel filtration experiments revealed that C1bβ-Y123W tended to form high-molecular weight aggregates at 50 mM NaCl (data not shown). Thus, experiments were limited to ionic strength above 150 mM salt.

Interaction of C1bβ-Y123W with Phosphatidylserine (PS) and Phosphatidylglycerol (PG)

The interaction of the C1 domain with anionic phospholipid has been shown to be specific for PS over PG (20). The mechanism of the C1 domain's interaction with PS, however, has not been established. Therefore, stopped-flow fluorescence spectroscopy was used to characterize this specific interaction. First, equilibrium experiments were performed in which C1bβ-Y123W was mixed with lipid vesicles

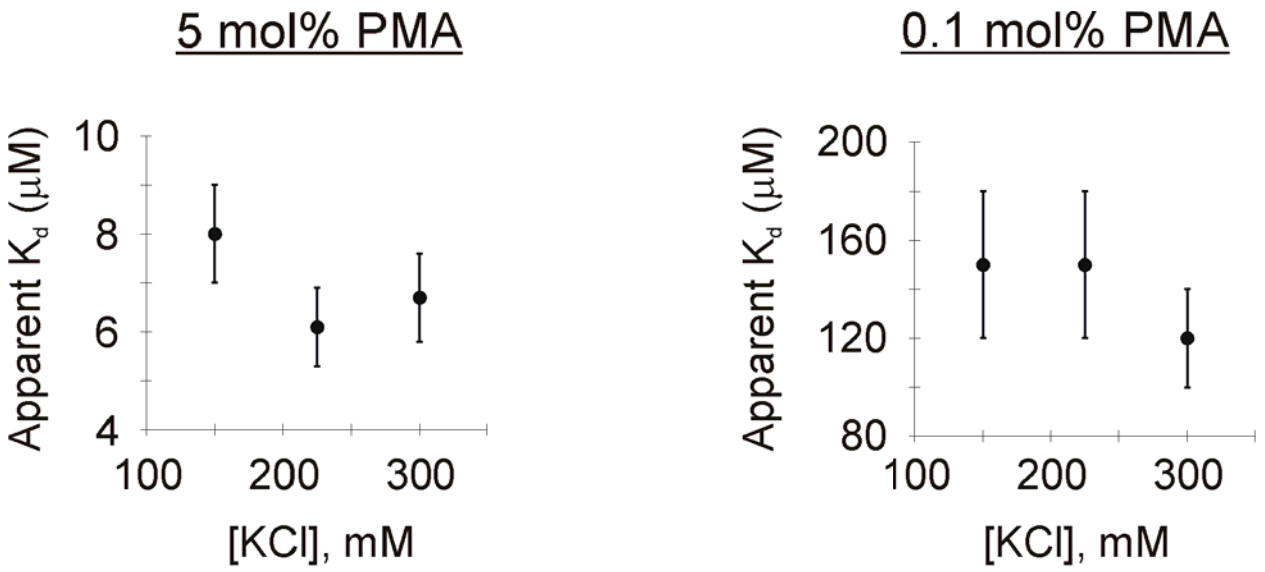


Figure 9. The association of C1bβ-Y123W with lipid vesicles containing 5 (*left*) or 0.1 (*right*) mol% PMA and 20 mol% PS is not sensitive to ionic strength above 150 mM KCl. The percent C1bβ-Y123W bound was determined by the sucrose-loaded vesicle assay at a fixed lipid concentration corresponding to ~50% bound, i.e., 10 μM and 150 μM for 5% and 0.1% PMA, respectively. Apparent K_d values were determined by using the Hill coefficient (n) for 150 mM KCl for each case (i.e., 2.1 and 1.3, respectively, see Table III) according to the equation: fraction bound = $[L]^n/([L]^n + K_d^n)$. Each data point represents the mean of triplicate experiments ± *S.E.*

Table 3. Binding of C1bβ-Y123W to lipid vesicles composed of 20 mol% PS and 5 *versus* 0.1 mol% PMA. Data are taken from the weighted, least-squares fit of data in Figure 11. Values are presented as the average of three experiments ± *S.E.*

		Apparent K_d (μM)		Hill coeff, *n*		PS
% PS	Ligand	PS	PG	PS	PG	Selectivity
20	0.1% PMA	150 ± 9	276 ± 8	1.3 ± 0.1	1.7 ± 0.2	1.8 ± 0.1
20	5% PMA	8.4 ± 0.5	9.3 ± 0.7	2.1 ± 0.2	1.5 ± 0.2	1.1 ± 0.1

containing 5 mol% PMA or DG and 30 mol% PS or PG (Figure 10). C1bβ-Y123W displayed no selectivity for PS over PG when the ligand was PMA (apparent K_d =5.3 ± 0.5 and 6.0 ± 0.9 μM, respectively, Figure 10 and Table 4). On the other hand, C1bβ-Y123W preferentially bound PS with 5.4-fold higher affinity than PG when the ligand was DG (apparent K_d = 24 ± 1 and 130 ± 10 μM, respectively, Figure 10 and Table 4). The non-selectivity for PS over PG in the context of PMA may be due to the high affinity of such conditions. Therefore, the binding of C1bβ-Y123W to vesicles containing 20 mol% PS or PG under conditions of high (5 mol% PMA) or low (0.1 mol% PMA) affinity was tested (Figure 11). Under both high and low affinity, C1bβ-Y123W displayed no selectivity for PS over PG (selectivities of 1.1 ± 0.1 and 1.8 ± 0.1 under high and low affinity, respectively). Thus, C1bβ-Y123W is selective for PS only when the ligand is DG.

Kinetic studies began with 5 mol% PMA and 30 mol% PS or PG. As in Figure 3A, kinetic traces showed monoexponential decay fits (Figure 12). C1bβ-Y123W showed nearly a twofold reduction in the rate of association with PG vesicles over PS vesicles (k_{on} = 0.67 ± 0.07 x 10^9 *versus* 1.05 ± 0.06 x 10^9 $M^{-1}s^{-1}$, respectively), yet the same domain dissociated from these vesicles at nearly the same rate (k_{off} = 0.111 ± 0.005 and 0.090 ± 0.003 s^{-1}, respectively, Table 5). The C1 domain's association with membranes has been proposed to involve long-range, *non-specific* electrostatic interactions. The data here, however, reveal that although a substantial portion of the association of the C1 domain with lipid membranes is due to non-specific interactions with anionic lipids, specific interactions with PS induce a further twofold increase in

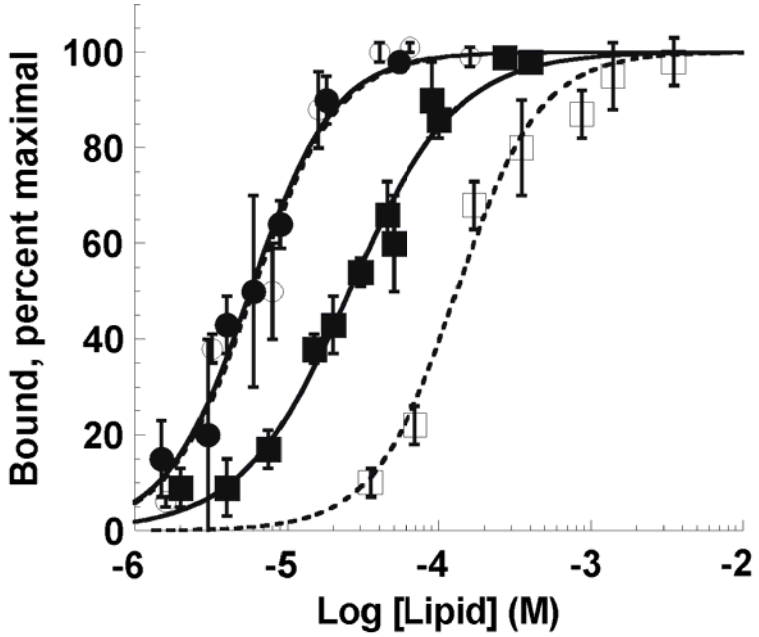


Figure 10. C1bβ-Y123W has selectivity for PS over PG only in the context of DG-containing membranes. Binding of C1bβ-Y123W to lipid PS- (*filled symbols*) or PG-containing (*open symbols*) vesicles containing 5 mol% PMA (● and ○) or 5 mol% DG (■ and □). Each data point represents the mean of triplicate experiments ± *S.E.*

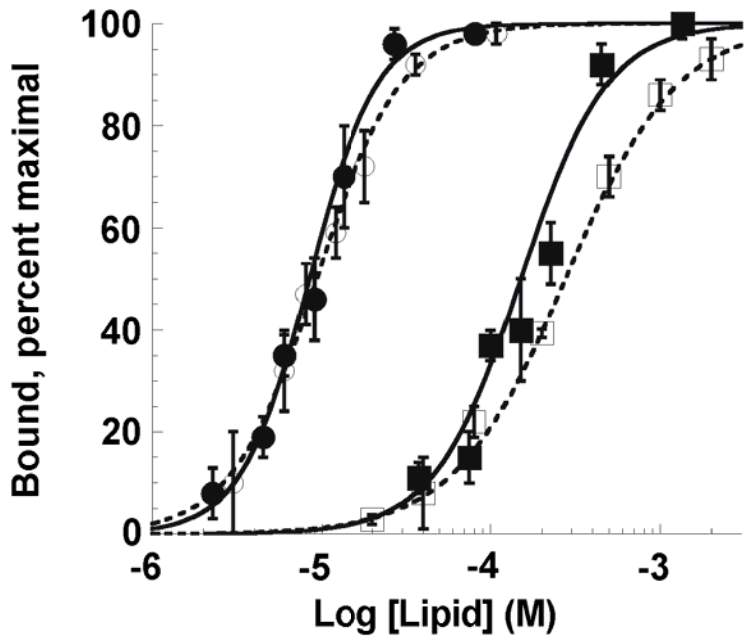


Figure 11. C1bβ-Y123W does not show selectivity for PS over PG in the context of PMA-containing membranes even under low-affinity conditions. Binding of C1bβ-Y123W to lipid vesicles containing 20 mol% PS (*filled symbols*) or PG (*open symbols*) and 0.1 (■ and □) or 5 mol% PMA (● and ○). Each data point represents the mean of triplicate experiments ± *S.E.*

Table 4. C1bβ-Y123W has selectivity for PS over PG only in the context of DG-containing membranes. Data are taken from Figure 10. Lipid vesicles were composed of 30 mol% PS or PG and either 5 mol% PMA or DG. PS selectivity was calculated as the ratio of the apparent K_d values for PG and PS. Values are presented as the average of at least three experiments ± *S.E.*

	Apparent K_d (μM lipid)		Hill coeff , n		PS
Ligand	PS	PG	PS	PG	Selectivity
5% PMA	5.3 ± 0.5	6.0 ± 0.9	1.5 ± 0.3	1.6 ± 0.2	1.1 ± 0.2
5% DG	24 ± 1	130 ± 10	1.7 ± 0.2	1.2 ± 0.1	5.4 ± 0.5

Table 5. Apparent equilibrium and kinetic parameters for the association of C1bβ-Y123W with lipid vesicles of 5 mol% PMA and 30 mol% PS or PG. Vesicles were composed of 5 mol% PMA and 30 mol% of the indicated anionic phospholipid, with the remainder composed of PC. Tabulated results are as in Table 1. Equilibrium data were taken from the weighted, least-squares fit of the data in Figure 10. Values are presented as the average of at least three experiments ± *S.E.*

Anionic phospholipid	Apparent K_d^{SLV} (μM lipid)	Hill coeff	k_{on} x 10^9 ($M^{-1}s^{-1}$)	k_{off} (s^{-1})	τ (s)	K_d^{calc} (μM lipid)
PS	5.3 ± 0.5	1.6 ± 0.2	1.05 ± 0.06	0.090 ± 0.003	7.7 ± 0.3	7.7 ± 0.5
PG	6.0 ± 0.9	1.5 ± 0.3	0.67 ± 0.07	0.111 ± 0.005	6.2 ± 0.3	15 ± 2

the association rate. Thus, the C1 domain specifically prefers to associate with PS membranes over PG membranes, despite the two phospholipids having the same net charge.

The resulting calculated K_d for PS vesicles was similar to that derived from SLV equilibrium experiments; the same was not true for PG vesicles, however, despite monoexponential fits to the data. Thus, similar to the experiments for increasing mol% PS (see above), kinetic K_d values do not match equilibrium K_d values very well. Also similar to the experiments with increasing mol% PS, the association with lipid vesicles shows monophasic behavior, suggesting a one-step association mechanism. While dissociation experiments were not performed for these conditions with PG, the above PS experiments indicate that dissociation rates obtained by extraction from k_{obs} *versus* lipid concentration in association experiments are accurate. Moreover, dissociation experiments from PS-containing vesicles indicate that dissociation is also monophasic. Therefore, the experiments performed here cannot account for a more calculated behavior than a simple, one-step association and dissociation.

Next, the mechanism by which C1bβ-Y123W is selective for PS over PG in the context of DG-containing membranes was tested. However, C1bβ-Y123W gave no change in fluorescence over time when vesicles containing 5 mol% DG and 30 mol% PG as the anionic phospholipid were used (Figure 12, *lower right*). The date show the highest the signal-to-noise ratio for vesicles containing PMA and PS (Figure 12, *upper left*), but the signal-to-noise ratio decreased when the ligand was changed to either DG (*upper right*) or PG (*lower left*). This suggested that the tryptophan fluorescence was being quenched by both PMA and PS.

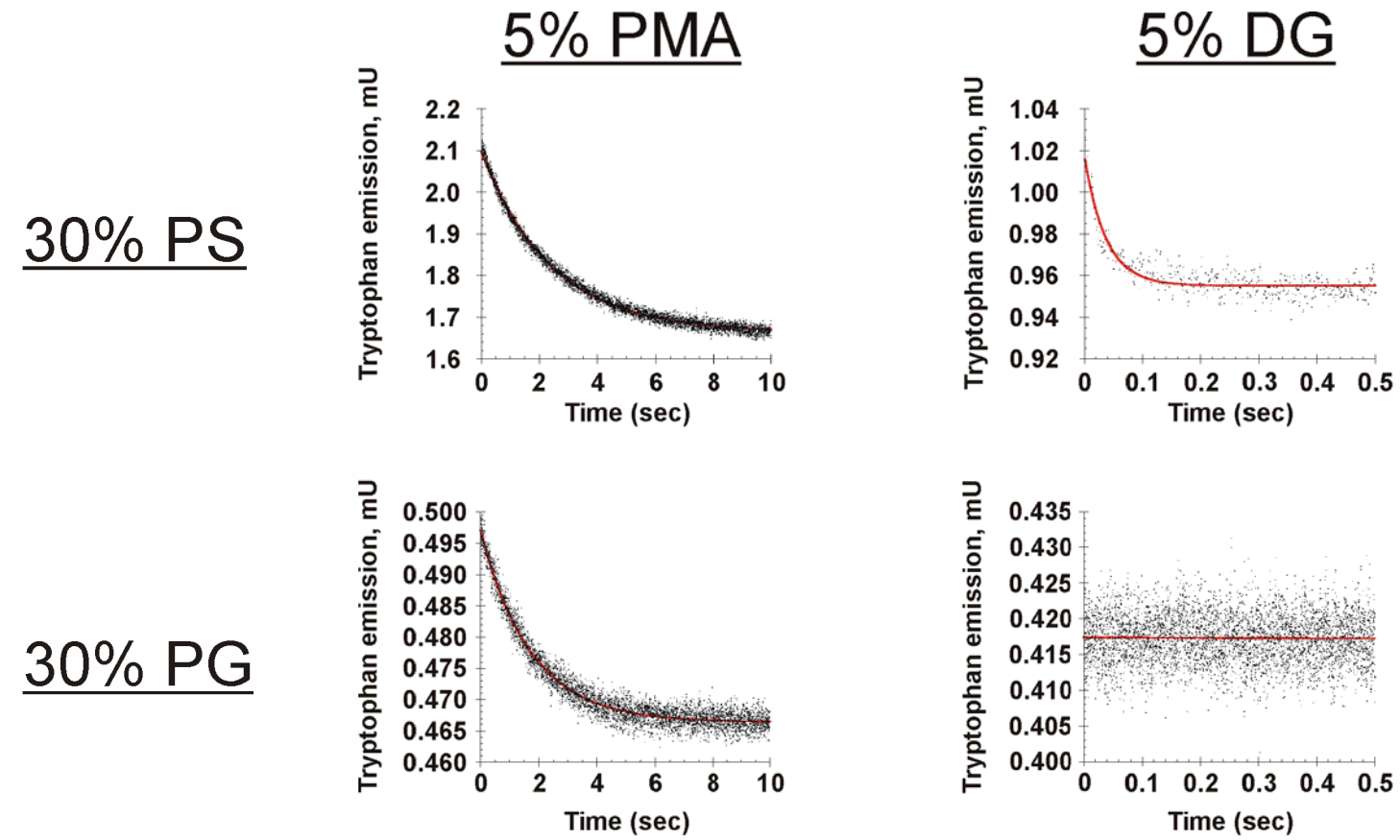


Figure 12. Sample traces for the association of C1bβ-Y123W with lipid vesicles containing 5 mol% PMA (*left panels*) or 5 mol% DG (*right panels*) and 30 mol% PS (*top panels*) or PG (*bottom panels*). Traces represent lipid concentrations at approximately 10 times the apparent K_d for each condition. Each trace is fitted to a monoexponential decay in tryptophan emission.

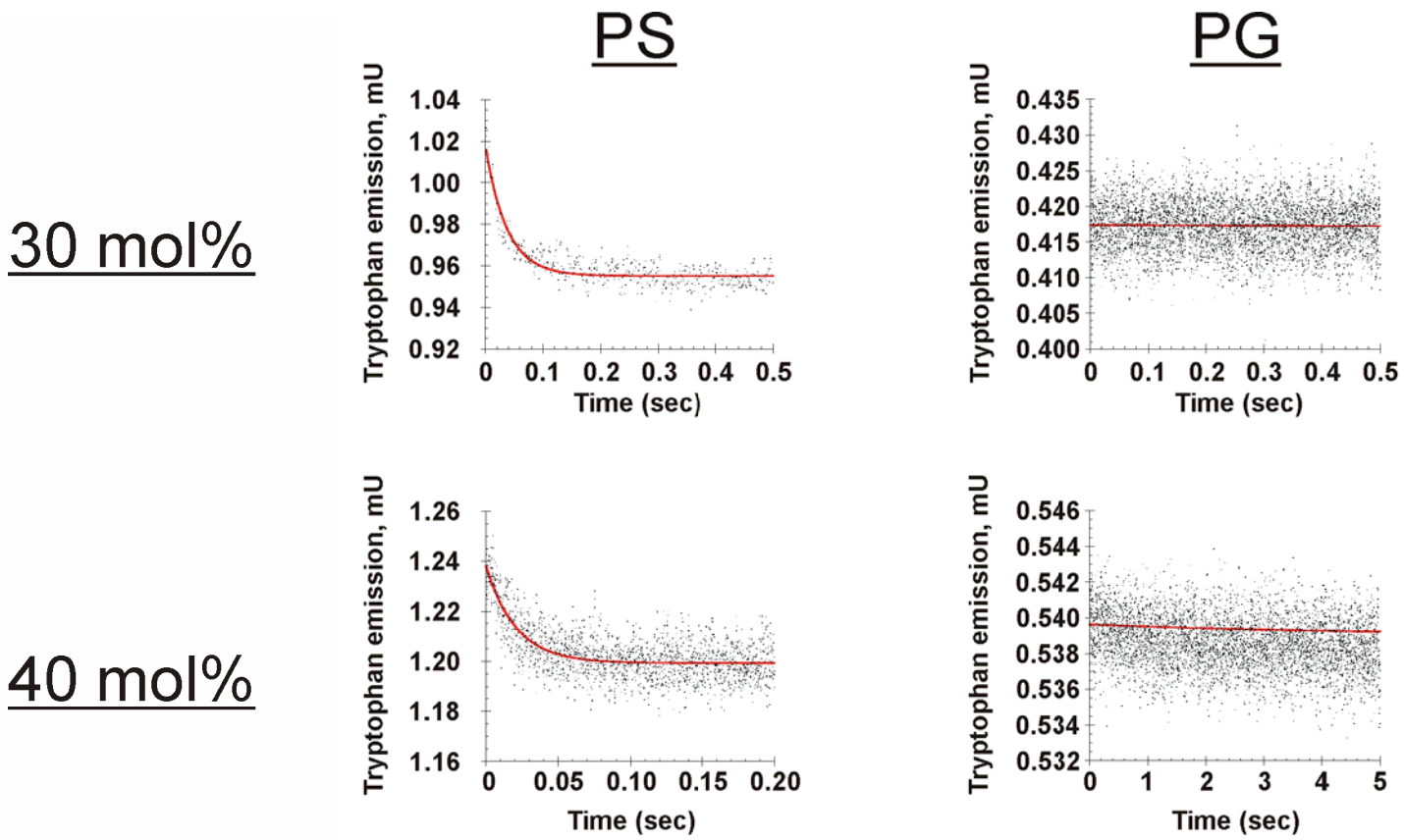


Figure 13. Sample traces for the association of C1bβ-Y123W with lipid vesicles containing 5 mol% DG and either 30 mol% (*top panels*) or 40 mol% (*bottom panels*) PS (*left panels*) or PG (*right panels*). Traces represent lipid concentrations at approximately 10 times the apparent K_d for each condition. Each trace is fitted to a monoexponential decay in tryptophan emission.

Another interpretation for these results could be that the interaction of C1bβ-Y123W with lipid vesicles was too weak to cause a fluorescence change in association experiments. Therefore, the association of C1bβ-Y123W with lipid vesicles of 5 mol% DG and 40 mol% PS or PG was tested (Figure 13), for which C1bβ-Y123W had higher affinity (data not shown). Similar to kinetic traces for 30 mol% PS (Figure 13, *top*), the interaction of C1bβ-Y123W with vesicles containing 5 mol% DG and 40 mol% PS showed a monoexponential decay, while that with 40 mol% PG showed no change in fluorescence (Figure 13, *bottom*). Thus, the fluorescence change from the interaction of C1bβ-Y123W with vesicles appeared to derive from two components: one dependent on its interaction with PS and a second on its interaction with DG. Unfortunately, this precludes the derivation of kinetic parameters describing the association of C1bβ-Y123W with PG vesicles in the context of DG.

Interaction of C1bβ-Y123W with Phorbol Ester *versus* Diacylglycerol

Figure 10 suggested that C1bβ-Y123W interacts differently with phorbol esters (i.e., PMA) and DG. Therefore, the mechanism by which C1bβ-Y123W binds to DG-containing membranes was characterized. First, the suitability of using C1bβ-Y123W as a surrogate for wild-type C1bβ was tested by equilibrium experiments in which these two proteins were allowed to bind to vesicles containing 5 mol% DG and 30 mol% PS. Figure 14 shows that C1bβ-Y123W binds to these vesicles with 32-fold higher affinity than wild-type C1bβ (apparent K_d = 780 ± 50 and 24 ± 1 μM for wild-type C1bβ and C1bβ-Y123W, respectively). However, C1bβ-Y123W is unusual

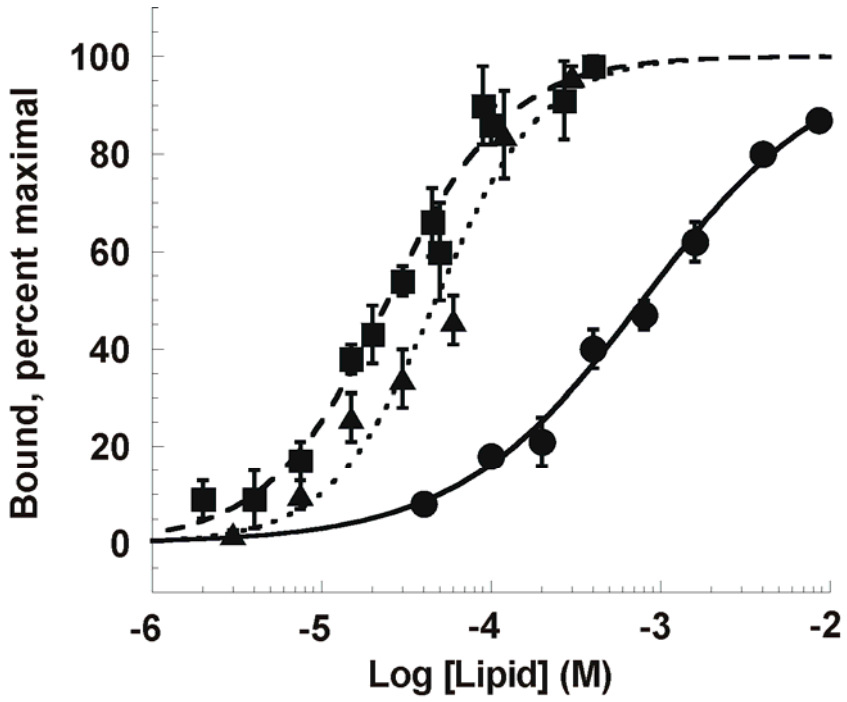


Figure 14. Binding of wild-type C1bβ, C1bβ-Y123W, and C1bδ to lipid vesicles containing 5 mol% DG and 30 mol% PS. C1bβ-Y123W (■) binds with 30-fold higher affinity to 5DG:30PS:65PC lipid vesicles than wild-type C1bβ (●), but with similar affinity to C1bδ (▲). Each data point represents the mean of triplicate experiments ± *S.E.*

across C1 domains, in that position 22 (123 in full-length PKCβI/II numbering) of C1bβ is typically Trp in nearly all PMA/DG-binding C1 domains (see Figure 20 in Chapter 3). In fact, Trp at this position allows C1 domains to respond to agonist-stimulated production of DG (Chapter 3 and (55)). Therefore, C1bβ-Y123W was compared to the C1b domain of PKCδ (C1bδ), which naturally has Trp at position 22 and better reflects most C1 domains (see Chapter 3). C1bβ-Y123W and C1bδ bound with similar affinity to vesicles composed of 5 mol% DG and 30 mol% PS (Figure 14). Thus, while C1bβ-Y123W is not an effective surrogate for wild-type C1bβ with respect to DG-containing vesicles, it can serve as an appropriate surrogate for C1bδ and those other C1 domains that bind with relatively high affinity to DG.

SLV equilibrium experiments revealed in two ways that the interaction of C1bβ-Y123W with vesicles containing PMA is five times tighter than that with DG (Figure 15). First, the interaction of C1bβ-Y123W with vesicles containing 30 mol% PS and 5 mol% PMA was five times higher than that with vesicles containing equimolar DG (apparent K_d = 5.3 ± 0.5 and 24 ± 1 μM, respectively). Second, C1bβ-Y123W bound with similar affinity to vesicles containing 30 mol% PS and either 5 mol% DG or 1 mol% (fivefold less) PMA (apparent K_d = 24 ± 1 and 35 ± 2 μM, respectively).

Next, stopped-flow fluorescence spectroscopy was used to extract kinetic parameters for the interaction of C1bβ-Y123W with membranes containing 40 mol% PS and either 5 mol% PMA or DG (Table 6). 40 mol% PS was used, as this condition yielded more reliable data with a higher signal-to-noise ratio and better amplitudes.

Equilibrium experiments showed tenfold higher binding of C1bβ-Y123W to PMA-containing vesicles than to DG-containing vesicles (Figure 16). C1bβ-Y123W bound to vesicles containing 5 mol% DG nearly four times faster than to vesicles containing 5 mol% PMA (k_{on} = 5.95 ± 0.03 x 10^9 *versus* 1.62 ± 0.09 x 10^9 $M^{-1}s^{-1}$, respectively). On the other hand, the faster association rate was outweighed by a dissociation rate over 200 times faster than from PMA-containing vesicles to give a net decrease in affinity for DG-containing vesicles (k_{off} = 14.20 ± 0.04 versus 0.063 ± 0.004 s^{-1} for DG and PMA, respectively). Thus, although C1bβ-Y123W bound to DG vesicles five times faster than to PMA vesicles, the domain remained at the membrane for only 0.05 seconds compared to 11 seconds when PMA was the ligand (Table 6). These results confirm an earlier hypothesis, in which studies with full-length PKCβII suggested a 200-fold reduction in k_{off} for PMA relative to DG (55,58). Again, the calculated apparent K_d was substantially higher than that derived from SLV equilibrium experiments, but monophasic behavior does not provide for a more complicated mechanism.

Conclusions

In this study, a mutant C1 domain, C1bβ-Y123W, was used to characterize the interaction of the C1 domain with lipid membranes. The data show that the association of the C1 domain with membranes is driven by long-range electrostatic interactions that are, in fact, specific for PS over PG. This binding is insensitive to ionic strength between 150 and 300 mM salt when the ligand is PMA; lower ionic

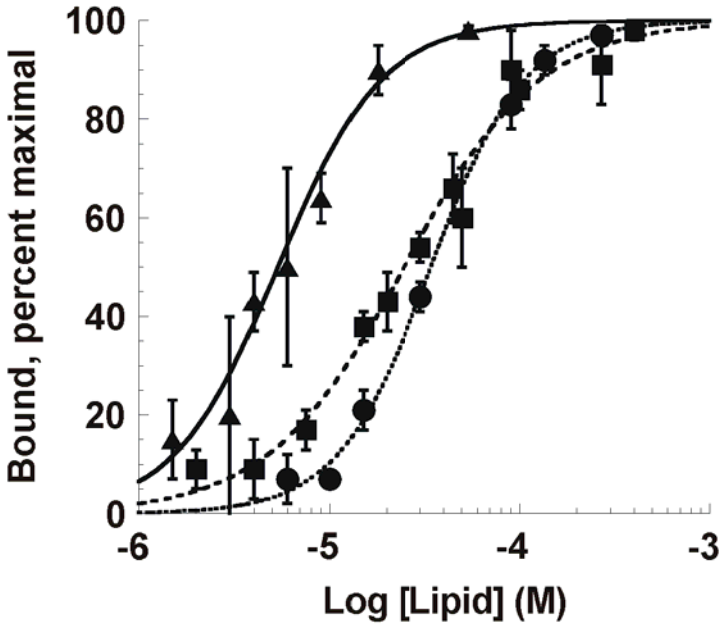


Figure 15. C1bβ-Y123W binds PMA-containing vesicles with five-fold higher affinity than DG-containing vesicles containing 30 mol% PS. Binding of C1bβ-Y123W to lipid vesicles containing 30% PS and 5% PMA (▲), 5% DG (■), or 1% PMA(●). Each data point represents the mean of triplicate experiments ± *S.E.*

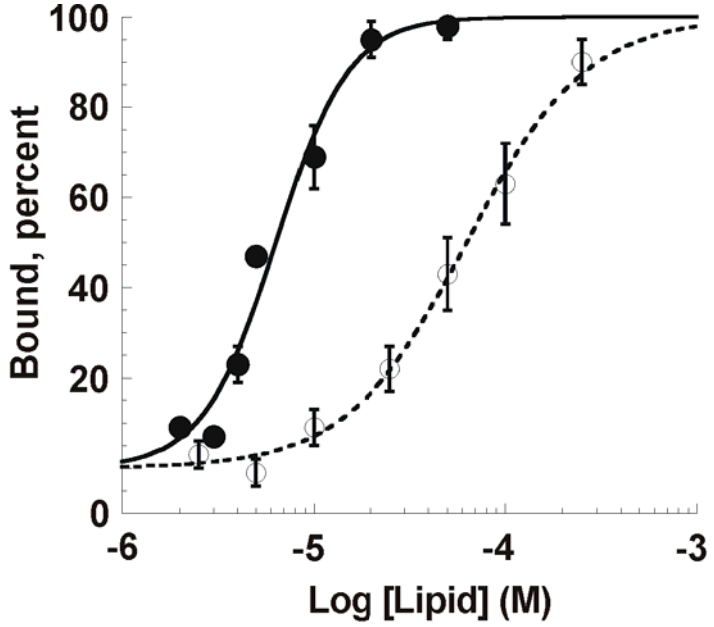


Figure 16. C1bβ-Y123W binds PMA-containing vesicles with ten-fold higher affinity than DG-containing vesicles containing 40 mol% PS. Binding of C1bβ-Y123W to lipid vesicles containing 40% PS and 5% PMA (●) or 5% DG (◯). Each data point represents the mean of triplicate experiments ± *S.E.*

Table 6. Apparent equilibrium and kinetic parameters for the association of C1bβ-Y123W with lipid vesicles of 40 mol% PS and either 5 mol% PMA or DG. Vesicles were composed of 40 mol% PS and 5 mol% of the indicated ligand, with the remainder composed of PC. Tabulated results are as in Table 1. Equilibrium data were taken from the weighted, least-squares fit of the data in Figure 16. Values are presented as the average of at least three experiments ± *S.E.*

Ligand	Apparent K_d^{SLV} (μM lipid)	Hill coeff	k_{on} x 10^9 ($M^{-1}s^{-1}$)	k_{off} (s^{-1})	τ (s)	K_d^{calc} (μM lipid)
PMA	6.3 ± 0.5	2.3 ± 0.4	1.62 ± 0.09	0.063 ± 0.004	11.0 ± 0.7	3.5 ± 0.3
DG	63 ± 3	1.4 ± 0.1	5.95 ± 0.03	14.20 ± 0.04	0.0488 ± 0.0001	215 ± 1

strength resulted in aggregation of the C1 domain. The interaction of C1bβ-Y123W with anionic membranes is specific for PS over PG, but only when DG is the ligand and not PMA. Experiments with PMA-containing membranes revealed that the association is specific for PS over PG, although the rates of dissociation are similar between the two. Finally, the data reveal that the affinity of C1bβ-Y123W for DG membranes is tenfold lower than for PMA membranes, primarily through a 200-fold increase in the rate of dissociation. The results support a model in which the interaction between C1bβ-Y123W and lipid membranes is mediated by a balance between electrostatic and hydrophobic interactions.

Many kinetic and equilibrium studies with wild-type and mutant domains have helped to tease apart the nature of the interaction of the C1 domain with lipid membranes (25,30,31,66). These studies have been an elegant way to dissect the mechanism of this binding interaction. However, these studies, which included surface plasmon resonance (SPR) and monolayer penetration, relied on a strictly two-dimensional plane of membrane or hydrophobic chip coated with lipid vesicles. Moreover, to date, no study has detailed the individual association and dissociation rates of an isolated C1 domain, although two studies do describe the kinetics of the interaction of full-length PKCα and δ with membranes (30,31).

Clearly, studies of the interaction of the full-length kinase with membranes describe the net effect of ligands and phospholipids on PKC activity. However, it is critical to dissect the individual components of the net effect in order to understand the nature of the PKC-membrane interaction and to design specific therapeutic compounds. Thus, the results here provide direct kinetic parameters for the interaction

of the isolated C1 domain with lipid vesicles. In many ways, these results agree with membrane penetration data and quantify the nature of such interactions. For example, membrane penetration data suggest that the C1 domain is first recruited to membranes by non-specific electrostatic interactions followed by membrane penetration via hydrophobic interactions (67). The data in this study support and quantify the parameters of this model. Indeed, many peripheral membrane-binding proteins follow this mechanism (25), and through the work presented here, this interaction can now be quantified.

Experiments with increasing mol% PS highlight the effect that anionic phospholipids have on the rate of association of the C1 domain with membranes. However, it cannot be ignored that there is also a slight (twofold) slowing of dissociation with an increase in PS content, suggesting that anionic lipids provide at least a minor role in controlling the rate of dissociation. Since electrostatic interactions are often long-range effects, perhaps the specificity of the domain for PS over PG resides in a slight increase in the retention at the membrane (for more, see below). Still, it is interesting to note the independence of this interaction to ionic strength. Occasionally, sensitivity to ionic strength is only seen at relatively low salt concentrations (68). However, at low salt, the C1 domain tends to aggregate, thereby confounding the results from kinetic data. Moreover, physiological salt concentrations are often between 150 and 300 mM, suggesting pharmacological irrelevance outside of this range.

There is much controversial evidence over the location of PS specificity in PKC. *In vitro* studies on isolated domains have concluded that the C1 domain confers

PS specificity, whereas non-specific interactions exist between anionic phospholipid and the C2 domain (24). Other studies, however, show no specificity for PS in the C1 domain, but instead show specificity in the C2 domain (67). The data presented here show no selectivity between PS and PG when the ligand is PMA, but selectivity when the ligand is DG. The kinetic parameters here show a twofold higher rate of association for PS membranes over PG even when the ligand is PMA. The dissociation from PS vesicles would have to be twofold higher in order to recapitulate equilibrium experiments, which show no selectivity with PMA. However, the data here show no difference in dissociation rates. Two complementary reasons may explain this phenomenon: 1) a kinetic parameter is missing in the model and/or 2) the dissociation is controlled primarily by PMA, such that any contribution from anionic lipids to the dissociation is negligible. These two explanations are further substantiated by the facts that 1) the calculated K_d values (k_{off}/k_{on}) do not match the apparent K_d values from equilibrium experiments and 2) PMA decreases the dissociation over 200-fold relative to DG (see below). Moreover, when PMA concentration is high relative to anionic lipid, ionic contributions to the interaction disappear, such that interactions with phorbol predominate (58).

As described above, the origin of PS specificity appears to reside in the presence of DG. Unfortunately, the fluorescent reporter used in this study did not show time-dependent changes with DG and PG, thereby precluding the drawing of conclusions between PS and PG in the context of DG-containing vesicles. However, one study using full-length PKCδ showed that PS, relative to PG, causes a threefold reduction in the dissociation and a twofold increase in association (31). (The latter

observation agrees with the data for PMA-containing vesicles – see above.) Since these studies were performed in the context of DG-containing bilayers, it is interesting to speculate that these parameters also reflect the kinetics of the individual DG-binding C1 domain.

The inability to detect fluorescence changes in C1bβ-Y123W with DG and PG is in itself an interesting topic. Several amino acids can quench tryptophan fluorescence, including cysteine, histidine, and the neutral amides of glutamine and asparagines. The backbone amides – even that of Trp itself, if in the right rotomer state – can participate in quenching (69). But the data here suggest that the quenching of Trp123 in this mutant is due to both PMA and PS. PMA contains several groups that may contribute to Trp quenching, including several hydroxyl groups, two alkene bonds, and a ketone functionality (Figure 17). The acyl moieties of the fatty acids most likely do not contribute to the quenching, as DG, which does not quench Trp emission (Figure 13, *right*), also contains these moieties (Figure 17). PS alone also quenches Trp emission, although to a lesser degree with lower amplitudes (Figure 12, *upper right*); PG, however, does not (Figure 13, *right*). Since the glycerol backbone (i.e., DG) does not quench Trp, this suggests that either the amine or carboxylic acid functionalities of PS can also quench Trp emission (Figure 18). Therefore, this study proposes that the interaction of the C1 domain with membranes places position 22 (i.e., Trp123 in C1bβ-Y123W) within 5-10Å of the phorbol and phospholipid headgroups. Such a model is consistent with a study that shows that the C1b domain of PKCβII does not penetrate the acyl chains of the lipid bilayer (58).

Finally, in this study, the differences between binding to PMA and DG vesicles

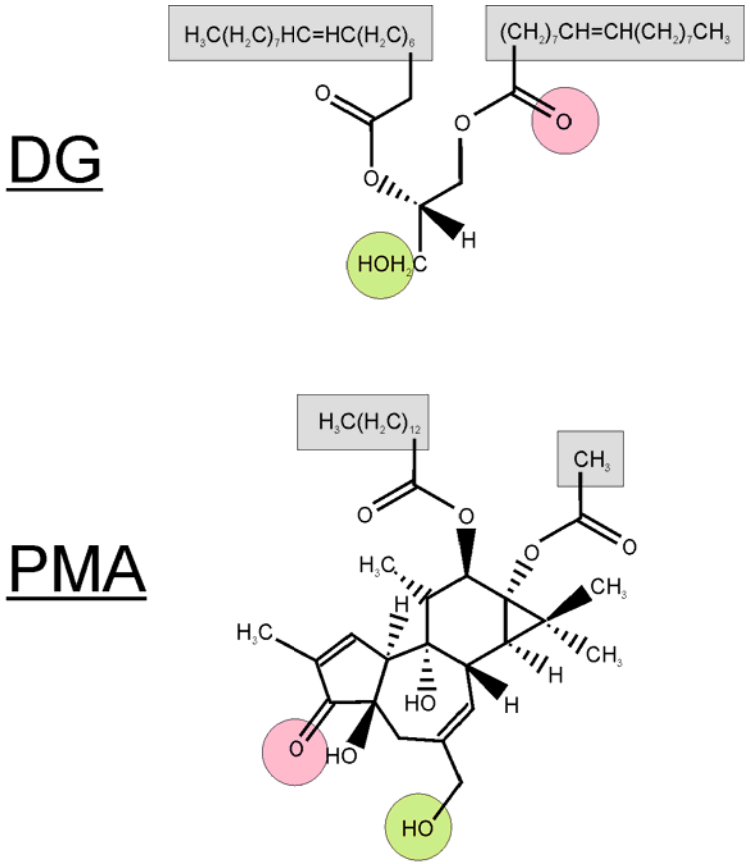


Figure 17. Chemical structures of dioleoylglycerol (DG, *top*) and phorbol-12-myristate-13-acetate (PMA, *bottom*). The proposed oxygens on PMA that mimic those of DG for binding to the C1 domain are colored similarly on the two structures. Acyl chains are boxed in *grey*.

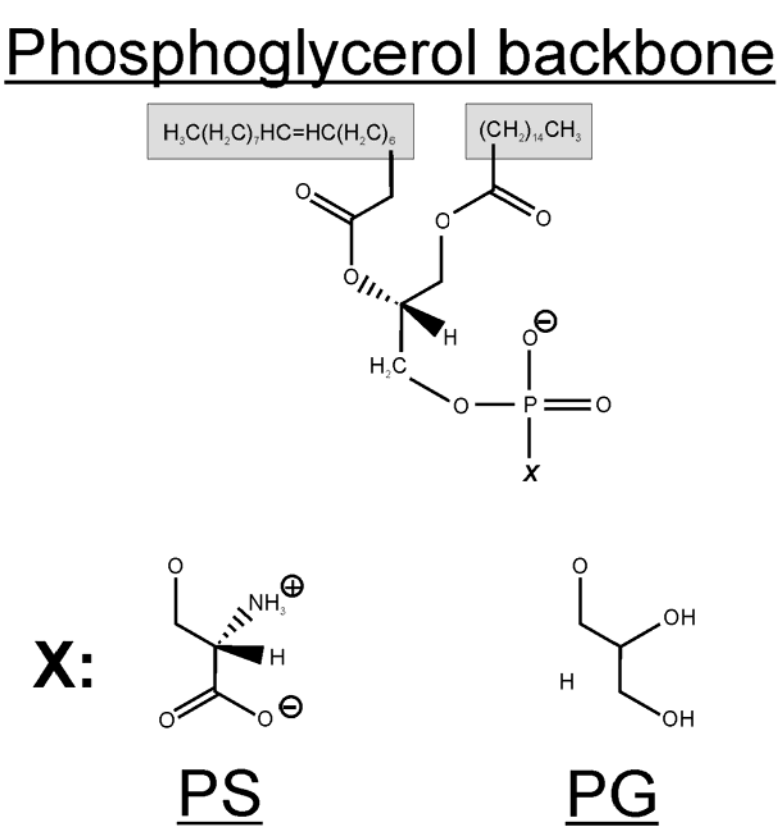


Figure 18. Chemical structures of the anionic phospholipids 1-palmitoyl-2-oleoyl-*sn*-glycero-3-[phospho-L-serine] (PS, *left*) and -[phospho-racemic-(1-glycerol)] (PG, *right*). The phosphoglycerol backbone is shown at *top*. "X" on the phosphate moiety is substituted with the lone oxygen at the top of the PS and PG structures.

were addressed. Similar to DG, PMA has a glycerol-like backbone with two acyl chains, but it also contains a polycyclic, highly hydrophobic phorbol headgroup (Figure 17). PMA is proposed to interact similarly with DG, and the phorbol oxygens that are analogous to DG have been identified (Figure 17, *like colors*). Yet PKC binds with two orders of magnitude higher affinity to PMA-containing vesicles than to DG-containing vesicles (58). A crystallographic study of the C1b domain of PKCδ with and without phorbol shows that phorbol does not significantly alter the overall structure of the domain. Rather, the ligand's main function is to provide a greasy cap to the C1 domain to promote its insertion into the lipid bilayer (34). Studies with full-length PKCδ revealed that DG increases the affinity of PKC for membranes by two orders of magnitude, doing so primarily via lowering the dissociation rate (25,31). However, whether this effect is a property of full-length PKC or whether the isolated domain also shows this behavior was unresolved. Indeed, the data here show that the individual domain has a net affinity tenfold higher for PMA- than DG-containing vesicles due to a 200-fold slower rate of dissociation. This corresponds to a difference of -3.2 kcal/mol in the dissociation rate, which, at a van der Waals interaction energy of 0.5 to 1.5 kcal/mol, could be explained as the energy of anywhere from two to six additional hydrophobic van der Waals interactions that do not exist in the interaction with DG. Indeed, the crystallographic data for C1bδ suggest that numerous hydrophobic interactions occur between C1bδ and the three-, five- and seven-membered rings and acetyl group of the phorbol (34).

While the 200-fold difference in dissociation rates between PMA and DG yielded useful thermodynamic information for the interaction of the C1 domain with

membranes, all other differences in the kinetics measured are small enough so as to yield energy differences less than or equal to 1 kcal/mol. Such calculations do not give much mechanistic information, as the low energy is most likely not due to hydrogen bonding (~1-5 kcal/mol) and is in the range of a single van der Waals interaction (~0.5-1.5 kcal/mol). It is interesting to propose that the *net* small difference in energy is the sum of a large energy gain due to electrostatic interactions and/or hydrogen bonding and a large entropy cost for the desolvation and ordering of the C1 domain sidechains and/or loops in the interaction with lipid. Indeed, several water molecules stabilize the unliganded C1 domain, and these water molecules are replaced with hydrophobic interactions in the ligand-bound structure (34). Such a balance between desolvation and charge-charge interactions has already been described as an "electrostatic switch for the interaction of the C2 domain with membranes (25,70).

As noted above, the kinetically- and equilibrium-derived K_d values differed from one another under nearly all conditions studied. Furthermore, cooperativity alone cannot reconcile the differences between these two K_d values, suggesting that the binding of the C1 domain to membranes is not a simple binding equilibrium with a single bimolecular association and single unimolecular dissociation step, i.e., $E + L \leftrightarrow E{\bullet}L$. Rather, the results here support a model in which the C1 domain binds to DG- or PMA-containing membranes via a two-step mechanism consisting of the formation of a weak encounter complex (*Step 1:* $E + L \leftrightarrow E{\bullet}L$) coupled to a transition equilibrium in which high-affinity, ligand-bound complex is formed (*Step 2:* $E{\bullet}L \leftrightarrow E{\bullet}L^*$, Figure 19). Such a model describes the binding equilibrium in terms of four rate constants:

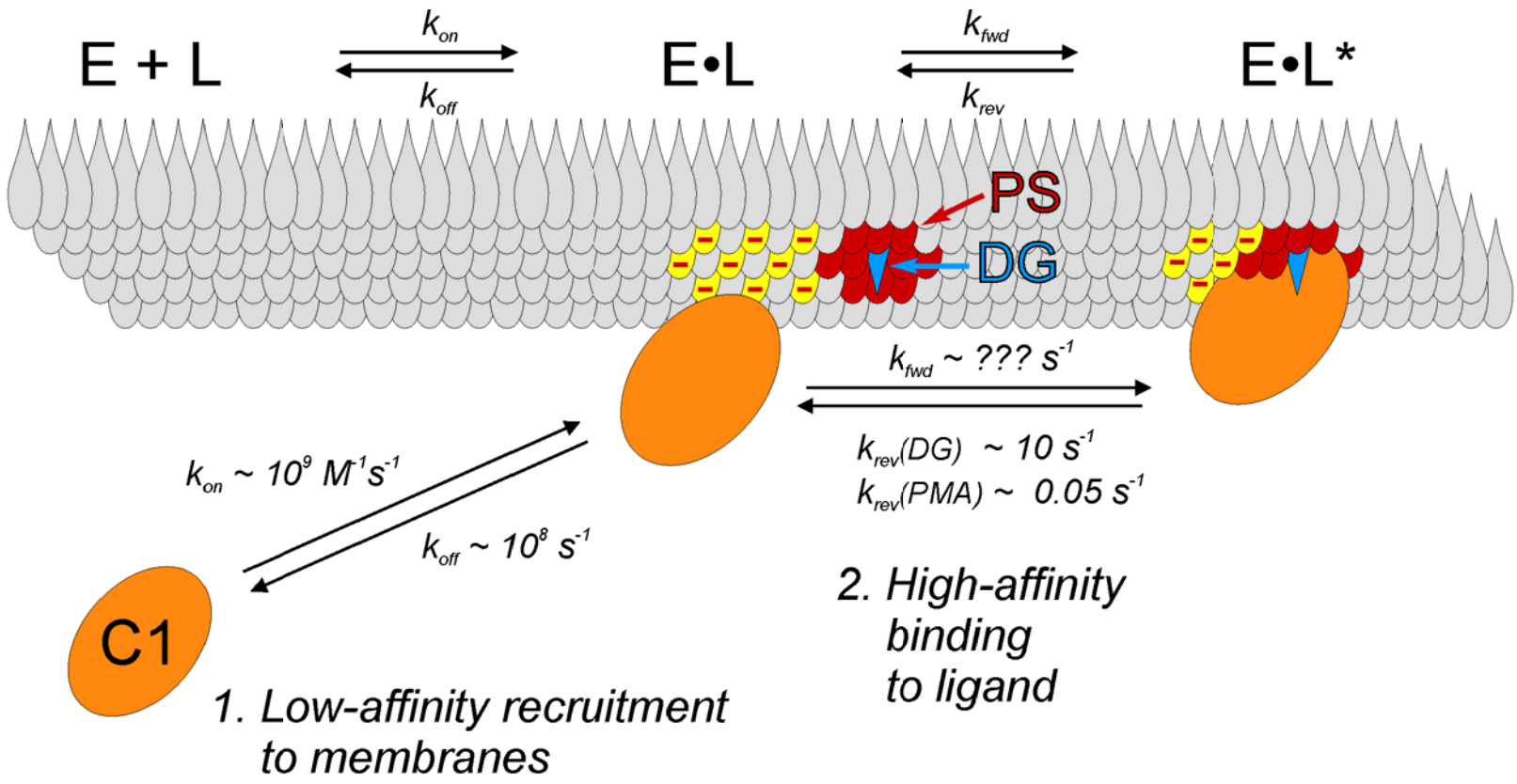


Figure 19. Model for the interaction of the C1 domain with lipid membranes. The interaction of the C1 domain with membranes occurs via two steps: the formation of an encounter complex followed by transition to a high-affinity species (*above*). (*1*) Long-range, specific electrostatic interactions with anionic lipids pre-target the C1 domain to the membrane through a diffusion-limited association and a rapid dissociation, resulting in a low affinity for membranes in the absence of ligand (i.e., DG or PMA). (*2*) High-affinity for ligand-containing membranes is achieved via coupling of this first weak equilibrium with a second, stronger interaction as the C1 domain searches along the lipid bilayer in two dimensions for specific interactions with its ligands PS and DG or PMA. The forward rate constant in step *2* (k_{fwd}) is infinitely high due to the reduction in dimensionality in searching for ligand. The net rate of dissociation depends primarily upon hydrophobic contacts with the ligand, with 200-fold higher retention at PMA-containing membranes than DG membranes (k_{rev}).

two that describe an initial low-affinity recruitment to membranes (k_{on} and k_{off}) and two that describe the equilibrium for the formation of a high-affinity transition complex (k_{fwd} and k_{rev}). Under such a scheme, the kinetically-derived association and dissociation rate constants from stopped-flow experiments are apparent (k_{on}^{app} and k_{off}^{app}) and contain components of both *Steps 1* and *2*. Nevertheless, the assumption can be made that once at the membrane, a reduction in dimensionality allows the C1 domain to very rapidly find its ligand, such that the rate of formation of the high-affinity complex (k_{fwd}) is very fast. This reduction in dimensionality has been shown to play an important role in the high-affinity binding of many membrane-binding domains as described in (25). Such an assumption implies that the initial recruitment is rate-limiting in the association of the C1 domain with membranes and simplifies the kinetics such that $k_{on}^{app} = k_{on} = 10^9\ M^{-1}s^{-1}$. This value for k_{on} is consistent with a diffusion-limited association driven by electrostatic interactions between the positive electrostatic potential of the C1 domain and the negatively-charged phospholipid bilayer.

Working on the above assumption, two other kinetic parameters can be assigned to the model depicted in Figure 19. First, it has been shown in this lab that in the absence of ligand (i.e. DG or PMA), the affinity of the C1 domain is approximately 100 mM (20,24). Consistent with this, data in Chapter 4 of this thesis shows that the C1 domain has an affinity of approximately 1 mM for 50 mol% PS membranes. In the absence of ligand, this K_d (equal to k_{off}/k_{on}) describes the recruitment equilibrium of *Step 1*. With K_d = 100 mM and $k_{on} = 10^9\ M^{-1}s^{-1}$, this yields a k_{off} value of $10^8\ s^{-1}$, consistent with a weak affinity in the absence of DG or PMA.

Second, the extremely high value of k_{off} implies that the initial release of the C1 domain from the ligand•PS cluster (k_{rev}) is rate-limiting in the dissociation of the C1 domain from membranes and simplifies the kinetics such that $k_{off}^{app} = k_{rev}$. Therefore, the measured apparent dissociation rates are direct measurements of k_{rev}, such that k_{rev} = 10 s^{-1} and 0.05 s^{-1} for DG and PMA, respectively.

The net effect of the above parameters is a mechanism as follows. First, specific electrostatic interactions guide the diffusion-limited association of the C1 domain towards an anionic patch on lipid membranes (*Step 1*). This weak recruitment to membranes facilitates the specific binding of the domain to DG or PMA by reducing the space in which the C1 must search for its ligand to two dimensions (25). As the C1 domain approaches the membrane, specific interactions with PS and ligand further guide the high-affinity association of the C1 domain with membranes (*Step 2*). *Step 2* is consistent with the observations that 1) DG is known to cluster PS into microdomains in the lipid bilayer (50) and 2) high-affinity binding to membranes requires interactions with both the PMA/DG ligand and anionic lipids (35). Finally, the time the C1 domain spends at the membrane is dictated by the extent of hydrophobic contacts with the ligand, with dissociation from DG-containing membranes occurring 200-fold faster than interactions with PMA-containing membranes (*Step 2,* k_{rev}). Thus, the dissociation of the C1 domain from its ligand, either DG or PMA, is rate-limiting in the dissociation of the C1 domain from membranes.

The above model accounts for a step missing from the kinetic analysis described above (*Step 2*), thereby explaining why K_d values calculated from k_{off}/k_{on}

varied from the apparent K_d values obtained through equilibrium measurements. Such a step may have been missed in the analysis if a) the step does not result in a fluorescence change in the reporter or b) the association or dissociation step consists of two steps so similar in rate that they could not be graphically resolved. Indeed, it is likely that our fluorescence-based method only detects changes deriving from *Step 1*. However, our model provides an excellent starting point for further, more detailed kinetic analysis of both steps. Importantly, more information is needed for the transition *Step 2* for a thorough analysis of the binding of the C1 domain with lipid membranes and for rigorous assignment of values to each of the four rate constants. Indeed, surface dilution kinetics (71), experiments substituting other anionic lipids for a portion of the PS used, or experiments at low temperature or in a viscous solution (e.g., glycerol) may resolve the difference between a diffusion-controlled association (*Step 1*) and a two-dimensional search for ligand at the membrane (*Step 2*).

The model above takes into account the cooperativity seen for both PS (43,44,47) and phospholipid in general, as shown in data above. Perhaps the missing kinetic parameter involved in *Step 2* in the above model involves the cooperative binding of the C1 domain to a specific number of phospholipid molecules. Moreover, non-specific interactions can, in fact, contribute to stereospecific interactions at the membrane, as domains pre-targeted to the membrane by a single contact point only need to find two specific contact points for stereospecificity, as opposed to the three needed for soluble ligands (35). Finally, the difference in the dissociation rates between PMA- and DG-containing membranes has profound implications in cellular signaling. For example, this explains PMA's chronic translocation of PKC to

membranes and PKC's consequent hyperactivation (28,72-74), whereas transient interactions with DG-containing membranes allows for acute signaling and translocation to cytosolic substrates, as well as rapid signal termination. Interestingly, the two-step association process outlined in Figure 19 provides for two means by which chronic activation of PKC may be achieved: a) shifting the equilibrium of the initial recruitment, for example by pre-targeting to membranes via the C2 domain in conventional PKC isoforms (*Step 1*) or b) shifting the equilibrium of the transition step, for example by increasing the extent of hydrophobic contacts as in PMA (*Step 2*). Thus, the results in this chapter and the resulting model allow a clearer understanding of PKC's activation and outline a better strategy for the design of therapeutic modulators of PKC signaling.

Acknowledgement

Chapter 2, in part, is a reprint of the material as it will appear in Dries, D. R., Newton, A.C. (2007) *Journal of Biological Chemistry*. The dissertation author will be the author of this paper; A. C. Newton is the principal investigator on the supporting grant.

CHAPTER 3: A SINGLE RESIDUE IN THE C1 DOMAIN SENSITIZES NOVEL PROTEIN KINASE C ISOFORMS TO CELLULAR DIACYLGLYCEROL PRODUCTION

Protein kinase C (PKC) is a critical transducer of intracellular signaling pathways, with a variety of outputs, most notably tumor promotion (4,6). The hallmark of PKC activation is its translocation to membranes (75). This translocation is mediated through the ligand-dependent engagement of two membrane-targeting modules: the C1 (ligand: diacylglycerol, or DG) and C2 (ligand: Ca^{2+}) domains. The regulatory domains vary within the PKC family, which is subdivided into three groups based on regulation. The conventional PKC isoforms (cPKCs: α, βI/II, γ) contain two tandem C1 domains and one conventional C2 domain; consequently, cPKCs are regulated both by DG and Ca^{2+}. The novel isoforms (nPKCs: δ, ε, η, and θ) contain two tandem C1 domains and a non-Ca^{2+}/membrane binding novel C2 domain; consequently, nPKCs are regulated only by DG. Atypical PKCs (aPKCs: ι/λ and ζ) contain a single non-DG binding ("atypical") C1 domain and no C2 domain; as a result, aPKCs are regulated by neither DG nor Ca^{2+} (20).

The C1 domain is an ~8 kDa domain that binds DG or the potent DG-mimicking phorbol esters, such as *p*horbol-12-*m*yristate-13-*a*cetate (PMA) and *p*horbol *di*bu*t*yrate (PDBu) (32). Structural studies have established that all C1 domains have a similar fold (34,36,56,57,59,76). An "unzipped" β sheet forms a groove lined by hydrophobic residues in which membrane-embedded diacylglycerol or phorbol esters bind (34). Membrane interaction is also facilitated by a ring of positive

charges around the middle of the domain that potentially interacts with phosphatidylserine (PS) and other anionic lipids (61).

Nearly all C1 domains have been shown to bind PS (33), but their affinity for ligand (DG/phorbol esters) varies substantially (31). The C1 domain of nPKCs has an intrinsic affinity for DG-containing membranes two-orders of magnitude higher than that of the C1 domain of cPKCs, allowing nPKCs to respond to agonists that trigger diacylglycerol production alone (60). In contrast, cPKCs must be pre-targeted to membranes by their C2 domain in response to an elevation of intracellular Ca^{2+} in order to respond to DG (65). The molecular basis by which nPKC C1 domains bind to DG membranes with two orders of magnitude higher affinity than those of cPKC C1 domains has not been elucidated.

Questions addressed in Chapter 3

The experiments presented in Figures 20-25 characterize a single conserved residue at position 22 in the C1 domain that tunes its affinity for DG-containing membranes. The results provide a molecular basis for why nPKCs respond to DG alone, whereas cPKCs require binding to DG with a coordinated elevation of Ca^{2+}.

Sequence alignment of various C1 domains

The C1 domains of nPKCs bind DG-containing membranes with two orders of magnitude higher affinity than those of cPKCs (60). Alignment of the sequences of the C1 domains of PKCs isoforms across species and other C1-domain-containing proteins revealed that the residue at position 22 is invariant as Trp in all C1 domains

that are regulated by DG except the C1b domains of cPKCs, where it is invariant as Tyr (Figure 20). This residue lies along one of the two loops that bind ligand and is on a surface that interacts with the membrane (61), suggesting that this is a likely candidate to modulate ligand-dependent membrane affinity.

Binding of C1bβ and C1bδ Domains to Lipid Vesicles *in vitro*

To test the hypothesis that position 22 controls the affinity of the C1b domain for lipid membranes, Tyr22 in the C1b domain of the cPKC PKCβI/II was mutated to Trp (C1bβ-Y22W), and the binding of the bacterially-purified wild-type and mutant domains to lipid vesicles containing 30 mol% PS and 5 mol% DG was measured (Figure 21, *filled symbols*). Wild-type C1bβ (C1bβ-WT) bound to vesicles containing 5 mol% DG with an apparent K_d of 780 ± 50 μM (*filled diamonds*). On the other hand, the mutant C1bβ-Y22W bound with 31-fold higher affinity to vesicles of the same composition (apparent K_d = 24 ± 1 μM, *filled squares*). Binding was dependent on the presence of DG, as there was no significant binding of the C1 domain to 2000 μM lipid containing 30 mol% PS and 0 mol% DG (2 ± 2% bound, data not shown). Next, the binding of these two domains to vesicles containing 30 mol% PS and 1 mol% PMA was measured (Figure 21, *open symbols*). C1bβ-WT and -Y22W bound with the same affinity to vesicles containing 1 mol% PMA (apparent K_d values of 35 ± 3 and 35 ± 2 μM, *open diamonds and squares*, respectively). These data reveal that mutation of Tyr22 to Trp in the C1 domain of PKCβ converts the domain from a low-affinity to a high-affinity DG binding module.

To confirm whether the isolated C1b domain of the nPKC PKCδ (C1bδ),

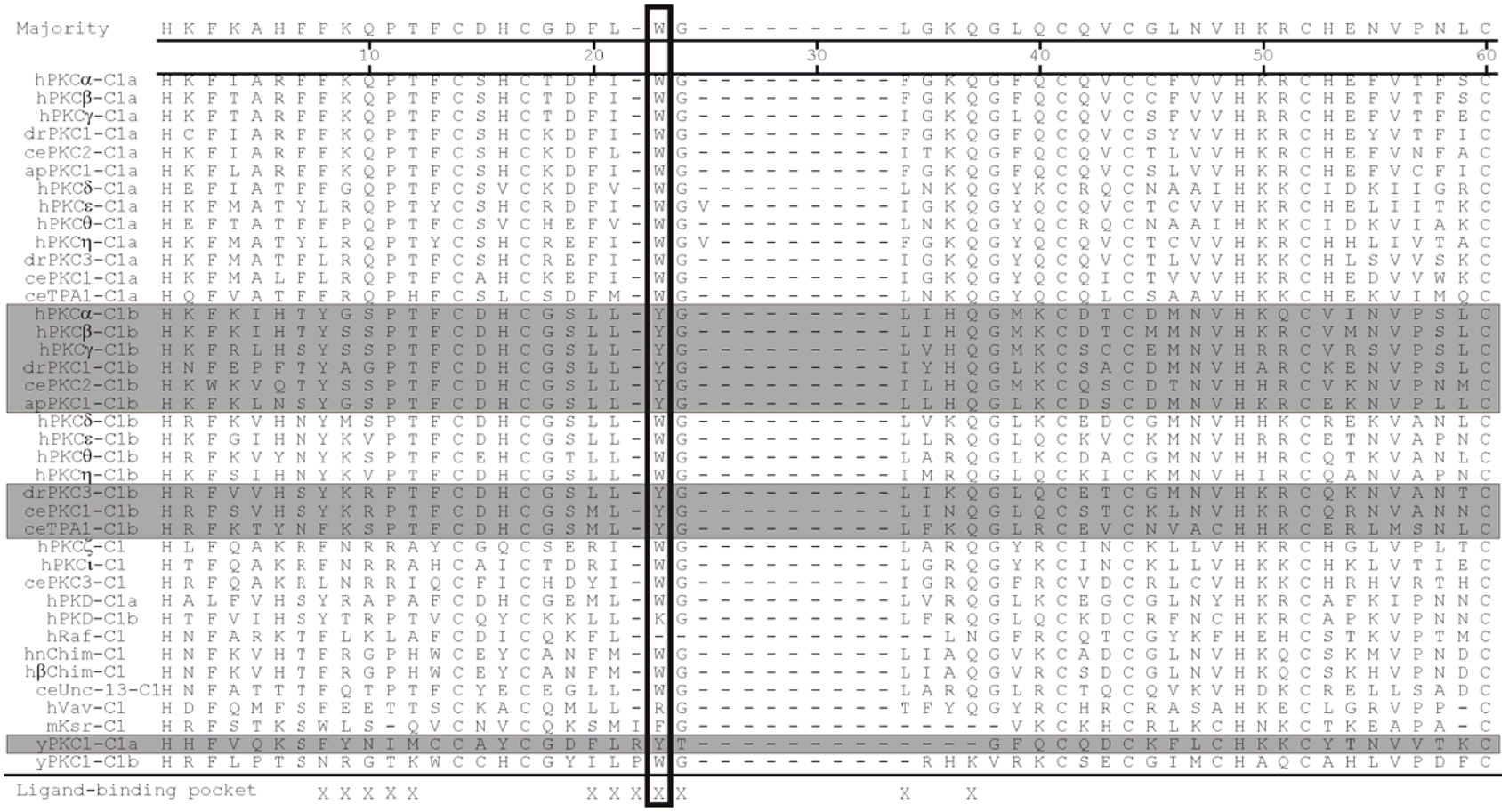


Figure 20. Sequence alignment of the C1 domains of representative conventional and novel PKC isoforms and other C1-domain-containing proteins across species. Position 22 (123 in PKCβII numbering) is boxed in black. Tyr at position 22 is highlighted in grey. Residues that are known to contact phorbol and/or to form the hydrophobic wall of the groove in which DG or phorbol binds are marked below with an "X".

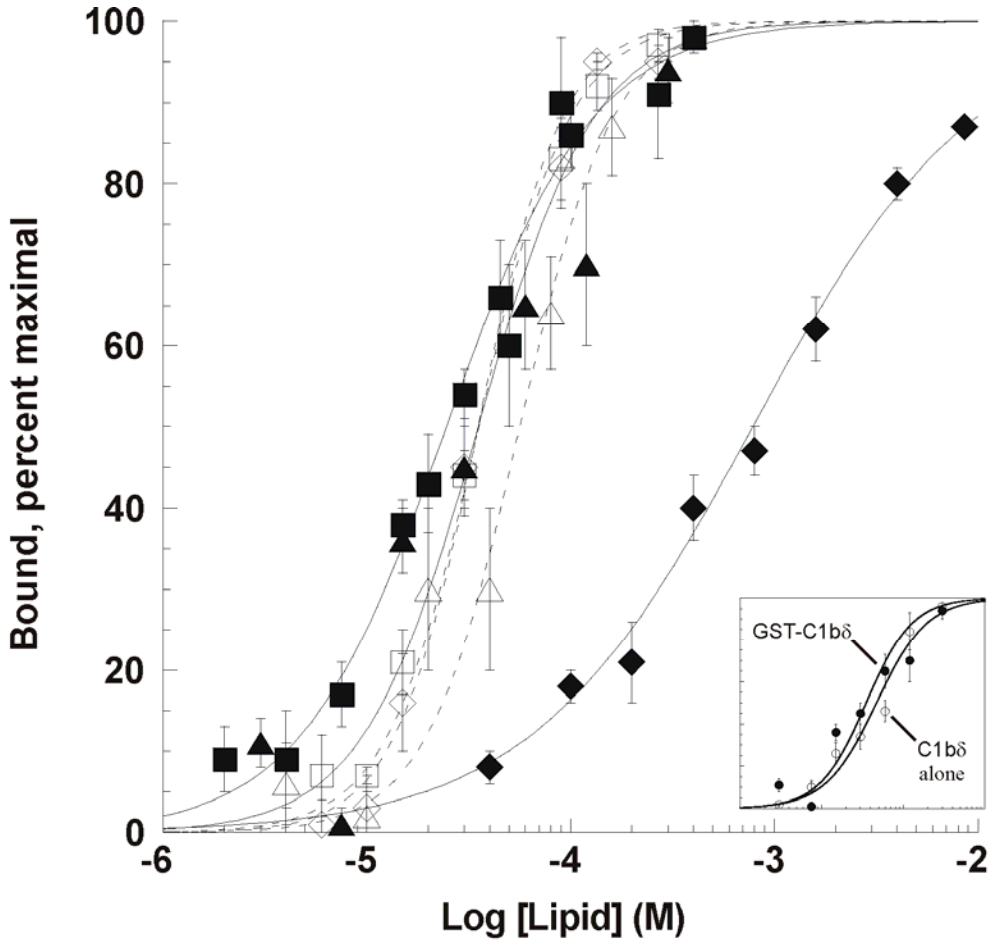


Figure 21. Mutation of Tyr22 to Trp in the C1b domain of PKCβ increases its affinity for DG-containing membranes and reduces selectivity for PMA over DG similar to the C1b domain of PKCδ. Binding of C1bβ-WT (◆ and ◇) and -Y22W (■ and □) and GST-C1bδ (▲ and △) to lipid vesicles containing 30 mol% PS and either 5 mol% DG (*filled symbols*) or 1 mol% PMA (*open symbols*). *Inset,* binding of GST-tagged (●) or untagged (○) C1bδ to lipid vesicles containing 5 mol% DG and 30 mol% PS. Each data point represents the mean of triplicate experiments ± *S.E.*

which has a Trp at position 22, also has higher intrinsic affinity for DG-containing membranes than C1bβ, the binding of these domains to DG-containing membranes was measured. A GST-tagged construct was used for C1bδ, as removal of the GST tag greatly reduced the stability of the protein. GST-C1bδ bound to vesicles containing 5 mol% DG and 1 mol% PMA with apparent K_d values of 35 ± 3 and 56 ± 6 μM, respectively (Figure 21, *triangles*). Low, but pure, amounts of untagged C1bδ showed that the GST tag had no effect on the affinity of the C1bδ for DG- or PMA-containing membranes (Figure 21, inset). Moreover, while C1bβ-WT showed a 110-fold preference for PMA over DG on an equimolar basis (Figure 21, *open vs. closed diamonds*), C1bβ-Y22W and GST-C1bδ showed modest 3.6- and 3.1-fold selectivities for PMA over DG, respectively (Figure 21, *open vs. closed squares* for C1bβ-Y22W and *triangles* for GST-C1bδ).

Binding of C1bβ and C1bδ Domains to Lipid Vesicles Containing Phosphatidylserine versus Phosphatidylglycerol

It was previously observed that the C1 domain exhibits selectivity amongst anionic lipids in the presence of DG, with preference for PS over phosphatidylglycerol (PG) (24,63). Since residue 22 is important for sensitizing the C1b domain to DG, this position should also allow the domain to discriminate between PS and PG. Therefore, the affinity of the C1bβ-WT, C1bβ-Y22W and GST-C1bδ domains for membranes containing 30 mol% PS or PG and 5 mol% DG or PMA was measured. Wild-type C1bβ (Tyr at position 22) showed 2-fold selectivity for PS over PG, regardless of

whether the ligand was DG or PMA (Table 7). Trp-containing C1 domains, however, showed selectivity for PS only in the context of DG membranes (5- and 20-fold selectivity for C1bβ-Y22W and GST-C1bδ, respectively). On the other hand, these proteins had no or 3-fold selectivity for PS for C1bβ-Y22W and GST-C1bδ, respectively, in the context of PMA-containing membranes. These data reveal that residue 22 also allows for the discrimination between PS and PG in the presence of DG. Taken together with data in the previous section, these results reveal that Trp at position 22 increases the affinity of C1bβ for DG-containing membranes, reduces selectivity between PMA and DG, and increases DG-dependent PS selectivity.

Translocation of C1bβ and C1bδ Domains to Membranes in Response to Natural Agonist *in vivo*

To monitor the real-time membrane translocation of isolated C1b domains in live cells, YFP was fused to the C-terminus of C1bβ and C1bδ. Also, YFP fusion constructs were generated for these two C1b domains containing point mutations reversing the identity of residue 22: C1bβ-Y22W and C1bδ-W22Y. COS7 cells were co-transfected with CFP that had been targeted to the plasma membrane (PM-CFP) and the indicated YFP-tagged C1b construct; translocation to the plasma membrane was monitored as an increase in the ratio of FRET-based YFP emission: CFP emission (FRET ratio) (77).

UTP, acting through endogenous P2Y receptors, stimulates the production of DG at the plasma membrane via phospholipase C-mediated lipid hydrolysis (for an

Table 7. Apparent binding constants (K_d) for the interaction of the C1b domain with membranes. Apparent K_d values were calculated from binding curves as described in "Materials & Methods." Data shown here are for lipid vesicles consisting of 5 mol% DG or PMA and 30 mol% PS or PG. Apparent K_d (in μM) is presented as the average of three experiments ± *S.E*.

	Apparent K_d (μM)					
	C1bβ		C1bβ-Y22W		C1bδ	
Ligand	DG	PMA	DG	PMA	DG	PMA
PS	780 ± 50	11.5 ± 0.5	24 ± 1	5.3 ± 0.5	35 ± 3	8.5 ± 0.6
PG	1690 ± 60	22 ± 1	130 ± 10	6.0 ± 0.9	700 ± 200	25 ± 3
PG:PS	2.2 ± 0.2	1.9 ± 0.1	5.4 ± 0.5	1.1 ± 0.2	20 ± 6	2.9 ± 0.4

example, see Figure 1 in Chapter 1; see also (78)). Figure 22 shows that stimulation of COS7 cells with UTP (100 μM) resulted in an increase in FRET ratio, which was further increased following addition of PDBu (200 nM), which causes maximal translocation of the domain to membranes. Upon stimulation of COS7 cells with UTP, C1bβ did not significantly translocate to membranes (Figure 22, *blue diamonds*). In contrast, UTP stimulation caused robust translocation of C1bδ (Figure 22, *green triangles*). Consistent with *in vitro* binding data (Figure 21), C1bβ-Y22W responded to UTP (Figure 22, *red squares*), resulting in a 10-fold increase in DG binding at the plasma membrane relative to C1bβ-WT (Figure 22, *blue diamonds*). Conversely, mutating the Trp 22 to Tyr in C1bδ (C1bδ-W22Y) reduced the translocation in response to UTP 10-fold relative to C1bδ without altering the maximal translocation driven by PdBu (Figure 22, *yellow circles*). These data reveal that Trp at position 22 in the C1b domain allows the domain to respond to DG generated by receptor-mediated phospholipid hydrolysis, whereas Tyr decreases the binding affinity to an extent to which the domain is unresponsive to agonist-produced DG.

Ca^{2+}-Independent Protein Kinase C Activity for Wild-Type and Mutant PKCβ and Wild-Type PKCδ

In order to determine whether binding differences arising from changes in the C1b domain affected the cofactor dependence of the full-length kinase, a full-length PKCβII construct was generated in which Tyr123 (position 22 of the C1b domain) was mutated to Trp (PKCβII-Y123W). COS 7 cells were transfected with either this

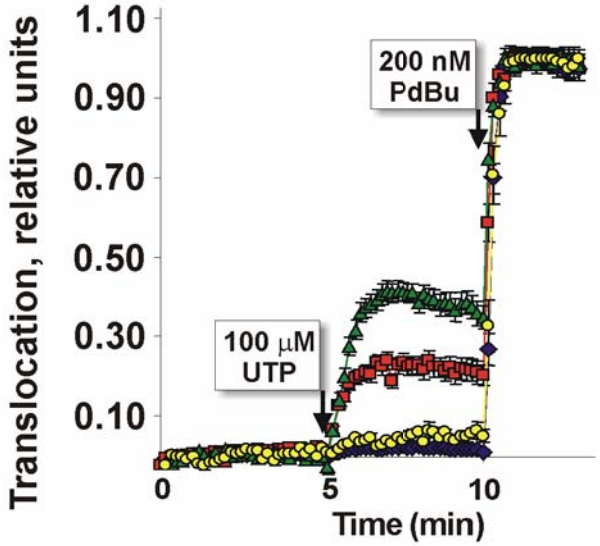


Figure 22. Trp at position 22 of the C1 domain is required for efficient translocation to membranes in response to natural agonist. COS7 cells were co-transfected with PM-CFP and the following YFP-tagged C1b domain constructs: C1bβ (◆), C1bβ-Y22W (■), C1bδ (▲), and C1bδ-W22Y (●). The relative translocation in response to UTP (100 μM) and PDBu (200 nM) treatment was calculated and plotted as a function of time. Data represent the average ± *S.E.* of 10-15 cells from at least three independent experiments referenced around the addition time point.

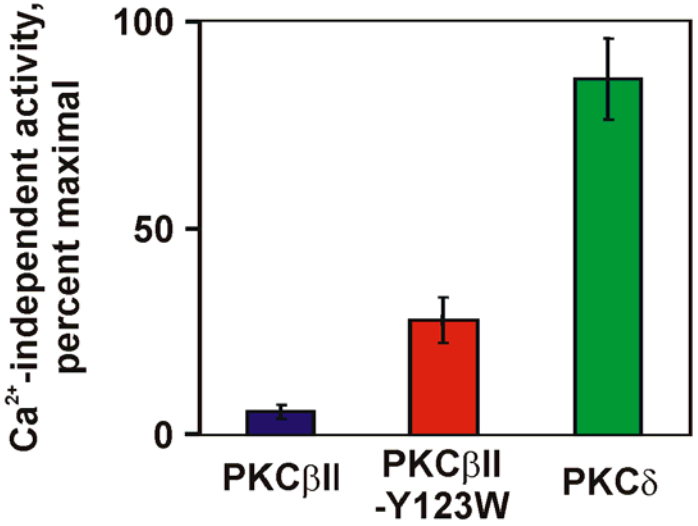


Figure 23. Trp at position 22 increases calcium-independent PKC activity. Lysates from COS7 cells transfected with PKCβII, PKCβII-Y123W, or PKCδ were assayed for PKC activity in the presence of PS, DG, and either Ca^{2+} (total PKC activity) or EGTA (calcium-independent PKC activity). Ca^{2+}-independent PKC activity was calculated as a percent of total activity; total activity was comparable for both PKCβII constructs and typically slightly lower for the PKCδ construct. These data represent the relative activity of the overexpressed kinases in response to lipid cofactors in the absence of Ca^{2+}. Data represent the average ± *S.D.* from three experiments.

mutant construct, wild-type PKCβII, or PKCδ, and kinase activity was assayed from the detergent-soluble supernatants of lysates compared to untransfected control cells. PKC activity was assayed in the presence of PS, DG, and either Ca^{2+} (for total PKC activity) or EGTA (for Ca^{2+}-independent activity). Background activity from untransfected cells was subtracted, and Ca^{2+}-independent activity was calculated as a percent of total PKC activity. Figure 23 shows the Ca^{2+}-independent activity of PKCβII, PKCβII-Y123W, and PKCδ. Consistent with the standard model where Ca^{2+}, DG, and PS are required for full activation of cPKCs (5,21), PKCβII had minimal (6%) activity in the absence of Ca^{2+}. In contrast, PKCδ was activated to near maximal levels in the absence of Ca^{2+}, consistent with the Ca^{2+} independence of novel PKC isoforms (5,21). Strikingly, the single point mutation of Y123W in PKCβII was sufficient to confer significant Ca^{2+}-independent activity (28% of maximal activity). These results are consistent with the tighter membrane affinity conferred by Trp vs. Tyr in the C1b domain, which results in reduced dependence on the C2 domain (and hence Ca^{2+}) for activation.

Basal Localization of Wild-Type and Mutant C1bβ and C1bδ Domains and Full-Length Proteins *in vivo*

Translocation of different PKC isoforms to discrete subcellular regions is an important mechanism for achieving specificity in PKC signaling. While the typical site of signaling for cPKCs is the plasma membrane (79), localization at endomembranes – particularly the Golgi – has been shown to be critical for PKCδ

activity (80). Striking differences were observed in the localization of the isolated, YFP-tagged C1bβ and C1bδ: C1bβ was localized diffusely throughout the cell (Figure 24A, upper left panel), while C1bδ was concentrated at a juxtanuclear region resembling Golgi membranes (Figure 24A, lower left panel). Localization at the Golgi was confirmed by treatment with brefeldin A, which abolished the juxtanuclear concentration of C1bδ (data not shown). Moreover, the reversion mutants C1bβ-Y22W and C1bδ-W22Y showed a complete reversal of the subcellular localization of their wild-type counterparts (Figure 24A, right panels). Next, wild-type and mutant full-length PKCβII and PKCδ were analyzed for differences in localization. In COS7 cells, PKCδ pre-localized to juxtanuclear membranes, while PKCβII was basally cytosolic (Figure 24B, left panels). Consistent with data from the isolated C1b domains, basal Golgi localization of the full-length PKCδ was greatly diminished upon mutation of Trp252 (position 22 of the C1b domain) to Tyr (Figure 24B, lower right panel). However, mutation of Tyr123 to Trp in PKCβII did not cause any change in its localization, as PKCβII remained cytosolic (Figure 24B, upper panels). Thus, in addition to affecting PKC function by regulating activation in response to DG, position 22 of the C1b domain may also regulate DG-dependent pre-localization of novel PKC isoforms.

Structure and Surface Properties of Representative C1 Domains

To gain insight into how Trp vs. Tyr at position 22 controls the affinity of the C1 domain for DG-containing membranes, the backbone structures and molecular

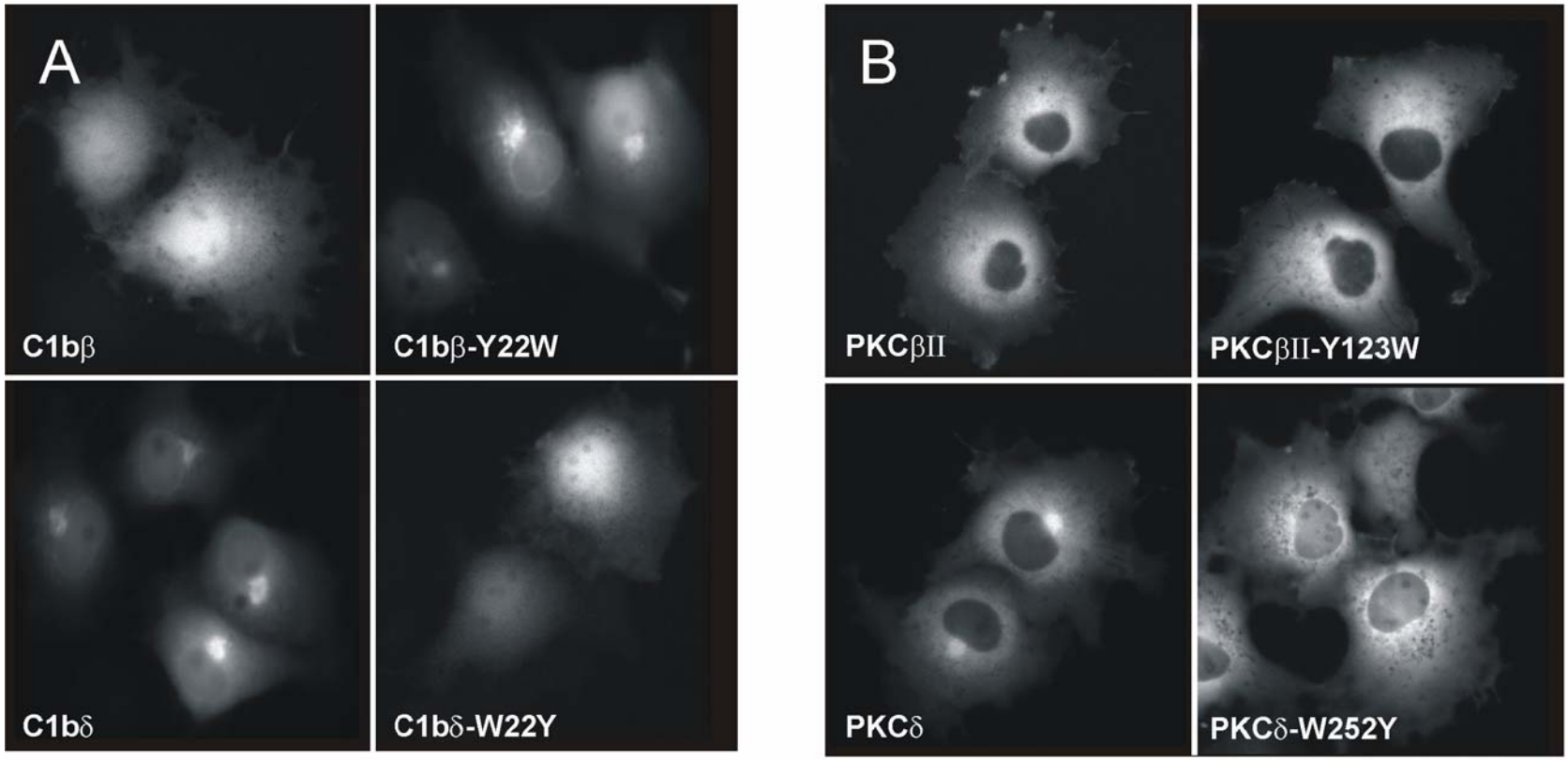


Figure 24: Residue 22 affects localization of the C1b domain (*A*) and full-length PKC (*B*). *A*, Representative images of COS7 cells transfected with YFP-tagged C1b domains: C1bβ (top left), C1bβ-Y22W (top right), C1bδ (lower left), and C1bδ-W22Y (lower right). *B*, Representative images of COS7 cells transfected with YFP-tagged full-length PKC: PKCβII (top left), PKCβII-Y123W (top right), PKCδ (lower left), and PKCδ-W252Y (lower right). Mutated residues correspond to position 22 of the C1b domain in the full-length protein. Data are representative of at least three independent experiments.

surfaces of several C1 domains were compared (Figure 25). Representatives of three C1 groups for modeling studies were chosen: those that bind DG membranes with relatively high affinity (C1bδ), those that bind DG membranes with relatively low affinity (C1bγ - a surrogate for C1bβ, with which C1bγ shares 80% identity and 92% similarity), and those that do not bind DG (C1ζ and C1-Raf). As described previously (33,34), there are two loops at the top of C1b domain of PKCδ, here designated β1/2 and β3/4, which form the phorbol/DG-binding pocket and contain the ligand- and membrane-binding determinants. As shown in Figure 25, comparison of the C1b domains of PKCγ and δ reveals large movements within the β3/4 loop, while the rest of the domain shows nearly identical overlap in backbone structure. The importance of this loop for ligand binding is further highlighted by the C1 domain from c-Raf, in which the entire β3/4 loop is deleted, thus rendering the domain unable to bind DG (Figure 20 and Ref. (56)). Curiously, the C1 domain of PKCζ retains this loop and has Trp at position 22, yet it still does not bind DG. Rather, C1ζ appears to lose the ability to bind DG by sterically and electrostatically occluding the ligand-binding pocket through substitution of hydrophobic residues (*grey*) for large basic amino acids (*blue*) (Figure 25). Consistent with this, Blumberg and coworkers have recently shown that mutation of Asn7, Ser10, Pro11, and Leu20 in the β1/2 and β3/4 loops to arginine in C1bδ results in complete loss of binding to phorbol ester-containing membranes (54). Thus, the affinity of the C1 domain for DG appears to be regulated by interactions with hydrophobic residues within the ligand-binding pocket and by the position of the β3/4 loop. Residue 22 lies at the apex of this highly mobile β3/4 loop,

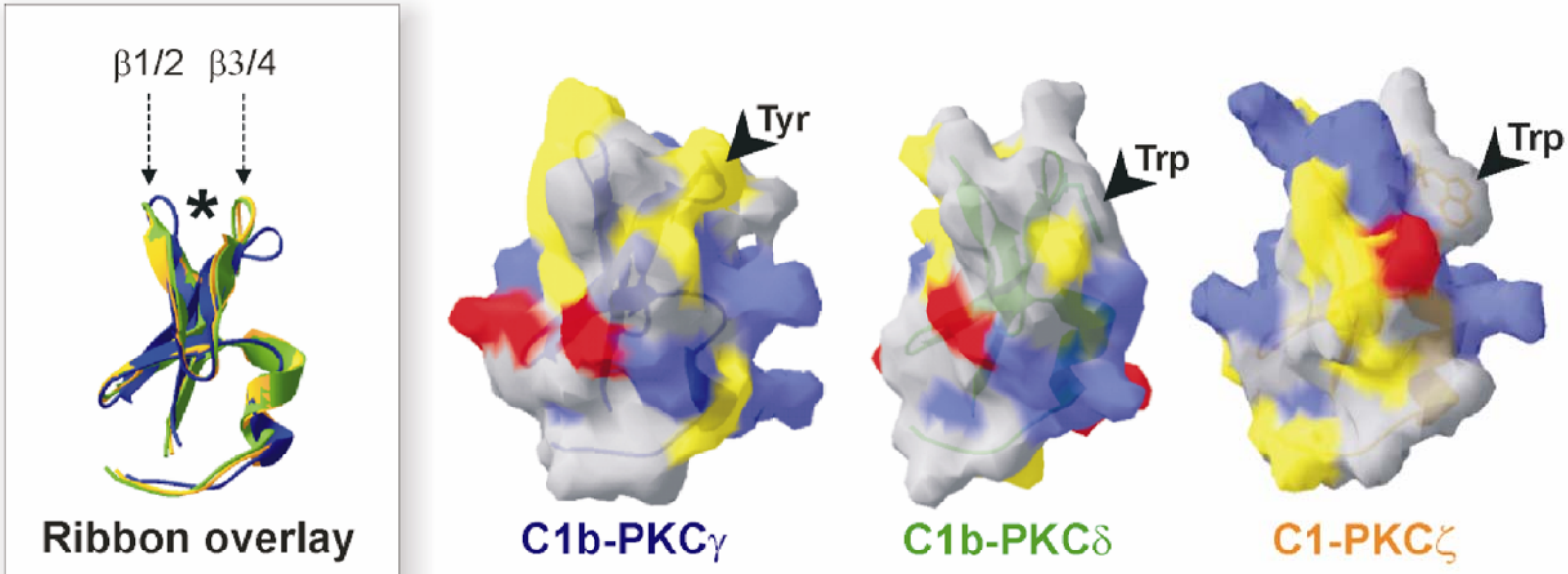


Figure 25. The C1 domain's ability to bind DG arises from modulation of the width and surface properties of the loops surrounding the hydrophobic DG-binding cleft. Ribbon diagram overlay and molecular surfaces of C1b-PKCγ (*blue*), C1b-PKCδ (*green*), and C1-PKCζ (*orange*). Phorbol binds between the two loops at the top of the domain as indicated with an asterisk (*). The identity of residue 22 is presented as a stick and marked with an arrowhead. Coordinates for C1b-PKCγ and C1b-PKCδ were taken from PDB IDs 1TBN and 1PTQ, respectively. Coordinates for C1-PKCζ were taken from a homology model as described in the "Methods" section. Surface coloring scheme is as follows: basic, *blue*; acidic, *red*; polar, *yellow*; nonpolar, *grey*.

in keeping with its role as a critical regulator for the C1 domain's ability to bind DG.

Conclusions

In this study, Trp vs. Tyr at residue 22 of the C1b domain was identified as a molecular switch that controls whether PKC isoforms can respond to DG alone, or whether the coordinated binding of a second membrane-targeting module (i.e., the C2 domain of cPKCs) is required to confer responsiveness to agonist stimulation. Specifically, the data show that C1b domains containing Trp at this position bind membranes with sufficiently high affinity to allow translocation following agonist-stimulated DG production, whereas those that contain Tyr at this position bind membranes with an order of magnitude lower affinity, making them unresponsive to agonist-produced DG. In keeping with this observation, mutation of position 22 in the C1b domain of the cPKC PKCβII (i.e., Tyr123) to Trp confers Ca^{2+}-independent activity; such a result is consistent with previous studies that showed that activation of PKC depends upon the affinity by which PKC binds to membranes (24). The increased membrane affinity conferred by having Trp rather than Tyr at position 22 provides a molecular explanation for why novel PKC isoforms are able to respond to DG alone, while conventional PKC isoforms require pre-targeting by Ca^{2+} via their C2 domains for translocation and activation (60,65).

The subcellular localization of PKC is a critical regulator of isoform-specific substrate phosphorylation (79). The studies here suggest that residue 22 is a key determinant in the localization of PKC. Here, the data show constitutive localization of the C1b domain of PKCδ to the Golgi, a site where PKCδ is known to signal (80).

C1bβ-Y22W also localizes to the Golgi, whereas domains containing Tyr at position 22 are cytosolic basally. A previous study also reported constitutive Golgi localization of the C1b domain of the nPKC PKCθ in unstimulated cells; this localization was redistributed to the cytosol upon inhibition of phospholipase C or phosphatidic acid phosphatase (81). Taken together, these data suggest that basal Golgi localization is mediated by basal levels of DG at this region. These effects are also evident in full-length PKCδ: mutation of Trp22 to Tyr in the C1b domain (i.e., Trp252) abolishes the localization of full-length PKCδ to the Golgi. Curiously, the reverse mutation, Tyr123 to Trp in full-length conventional PKCβII, does not confer Golgi localization. Thus, merely increasing the C1b domain's affinity for DG is not sufficient to determine the subcellular distribution of PKC. This suggests that other determinants control cPKC localization. For example, the Ca^{2+}-binding C2 domain of cPKCs – a feature absent from nPKCs – may override targeting to the Golgi (82,83). These results suggest a model of activation in which low DG levels allow pre-targeting of PKCδ to the Golgi through the C1b domain, with a shift in equilibrium to full binding and full activation following an additional agonist-stimulated increase in DG.

Numerous elegant studies delineating the residues in the C1 domain involved in ligand binding have identified residue 22 as participating in DG-dependent membrane binding (66,67,84,85). Interestingly, no significant effects of the residue at this position were noted in studies examining phorbol ester binding (84,85). Here, the data show that Trp vs. Tyr at position 22 selectively alters the affinity for DG but not PMA. In addition, the DG-dependent selectivity of the C1b domain for PS (24,63) is

regulated by the residue at this position. The functionality of this residue is further highlighted by the fact that C1 domains that contain Tyr at position 22 cluster both within and across species, with Tyr22-containing C1 domains found in the fly, nematode, mullosks, and even yeast (see Figure 3, Chapter 1).

Kinetic analysis has shown that position 22 of C1bδ participates in membrane penetration by controlling dissociation from membranes, and it appears to be in direct contact with phospholipids when bound to membranes (31,59,66). Yet the exact mechanism by which residue 22 regulates the binding of ligand is unknown. The modeling studies here suggest that position 22 may regulate the size of the ligand-binding pocket (Figure 25). The phenol ring of Tyr22 in C1bγ lies in a very different orientation relative to the membrane compared to the indole ring of Trp22 in C1bδ. Moreover, these two amino acids are known to be positioned very differently at the water/lipid bilayer interface (86,87), suggesting that mobility in the β3/4 loop may dictate the width and depth of the ligand-binding pocket. Indeed, several studies have shown flexibility within this loop, whereas the rest of the structure tends to remain static (34,59,88). The presence of two highly conserved Gly residues within the β3/4 loop (Gly23 and 28) suggests that such flexibility is not only possible, but may also be required for function.

Particularly relevant to this study, the ligand-binding cavity in C1bδ is narrow and deep, while that of the non-DG binding C1bγ is wide and shallow. Phorbol does not significantly alter the structure of the C1b domain of PKCδ, suggesting that phorbol esters and DG simply match the molecular surface of their targets (34). Thus,

whereas the smaller DG can bind well to C1bδ, only the larger phorbol esters can make hydrophobic contacts across the wide gorge of C1bγ. Moreover, C1bγ has polar uncharged residues on the binding loops, while C1bδ has strictly hydrophobic loops, suggesting that hydrophobic match between the C1 domain and DG/phorbol esters may also play a role in distinguishing between the two ligands.

The data presented in this chapter reveal that Trp vs. Tyr at position 22 of the C1b domain switches PKC from an isoform that can respond to DG alone to one that requires pre-targeting to membranes by the C2 domain for activation (60). This residue also governs the subcellular localization of PKC isoforms: the higher affinity of novel C1b domains for DG promotes the localization of novel PKC isoforms at the Golgi (81). The finding that DG selectively activates novel PKC isozymes, whereas phorbol esters do not discriminate between novel and conventional PKCs, cautions against drawing physiological conclusions when substituting phorbol esters for DG in the context of cellular signaling, an idea that has also been suggested by other groups (66). Taken further, the results also suggest that therapeutic compounds designed to target the C1 domain of a specific isoform should more closely resemble DG than phorbol, an approach taken by Blumberg and coworkers (89).

Acknowledgement

Chapter 3, in part, is a reprint of the material as it appears in Ref. (55). The dissertation author and L. L. Gallegos contributed equally to the work and co-authored this paper; A. C. Newton was the principle investigator.

CHAPTER 4: THE INCREASED ELECTROSTATIC POTENTIAL OF THE ATYPICAL C1 DOMAIN OF PROTEIN KINASE C ζ DOES NOT INCREASE ITS AFFINITY FOR ANIONIC LIPIDS RELATIVE TO TYPICAL C1 DOMAINS

Protein kinase C (PKC) is involved in a myriad of intracellular signaling pathways (4). However, one of the most important roles for PKC is in tumor promotion (4,6). The hallmark of PKC activation is its translocation to membranes (75). This translocation is mediated through the engagement of its regulatory domain to membranes, with the energy released in this interaction used to remove a pseudosubstrate from PKC's active site (Figure 2 and (24)). The conventional and novel isoforms contain two lipid-targeting modules, the C1 and C2 domain, that are involved in the DG- and Ca^{2+}-dependent translocation of PKC to membranes, respectively (Figure 2 and (20)). However, the atypical isoforms, aPKCs: ι/ λ and ζ, contain a single non-DG binding ("atypical") C1 domain and lack a C2 domain; as a result, aPKCs are regulated by neither DG nor Ca^{2+} (20,54). Instead, the aPKCs contain a PB domain, which can interact with a variety of proteins (27). Thus, clear evidence for why aPKCs contain an atypical C1 domain and what lipid second-messengers they bind, if any, for activation has remained elusive.

Regulation of Atypical PKCs by Phospholipids

Although the atypical C1 domain of aPKCs does not bind DG (or phorbol ester), aPKCs have been shown to be regulated *in vitro* and *in vivo* by a variety of lipids (27). Indeed, the original cloning of PKCζ showed a strong dependence for

activity on phospholipid, but no dependence on Ca^{2+} or DG (90). Shortly afterwards, a study showed that phosphatidic acid, the product of phospholipase D activation, can activate PKCζ through direct binding (91). Soon, however, the focus turned to phosphoinositides (PIs) in the regulation of PKCζ activity. One early report identified phosphoinositide-3,4,5-trisphosphate (PIP_3), the product of phosphoinositide-3-kinase (PI3K), as a direct activator of PKCζ (92). Indeed, an increase in nuclear PI3K activity was found to precede the translocation of PKCζ into the nucleus (93). In addition, ceramide had been shown to activate PKCζ with downstream effects in two separate pathways – mitogenic signaling through nuclear factor kappa B (NF-κB) (94) and the stress activated protein kinase cascade (95). A later report, however, showed that ceramide activates PI3K, with PIP_3-dependent translocation of PKCζ to the nucleus for activation (96).

The most obvious way for PIP_3 to regulate PKCζ activity would be through activation of PKCζ's upstream kinase phosphoinositide-dependent kinase (PDK) (21). However, one report has shown that PIP_3 can activate PKCζ through both PDK-dependent and -independent mechanisms (97). Contrary to all of the above, one early report showed that a variety of phosphoinositides do not activate baculovirus PKCζ, which was instead constitutively active (98). Finally, one of the original papers characterizing PKCζ suggested that anionic lipid participates in the optimal presentation of substrate to the kinase, rather than through a direct activation mechanism (99). Although many of the aforementioned studies implicate anionic lipids – in particular PIP_3 – in the activation of aPKCs – in particular PKCζ – no

reports isolate the particular domain(s) responsible for direct regulation by these lipids. A prime candidate for such an interaction would be the aPKC C1 domain since a) the C1 domain in the conventional and novel PKC isoforms, as well as in many other C1 domain-containing proteins, is a membrane-targeting domain with specific lipid ligands, and b) the C1 domain is immediately preceded by the pseudosubstrate, whose membrane-dependent removal from the active site of PKC is required for full activation (see above). However, to date, no study has examined the direct binding of the aPKC C1 domains to specific phospholipids.

Structures of Typical and Atypical C1 domains

The C1 domain is an ~50 amino acid domain with a small, globular fold (35). The C1 domains can be divided into the typical, which bind DG or the potent DG-mimicking phorbol esters (e.g., *p*horbol-12-*m*yristate-13-*a*cetate (PMA) and *p*horbol *di**bu*tyrate (PDBu) (32)), and the atypical, which do not bind these ligands (27). Despite these two subclasses of C1 domains, structural studies have established that all C1 domains have a similar fold (34,36,56,57,59,76). The ligand-binding pocket of typical C1 domains is formed by an "unzipped" β sheet lined with hydrophobic residues to promote its insertion into membranes (34). Membrane interaction is also facilitated by a ring of positive charges around the middle of the domain that potentially interacts with phosphatidylserine (PS) and other anionic lipids (61).

Yet while much is known about the structural and molecular properties of typical C1 domains, few structures have described the atypical C1 domains. The first description of an atypical C1 domain was that of Raf. The C1 domain of Raf was

shown to adopt a fold and topology similar to that of other C1 domains, with coordination to two zinc ions being critical for proper folding. However, the second of two loops that form the DG-binding cavity in typical C1 domains was found to be truncated, thus explaining the inability of this C1 domain to bind to DG or phorbol esters (56). A second structure of an atypical C1 domain – that of *k*inase *s*uppressor of *R*as (KSR) – later confirmed the importance of these loops in binding to DG and phorbol ester (57). Similar to C1-Raf, this structure had a truncated second loop in the ligand-binding pocket. However, the study of KSR highlighted the importance of the increased number of basic amino acids that lined an amphipathic β-sheet at the core of the C1 domain. Consequently, this patch was proposed to form a binding site for anionic lipids. Moreover, the KSR study drew comparisons between the atypical C1 domains of Raf and KSR and found that the two differ in the pattern of basic amino acids lining the "upper" membrane-binding half of the domain, possibly explaining why these two cannot substitute for one another (57).

While the C1 domain is an atypical C1 domain which, like those of Raf and KSR, does not bind DG or phorbol ester, the C1 domains of the atypical PKCs ζ and ι are the most similar atypical C1 domains to the typical, DG-binding C1 domains. For example, as opposed to C1-Raf and -KSR which have a truncation in the second ligand-binding loop, C1ζ and C1ι have – by all appearances – a fully intact DG binding site that shares substantial similarity to typical, DG-binding C1 domains (33). Thus, mere sequence alignment of C1 domains and comparison with those domains whose structures are known do not offer a clear explanation of why the C1 domains of atypical PKCs cannot bind DG, nor if or how they are regulated by anionic lipid.

The experiments presented in Figures 26-28 describe a model of the C1 domain of PKCζ (C1ζ) and compare the structural and molecular properties of the C1ζ to those of the C1b domains of PKCβI/II and PKCδ (C1bβ and C1bδ, respectively). Furthermore, the experiments in Table 8 and Figure 29 reveal that C1ζ cannot use its high electrostatic potential to bind to PS or a variety of other anionic phospholipids, including a panel of phosphoinositides, in order to compensate for its inability to bind to DG or phorbol esters.

Molecular Modeling and Electrostatic Potential Maps of the C1b Domain of PKCγ and the C1 Domain of PKCζ

In order to gain insights into the mechanism by which PKCζ is regulated by PS, the C1 domain of PKCζ (C1ζ) was modeled by homology against several known C1 domain structures. Both PKC and non-PKC C1 domains were used as templates for modeling and included the C1b domains of PKCδ, PKCγ, and DGKδ and the C1 domains of Raf, Ksr (kinase suppressor of Ras), β2-chimaerin, and munc-13 (see "Materials and Methods" for details). Modeling revealed all C1 domains adopt a similar fold, with most of the variation in structures occurring within the two loops that comprise the ligand-binding cavity (Figure 26A). Moreover, modeling revealed that the C1 domain of PKCζ (C1ζ) adopts a fold most similar to that of the C1b of PKCδ (C1bδ) and the C1 domain of β2-chimaerin (Figure 26A). Since the overall fold of the atypical C1ζ domain was similar to that of the typical C1 domains of PKCδ and β2-chimaerin, the surface properties of C1bδ (which binds both PS and DG) and

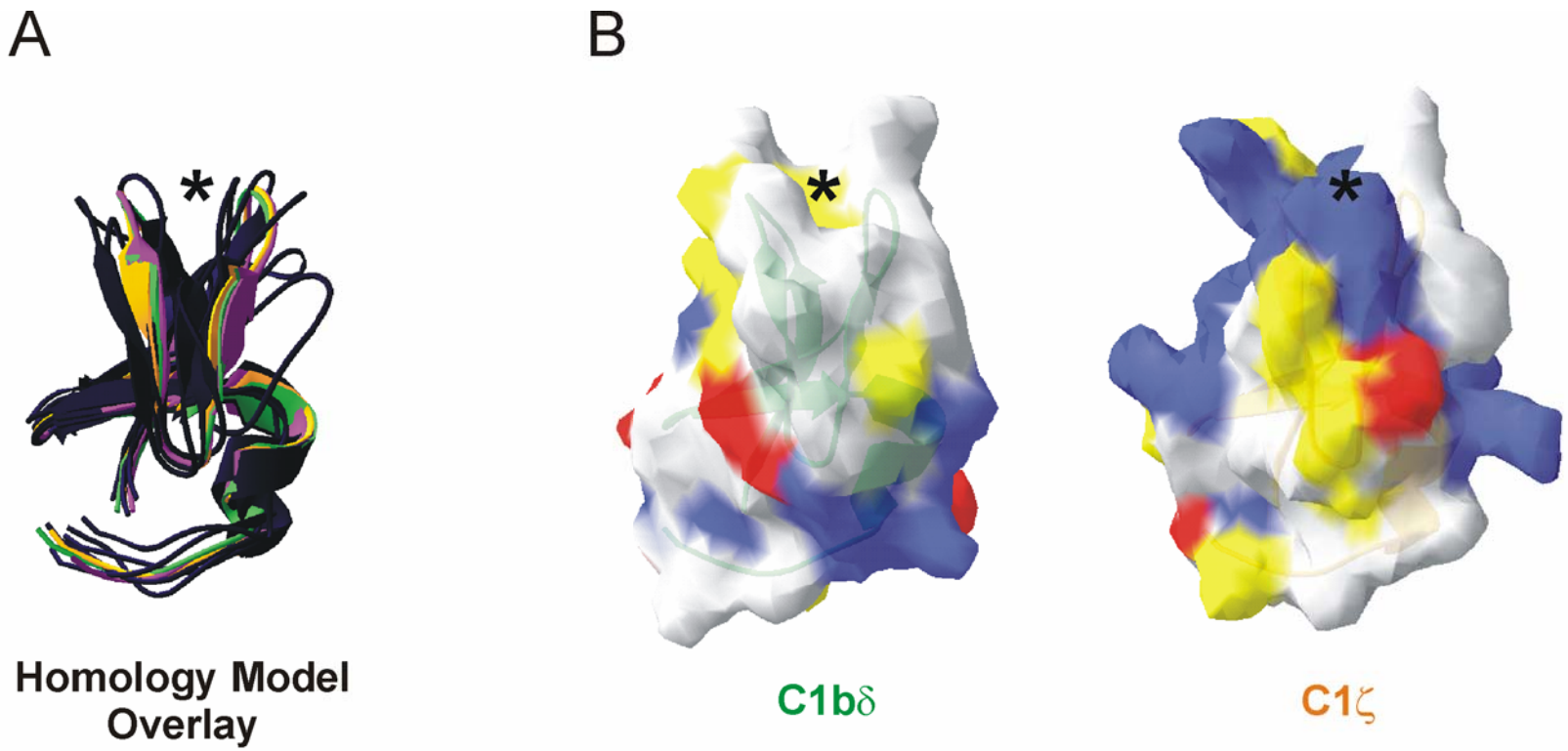


Figure 26. Homology modeling of the C1 domain of PKCζ (C1ζ) and comparison with the C1b domain from PKCδ (C1bδ). *A*, overlay of all structures that were used as templates for the modeling of C1ζ. Shown in color are the C1b domain of PKCδ (*green*) and the C1 domains of PKCζ (*orange*) and β2-chimaerin (*purple*). The remaining structures used for modeling are shown in *dark blue*. The cavity in which ligand (DG or phorbol ester) binds is marked with an asterisk (*). *B*, comparison of the surface properties of C1bδ and C1ζ. Surfaces are colored according to property of amino acid as follows: basic, *blue*; acidic, *red*; polar, *yellow*; nonpolar, *grey*. As in panel *A*, the cavity in which ligand binds is marked with an asterisk (*).

C1ζ (which binds PS only) were compared. Figure 26B revealed that although the backbone structures of C1bδ and C1ζ are nearly identical, the surface properties are markedly different. In particular, the β1/2 (*lefthand*) loop is lined with basic residues, many of which occlude the DAG-binding cleft. This would both prevent the docking of a large hydrophobic ligand such as DAG or phorbol within the cleft and also increase the electrostatic potential to allow for interactions with the anionic lipid PS.

To confirm the hypothesized increase in electrostatic potential in C1ζ due to the replacement of hydrophobic residues with basic residues, electrostatic potential maps were generated for C1bδ and C1ζ. In the generation of electrostatic potential maps for these two domains, it was found that the isoelectric point for C1ζ is two full units more basic than that of C1bδ (pI = 8.304 and 10.213, respectively). In keeping with the higher pI, C1ζ has a large positive electrostatic potential throughout most (~80%) of the domain, whereas C1bδ replaces most of this positive electrostatic potential with an acidic patch on the bottom half of the domain (Figure 27C). This highly basic patch suggests that C1ζ may compensate for its inability to bind DG by increasing its affinity for anionic lipid, in particular, PS.

Binding of C1bβ and C1ζ to Phosphatidylserine-Containing Membranes

In order to test the intrinsic affinity of C1ζ for PS, its ability to bind to vesicles containing 50 mol% PS and 50 mol% PC was compared with that of C1bβ. For these studies, GST-tagged C1ζ and C1bβ were used, as C1ζ is extremely insoluble in isolation. GST-tagged C1bβ was also used as a comparison, as this domain, which

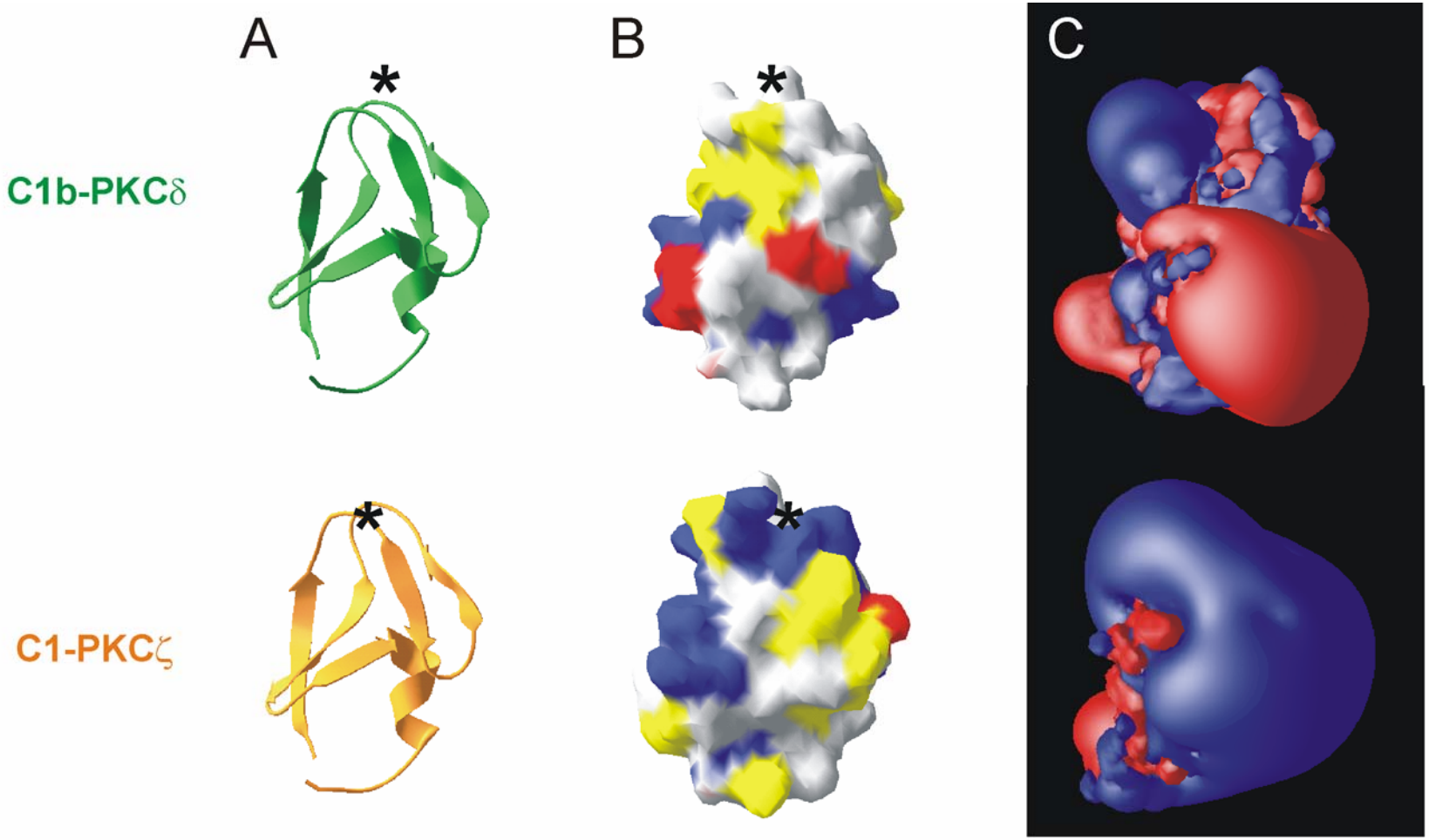


Figure 27. C1ζ has a greater electrostatic potential than C1bδ due to a cluster of basic residues occluding the ligand-binding cavity. *A and B,* re-representation of Figure 7. Structures are rotated 90 degrees to the right relative to those in Figure 7. All coloring is as in Figure 7. *C*, electrostatic potential isocontour of C1bδ (*top*) and C1ζ (*bottom*). Negative contours are colored in *red*; positive in *blue*.

binds both DG and PS, is often used as a prototypical C1 domain and, as such, has been extensively biochemically characterized (24,53,55,60). In fact, C1bβ and C1bδ have very similar electrostatic potential maps (Figure 28), suggesting that many typical C1 domains share a similar electrostatic potential. The data in Table 8 reveal that GST-tagged C1bβ and C1ζ bind to vesicles containing 50 mol% PS and 50 mol% PC with similar affinity. In fact, despite C1ζ having a higher pI and greater electrostatic potential (Figure 27C), GST-C1ζ binds with 5-fold lower affinity to these vesicles than does GST-C1bβ (Table 8, apparent $K_d = 4.9 \pm 0.8$ *versus* 1.10 ± 0.05 mM, respectively). Therefore, the higher electrostatic potential of C1ζ does not compensate for its inability to bind DG by increasing its intrinsic affinity for PS-containing membranes.

Binding of C1ζ to a Panel of Phosphoinositides and Phospholipids

Several studies have suggested that PKCζ can be regulated by ceramide and anionic lipids, including PS, phosphatidic acid, and the phosphoinositides, in particular PIP_3 (see above and (27)). However, none of these studies show direct binding to acidic phospholipids via the C1 domain. Figures 26 and 27 established that the C1 domain of PKCζ has a large electrostatic potential due to a large basic patch, suggesting that the domain would readily bind anionic lipids. However, data in Table 8 showed that the intrinsic affinity of C1ζ for PS-containing membranes is not substantially higher than that of a domain with a lower electrostatic potential. Thus, the isolated C1ζ domain was tested for binding to a panel of other phospholipids,

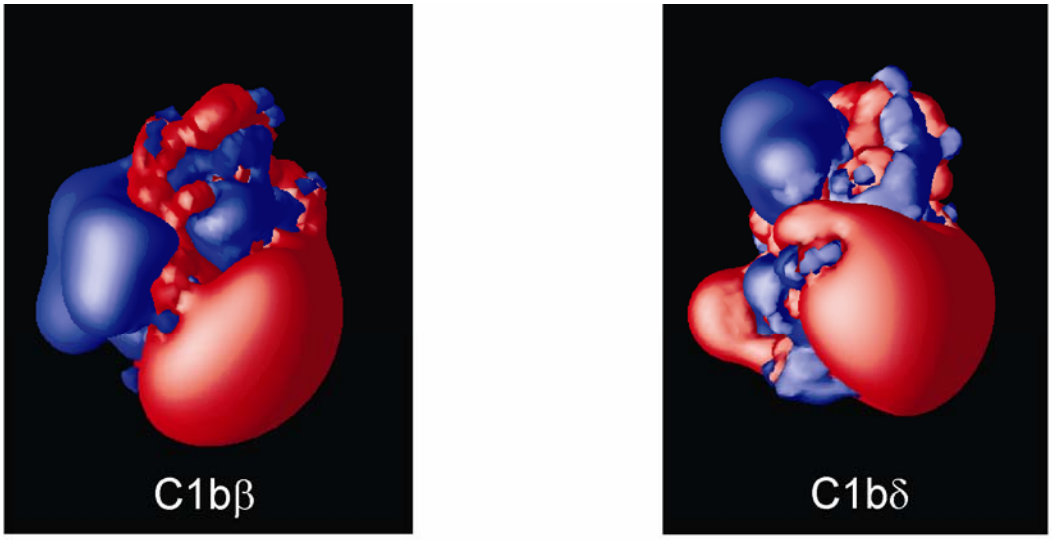


Figure 28. C1bβ and C1bδ have similar electrostatic potential maps. Electrostatic potential isocontour of C1bβ (*left*) and C1bδ (*right*). Negative contours are colored in *red*; positive in *blue*.

Table 8. Binding affinity for the interaction of the C1bβ and C1ζ with PS-containing membranes. Apparent K_d values were calculated according to the following equation: % bound = [Lipid]/([Lipid] + K_d). Data shown here are for 7.4 mM lipid consisting of 50 mol% PS and 50 mol% PC as small unilamellar vesicles. Apparent K_d (in μM) is presented as the average of three experiments ± *S.E.*

C1 Domain	Bound, percent maximal	Apparent K_d (mM)
GST-C1bβ	87 ± 4	1.10 ± 0.05
GST-C1ζ	60 ± 10	4.9 ± 0.8

including several PIs.

Figure 29 shows the results of an overlay assay in which YFP-tagged C1ζ was screened against a panel of phospholipids and PIs. YFP-tagged C1ζ was not found to interact with any tris-, bis-, or monophosphorylated PIs (Figure 29). Neither did C1ζ interact with the charge-neutral phospholipids phosphatidyldimethylethanolamine (PDME), phosphatidylmonomethylethanolamine (PMME), phosphatidylethanolamine (PE), or phosphatidylcholine (PC) or the anionic phospholipids sphingosine-1-phosphate (S1P) and phosphatidic acid (PA). The specificity of this assay was confirmed by testing four control proteins with known specificity for a variety of PIs. Thus, taken together with the previous sections, the isolated C1 domain of PKCζ does not bind with appreciable affinity to a variety of anionic lipids, including PS, S1P, PA, and an array of PIs.

Conclusions

In this study, a model for the "atypical", non-DG-binding C1 domain of the atypical PKCζ is derived. The data show that C1ζ has a more positive electrostatic potential than its counterparts in PKCβI/II and PKCδ, primarily due to a large number of substitutions of polar and nonpolar amino acids in the latter for basic amino acids in the former. It may be hypothesized that this increase in electrostatic potential helps to regulate PKCζ by increasing its intrinsic affinity for PS in the absence of DG; however, C1ζ does not bind with any higher affinity to PS than does C1bβ, nor does it bind with appreciable affinity to a variety of other negatively-charged lipids. Thus, it

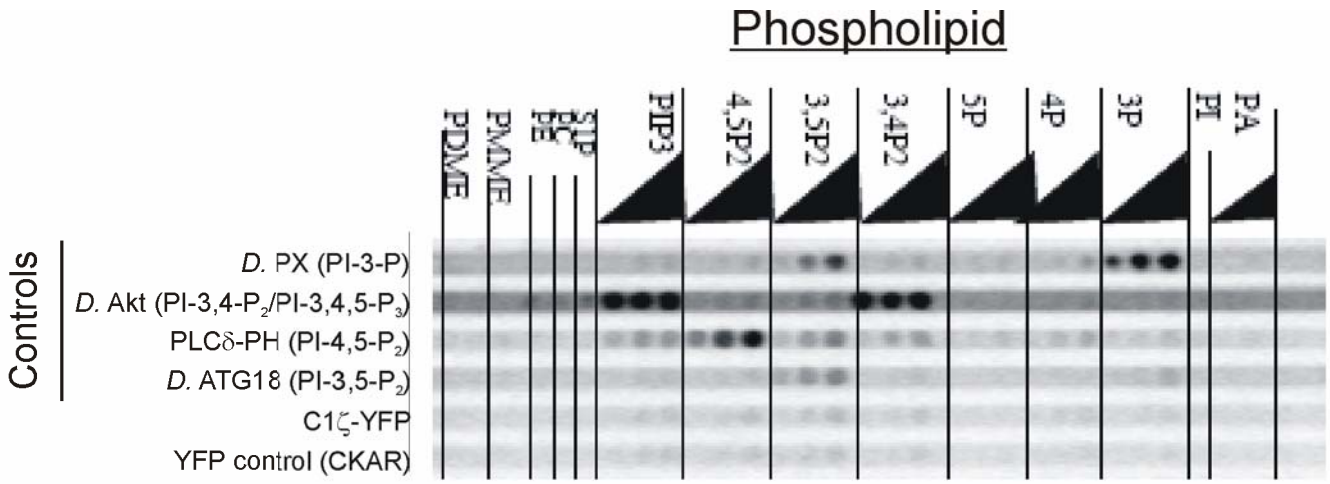


Figure 29. C1ζ does not bind to a panel of phospholipids. Modified PIP strip assay in which select phosphoinositides were blotted in increasing concentrations from left to right. Also tested are phosphatidyldimethylethanolamine (PDME), phosphatidylmonomethylethanolamine (PMME), phosphatidylethanolamine (PE), phosphatidylcholine (PC), sphingosine-1-phosphate (S1P), and phosphatidic acid (PA). The top four proteins tested are positive controls, with the specific phosphoinositide to which they bind in parentheses. Also tested is a negative control, CKAR, to test for any interactions with YFP.

appears that C1 domain of PKCζ does not directly interact with, nor is directly regulated by, phospholipids – in particular, phosphoinositides – *in vitro*.

One of the earliest experimental attempts at explaining the inability of atypical C1 domains to bind DG identified Pro11 as a potentially critical residue, as this was the only residue out of the 13 consensus residues that was lacking in the C1 domain of PKCζ. However, mutation of this residue (Gly11) to Pro did not restore the ability to bind phorbol ester, suggesting that other residues were critical for this interaction. The modeling studies presented here indicate that the more critical determinants for lack of DG binding are the basic residues that sterically occlude the ligand-binding pocket.

Indeed, Blumberg and coworkers recently used a combination of modeling and mutagenesis to dissect out which residues make the C1b domain of PKCδ "typical" and which make the C1 domain of PKCζ "atypical" (54). Similar to the modeling studies above, the authors found that C1ζ adopts a fold quite similar to that of C1bδ. The Blumberg study, too, finds a cluster of positively charged amino acid substitutions in the second loop that forms the ligand-binding pocket. The study notes that these substitutions block the ligand-binding cavity and increase the net charge on the domain. These authors, however, pinpoint four residues – Arg7, Arg10, Arg11, and Arg20 – that block phorbol ester binding only if done in combination, but not as single mutations. Interestingly, these authors find that when the corresponding residues in C1bδ are mutated to Arg, the resulting domains bind PS with higher affinity (54), an observation that directly opposes the results presented here which shows that C1bβ and C1ζ bind to anionic membranes with approximately equal affinity (Table 8). The

best explanation for this discrepancy is that the experiments above look at intrinsic PS affinity in the absence of ligand, whereas Pu, *et al.* perform their experiments in the presence of the phorbol ester PDBu. Moreover, the increase in PS sensitivity was seen for the single mutants, although only the quadruple mutant shows reduced PDBu binding comparable to that of C1ζ (54). Thus, it appears that while Arg substitutions in the C1b domain of PKCδ may increase its sensitivity to PS, the C1 domain of PKCζ does not appear to have a higher intrinsic affinity for PS in the absence of phorbol ester or DG.

The data in Figure 29 support no direct binding of the C1 domain of PKCζ to a panel of lipids. Yet several lipids have been shown to activate of PKCζ *in vitro* and *in vivo* (27). For example, several initial reports identified ceramide as a direct activator of PKCζ (94,95), while others found no direct activation by ceramide (98). Later reports, however, showed an indirect effect of ceramide on PKCζ signaling through PI3K (93,96,97). Another report showed direct activation of PKCζ by PIP_3 *in vitro* (92); such activation is direct in catalysis and independent of the PDK-dependent activation loop phosphorylation, as purified PKCζ is constitutively phosphorylated at this position (98). However, many of these studies use highly basic substrates, offering the possibility that these highly anionic lipids function through optimal presentation of PKCζ substrates and/or through binding of the highly basic pseudosubstrate to remove it from PKCζ's active site (27). Perhaps the most convincing explanation for all of these observations is the effect of phosphoinositides on activation of PDK, the upstream kinase of the PKC family that phosphorylates the

activation loop and primes PKC for catalysis (27).

While the dot blot presented in Figure 29 is an admittedly artificial way to detect interactions with PI-binding proteins, the control proteins tested provide evidence that meaningful interactions can be extracted. The controls tested have affinities for their cognate PIs in the 0.1 to 10 μM range (100-104). This suggests that if, in fact, C1ζ does bind to PIs or the other represented lipids, the affinities for such ligand is in the high micromolar range to millimolar range, making such an interaction highly unlikely *in vivo*. Moreover, the inability of the C1 domain to bind these lipids on its own does not rule out the possibility of direct binding of these lipids to the full-length kinase or to other subdomains of PKCζ. Experiments based on binding to phospholipids would clarify what interactions with phospholipids, if any, are direct and eliminate affects of the phospholipids on activity and presentation of substrate (see previous paragraph).

If the C1 domain of PKCζ does not directly bind a specific lipid second messenger, why might atypical PKCs retain a C1 domain? Atypical PKC C1 domains have been shown to be an important site for interactions with other proteins, some of which activate the C1-domain-containing protein (26,27,105). For example, the C1 domain of Raf plays an autoinhibitory role; this autoinhibition is relieved through interaction with Ras via its C1 domain (106,107). Such an interaction might still expose a PS-binding site so as to give the appearance of activation by PS, although only in concert with its binding interaction with Ras (56,108). Indeed a similar situation might occur with the C1 domains of atypical PKCs, as both activators (e.g. LIP, *l*ambda-*i*nteracting *p*rotein) and inhibitors (e.g. Par-4, *p*rostate *a*ndrogen

*r*esponse-4) can bind to and affect PKCι/λ and ζ activity (26). Another possible explanation for the retention of a "non-functional" C1 domain is described in a report that identified nuclear localization and export signals (NLS and NES, respectively) in the C1 domain and linker region between the C1 and catalytic domains (109). Such a finding provides the intriguing possibility that the C1 domain has a critical function in localization, specifically in the nucleocytoplasmic shuttling of atypical PKCs.

The data presented here show that despite a high electrostatic potential for interaction with anionic partners, the C1 domain of PKCζ does not have a higher affinity for PS than the C1b domain of PKCβI/II, nor does it interact directly with a variety of negatively-charged lipids. Therefore any regulation of PKCζ by phospholipids and/or phosphoinositides appears to be either indirect or mediated by other domains of the kinase. Thus, the direct regulation of PKCζ by lipid second messengers remains a controversial puzzle.

Acknowledgement

Thank you to Dr. Seth Field, who performed the phospholipid dot blot in Figure 29. Thank you also to Mrs. Lisa L. Gallegos for preparation of the YFP-C1ζ and CKAR constructs used for the phospholipid dot blot in Figure 29.

CHAPTER 5: SUMMARY AND CONCLUSIONS

The results presented here have explored the molecular properties of protein kinase C (PKC)'s C1 domain and its interaction with lipid membranes. First, design of a fluorescent reporter has allowed the dissection of the kinetics of the interaction of the C1 domain with membranes with respect to both phosphatidylserine (PS) and diacylglycerol (DG) or phorbol ester (PMA). PS functions by driving the C1 domain's diffusion-limited recruitment to membranes. However, this interaction is relatively insensitive to ionic strength. While specific interactions are partly responsible for retention of the C1 domain at membranes, the rate of dissociation is primarily driven by hydrophobic interactions with the ligands DG or PMA, with a 200-fold higher retention rate for PMA-containing vesicles. When PMA is the ligand, hydrophobic contributions far outweigh electrostatic contributions from PS. Due to the difference in free energy as calculated from the dissociation constants for both PMA and DG, PMA appears to make somewhere between two and six more van der Waals interactions with the C1 domain than does DG. Finally, the nature of the interaction of the fluorescent probe with membranes provide further biochemical evidence that the tip of the C1 domain does not penetrate much farther than the phospholipid headgroup. This kinetic analysis allows the formation of a new model for the interaction of the C1 domain with lipid membranes.

Next, a conserved point mutation has been identified that allows regulation of the domain by diacylglycerol. Position 22 in the consensus sequence of all C1 domains is typically tryptophan; the C1b domains of conventional PKC isoforms,

however, contain tyrosine at this position. The results presented here show that Trp at position 22 increases the affinity of the C1 domain 30-fold over domains containing Tyr; however, both domains bind PMA with nearly identical affinity. The *in vitro* results are recapitulated *in vivo*, as Trp-containing C1 domains translocate to the membrane in response to agonist-stimulated DG production, while Tyr-containing domains remain unresponsive. Moreover, the incorporation of Trp into position 22 of the C1b domain of full-length PKCβII increases Ca^{2+}-independent PKC activity to a level approaching that of PKCδ. This position also appears to be critical for the pre-targeting of individual domains and the novel PKCδ to Golgi membranes. Finally, modeling studies reveal that due to differences in the way the two amino acids partition into the water/lipid bilayer interface, the Tyr-containing C1b domains of conventional isoforms have a wider and shallower ligand-binding pocket in which only the larger PMA can bind. On the other hand, the remaining Trp-containing C1 domains DG-activated PKC isoforms have a narrower, deeper pocket to allow the binding of both DG and PMA. These studies have helped to explain why 1) the C1 domains of novel PKC isoforms bind with two orders of magnitude higher affinity than those of conventional isoforms and 2) the conventional isoforms require a C2 domain for pre-targeting to membranes.

Finally, the structure and function of an atypical, non-diacylglycerol-binding C1 domain has been explored. Homology modeling shows that the atypical C1 domain of the atypical PKCζ has a fold most similar to the C1b domain of PKCδ. A number of basic residues replace small, uncharged residues to sterically occlude the ligand-binding site. This large number of basic residues greatly increases the

electrostatic potential of the C1 domain, suggesting that the domain may have a higher affinity for anionic membranes than that of typical C1 domains. The results presented here, however, show that the C1 domain of PKCζ does not have a higher intrinsic affinity for anionic membranes that a typical C1 domain; nor does it bind to a panel of other phospholipids. Therefore, the C1 domain of PKCζ does not directly bind to anionic membranes, suggesting that the determinants for the regulation of PKCζ by anionic lipid reside elsewhere on the full-length kinase.

Significance

Protein kinase C (PKC) is a critical component of a myriad of signaling pathways (1), and its chronic activation can lead to the promotion of cancer (6). The activation of PKC is achieved through the membrane-dependent engagement of its regulatory region. A common domain within the regulatory region to all PKCs is the C1 domain. The C1 of conventional and novel isoforms binds to membranes in response to the presence of its physiological ligand, DG. Moreover, phorbol esters chronically activate PKC as potent DG analogs. Therefore, the understanding of PKC activation through its C1 domain is critical to the understanding of PKC's role in biological signaling pathways, particularly cancer.

The foregoing results have defined the molecular mechanisms driving the interaction of the C1 domain with lipid membranes. Figure 30 depicts the three key findings contained in the work presented here. First, the data in Chapter 2 support a model by which the C1 domain is recruited to membranes in a diffusion-limited manner; this recruitment is driven by long-range, non-specific electrostatic

interactions between the C1 domain and anionic membranes (*Step Ia*). Once at the membrane, the initial weak encounter complex is coupled to a second step in which the C1 domain searches in two dimensions for its ligand, DG (*Step Ib*). This second step is rapid due to a reduction in dimensionality and contains a component guided by specific interactions with the anionic lipid PS. Finally, release of the domain from membranes is primarily determined by the rate-limiting dissociation of the C1 from its ligand(s) DG or PMA, a process that is governed primarily by hydrophobic interactions (*Step Ib*). Second, the data in Chapter 3 identify tryptophan at position 22 of the C1 domain as a critical determinant in the regulation of the domain by diacylglycerol. Tyrosine at this position, as occurs in all C1b domains of conventional PKC isoforms, does not allow the C1 domain to respond to DG; tryptophan at this position, however, as occurs for all other DG-responsive C1 domains, sensitizes the domain to agonist-stimulated increases in DG production (*Step IIa*). PMA, however, binds equally well to both domains (*Step IIb*). Tryptophan also pre-targets the C1 domain to endomembranes, whereas tyrosine releases the domain into the cytosol for signaling at the plasma membrane (*Step IIc*). Third, the data in Chapter 4 reveal that the atypical C1 domain of PKCζ cannot bind ligand due to a cluster of basic residues blocking the ligand-binding site (*Step IIIa*). The increase in electrostatic potential due to these basic substitutions does not allow additional regulation by anionic phospholipids (*Step IIIb*).

Thus, the interaction of the C1 domain with membranes is governed by a variety of molecular properties, the manipulation of which subtly modulates the strength of this interaction. In particular, the data here provide two mechanisms for

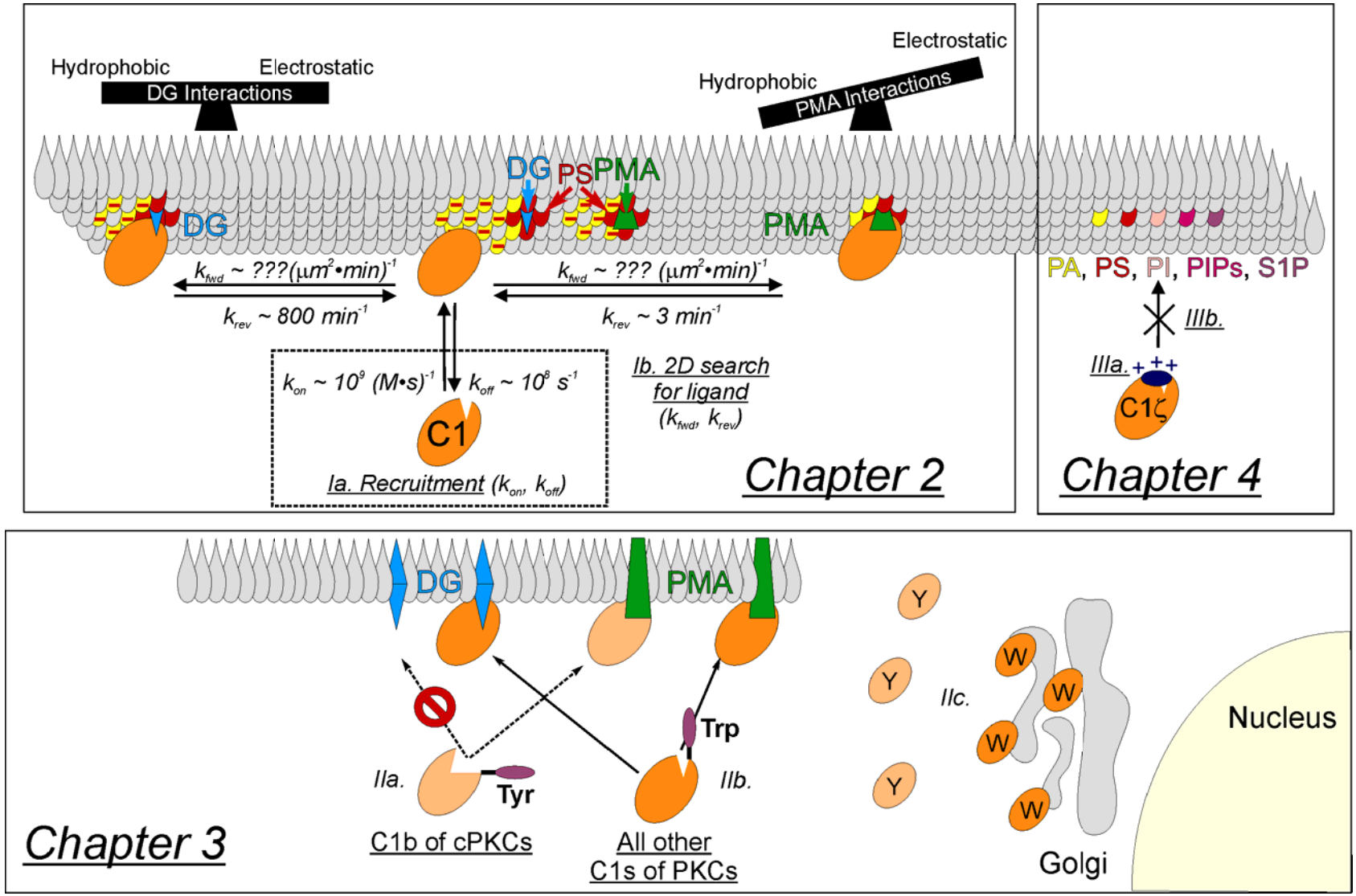
the potency of PMA in the promotion of cancer: chronic activation of PKC by 1) high retention rates at the membrane (Chapter 2) and 2) non-discriminate binding to all C1 domains, including those that do not bind to DG (Chapter 3). Moreover, the emphasis placed on hydrophobic contacts with the mostly nonpolar ligand sets the C1 domain apart from the other lipid-targeting molecules, most of which normally have highly charged or polar ligands, such as PKC's C2 domain that uses Ca^{2+} to bind to membranes and the PH and FYVE domains that bind phosphoinositides. Therefore, the data presented in this dissertation detail the activation of PKC through its C1 domain and provide insights for the rational design of PKC-based therapeutics.

Figure 30. Summary of the results from Chapters 2 through 4.

Upper left: The data in Chapter 2 analyzes the kinetics of the interaction of the C1 domain with lipid membranes. The data reveal that the C1 domain binds to DG- or PMA-containing membranes via a two-step process: weak membrane association coupled to a rapid two-dimensional search for its membrane-bound ligand. The diffusion-limited association of the C1 domain is driven by non-specific electrostatic interactions with anionic lipid, independent of DG or PMA as the ligand (Ia, dashed box). Once at the membrane, the C1 domain very rapidly scans in two dimensions for its ligand, DG or PMA (Ib). Specific electrostatic interactions between the C1 domain and PS or PG guide the rapid association, while hydrophobic interactions with its ligand (i.e., DG or PMA) dictate the retention time for the C1 domain's residence at membranes. Specifically, the C1 domain is released ~200 times faster when DG is the ligand, with a delicate balance of electrostatic and hydrophobic interactions governing the C1 domain's affinity for membranes. PMA, however, sequesters the C1 domain at the membrane through extensive hydrophobic contacts, such that hydrophobic contacts outweigh electrostatic contributions in the C1 domain's affinity for membranes.

Bottom: The data in Chapter 3 identify a single residue as a critical regulator for the ability of the C1 domain to bind DG. Most PKC C1 domains contain tryptophan at position 22 (consensus numbering), whereas the C1b domains of conventional isoforms contain tyrosine at this position (Figures 3 and 20). Tyrosine at position 22 lowers the affinity of the C1 domain for DG without affecting its affinity for PMA; in so doing, these C1 domains bind with weak affinity to DG in vitro but are unresponsive to physiological generation of DG in vivo (IIa). Trp-containing C1 domains, on the other hand, bind equally well with high affinity to both DG and PMA; as such, these domains do respond to agonist-stimulated production of DG (IIb). Modeling suggests that tyrosine interacts differently with the membrane so as to widen the ligand-binding cavity; DG can no longer bind, although the larger PMA can span the width of the gorge. Both DG and PMA, however, can fit into the more narrow binding groove of Trp-containing C1 domains. Moreover, C1 domains that contain Tyr (Y) at this position are localized in the cytosol, whereas Trp (W)-containing C1 domains are pre-targeted to endomembranes, such as the Golgi (IIc).

Upper right: The data in Chapter 4 reveal that the atypical C1 domain of PKCz cannot bind DG or PMA due to several substitutions of small, uncharged amino acids with large, positively-charged residues. These positively-charged substitutions sterically occlude the ligand-binding pocket (IIIa). The resulting basic patch does not allow for an increased intrinsic affinity for a variety of phospholipids (IIIb), including phosphatidic acid (PA), phosphatidylserine (PS), phosphatidylinositol (PI), poly-phosphorylated PIs (PIPs), or sphingosine-1-phosphate (S1P).


Hydrophobic
Electrostatic
DG Interactions
Electrostatic
Hydrophobic
PMA Interactions
DG
PS
PMA
DG
PMA
k_{fwd} ~ ???(μm^2•min)$^{-1}$
k_{rev} ~ 800 min^{-1}
k_{fwd} ~ ??? (μm^2•min)$^{-1}$
k_{rev} ~ 3 min^{-1}
k_{on} ~ 10^9 (M•s)$^{-1}$
k_{off} ~ 10^8 s^{-1}
C1
Ia. Recruitment (k_{on}, k_{off})
Ib. 2D search for ligand (k_{fwd}, k_{rev})
Chapter 2
PA, PS, PI, PIPs, S1P
IIIb.
IIIa.
C1ζ
Chapter 4
DG
PMA
Y
Y
Y
IIc.
W
W
W
W
Nucleus
Golgi
Trp
IIa.
Tyr
IIb.
C1b of cPKCs
All other C1s of PKCs
Chapter 3

APPENDIX: EXPERIMENTAL

I. Materials

1-palmitoyl-2-oleoyl-*sn*-glycero-3-phosphocholine (POPC), 1-palmitoyl-2-oleoyl-*sn*-glycero-3-phospho-L-glycerol (POPG), 1-palmitoyl-2-oleoyl-*sn*-glycero-3-phospho-L-serine (POPS), and 1,2-*sn*-dioleoylglycerol (DG) in chloroform were purchased from Avanti Polar Lipids, Inc. L-α-dipalmitoyl,[2-palmitoyl-9,10-^{3}H(N)]-phosphatidylcholine (60 Ci mmol^{-1}) was purchased from American Radiochemical Co. γ-^{32}P-ATP was purchased from PerkinElmer, Inc. DNase I, thrombin, phorbol-12-myristate-13-acetate (PMA), phorbol-12,13-dibutyrate (PDBu), BAPTA/AM were purchased from CalBiochem. The pGEX-6P3 vector (Amersham Pharmacia Biotech), glutathione-Sepharose 4B, and PreScission Protease were purchased from Amersham Biosciences. Electrophoresis reagents were purchased from Bio-Rad Laboratories, Inc. Oligonucleotides used in PCR were purchased from GenBase, Inc. Restriction enzymes were purchased from New England Biolabs, Inc. All other reagents and chemicals were reagent-grade. The pH of all buffers was taken as the reading at room temperature (~25 °C).

II. Methods

Cloning of Protein Kinase C and C1 Domains

Rat C1bβ was subcloned into pGEX-KG for bacterial expression as described previously (24). Murine C1bδ (Gln221 to Ala290) was subcloned into the BamHI and SalI sites pGEX-6P3. Human C1ζ (Arg120 to Pro189) was subcloned into the BamHI and HinDIII sites of pGEX-KG. PM-CFP (MyrPalm-CFP) was constructed as described previously (110). C1b-YFP constructs were made by fusion of monomeric YFP to the 3' end of the C1b domain of PKCβ (Pro93 to Gly152) or PKCδ (Phe225 to Gly281) in pcDNA3. Full-length PKC-YFP constructs were made by fusion of monomeric YFP to the 3' end of rat PKCβII or murine PKCδ in pcDNA3.

Mutagenesis

All mutagenesis was performed using QuikChange site-directed mutagenesis (Stratagene, Inc.) according to manufacturer's instructions. For bacterial purification and imaging experiments, the Y123W and W252Y mutations were introduced, respectively, into the C1b domains of PKCβII and PKCδ as described previously (55).

Bacterial Production of Recombinant Protein and Bacterial Cell Lysis

Wild-type C1bβ was expressed in the BL21-pLysS strain of bacteria and purified as described previously (24). An overnight culture was expanded 1:10 in fresh Luria broth media containing 1X antibiotic. Cultures were shaken to an optical

density of 0.3-1.0 at 600 nm before induction with 0.3 mM (final concentration) isopropyl-β-D-thiogalactopyranoside. 10 μM (final concentration) zinc sulfate was also added at the time of induction. Cultures were shaken for 4 hours at 25 °C before pelleting at 6,000 x g for 15 minutes at 4 °C. Cell pellets were transferred to 50 ml polypropylene conical tubes for storage at -80 °C.

Cell pellets were rocked for 1 hour at 4 °C in lysis buffer containing the following: 50 mM Tris, pH 7.8, 200 mM NaCl, 1 mM EDTA, 0.4 mM phenylmethylsulfonylfluoride (PMSF), 2 mM benzamidine, 40 μg/ml leupeptin, 5 mM DTT, and 1 mg/ml lysozyme. Cell suspensions were then rocked for another 30 minutes at 4 °C after addition of 1 mM $MgCl_2$, 1 mM $MnCl_2$, and 100 μg/ml DNase I (final concentrations). A Dounce tissue homogenizer was used to homogenize the resulting cell suspensions before lysis by either French press or syringe. Syringe lysis was achieved by two passages successively through needles of gauge 18 ½ G, 20 ½ G, 22 ½ G, 25 ½ G, and 27 ½ G. Resulting lysates were spun down at 10,000 x g for 30 minutes at 4 °C.

Purification of C1 Domains

Bacterial cell lysates were passed slowly over glutathione-Sepharose beads in a disposable column at room temperature. Beads were washed extensively with at least three bed volumes of column buffer containing 50 mM Tris, pH 7.8, 200 mM NaCl, and 1 mM EDTA at room temperature. Glutathione-*S*-transferase (GST)-tagged C1bβ was purified by elution from these beads in column buffer supplemented with 10 mM

glutathione. Untagged C1bβ were purified by on-column cleavage with thrombin in column buffer overnight at 4 °C according to manufacturer's instructions. Subsequent elutions were conducted at room temperature. Fractions were qualitatively tested for protein content using BioRad reagent. GST-tagged and untagged C1bβII-Y123W and C1bδ domains were purified similarly, with the substitution of PreScission Protease for thrombin. Fractions of recombinant protein were pooled, spun at 80,000 x g at 4 °C for 15 minutes to remove insoluble material, and cleaned to homogeneity through passage over a Superdex 75 10/300 GL column at 4 °C using the BioLogic HR chromatography system (Bio-Rad Laboratories, Inc.). Samples were concentrated in Centriprep and Centricon devices using a 3,000 Dalton molecular weight cutoff (Millipore). Protein concentrations were determined by dissolution in 5 M guanidinium hydrochloride and using absorbance at 280 nm and the Beer-Lambert law, where ε^{1M}_{280} was calculated, in $M^{-1}cm^{-1}$, from the number of tryptophan residues x 5690 plus the number of tyrosine residues x 1280 plus the number of cysteine residues x 120.

Lipids

Phospholipids were purchased as chloroform stock solutions and stored at -20 °C. Concentrations for all phospholipid stock solutions were determined by a phosphate analysis modified from (111). From 0 to 7 µl of stock phospholipid of unknown concentration and from 0 to 7 µl of known phosphate concentration (1 to 100 mM Na_2HPO_4) were placed into disposable borosilicate glass test tubes. 100 µl of

5 M (10 N) sulfuric acid was added to each tube, and all samples were heated at 150 °C for at least three hours. 30 µl of a 30% hydrogen peroxide solution (kept at 4 °C) was added to each tube, and the reaction was heated for an additional 90 minutes at 150 °C. Samples were removed from heat, and 920 µl of 0.22% (w/v) ammonium molybdate tetrahydrate and 50 µl of 10% (w/v) ascorbic acid were added to each tube, after which the reactions were heated at 100 °C for an additional 15 minutes. Reactions were diluted fourfold with distilled water, and 1ml aliquots were assayed for absorbance at 830 nm, using one 0 µl tube as a representative blank for all samples. Absorbance was plotted against the volume of solution added, and linear regression analysis was performed on the resulting plots. The concentration of stock phospholipid (in mM) was then calculated as the concentration of known phosphate standard (Na_2HPO_4, in mM) multiplied by the slope of the unknown divided by the slope of the known standard. Dioleoylglycerol (DG) stock concentrations were assumed to be that indicated from the manufacturer. Lipid concentrations were converted to vesicle concentrations by assuming 90,000 lipids per vesicle (112).

Preparation of Lipid Vesicles for Stopped-Flow Spectroscopy

Lipid vesicles were prepared as described elsewhere (60). Volumes of lipid stocks in chloroform required for the desired mole percent of a given phospholipid were transferred to disposable flint glass tubes using a dialamatic microdispenser (Drummond Scientific Co.). PMA was included as a lipid component in the calculation of the mole percent of each desired lipid. Phosphatidylcholine (PC) was used as a neutral diluent to comprise the remaining mole percent of phospholipid. The

mixture was dried to a thin, transparent film under a gaseous nitrogen stream, and the sample was further evacuated of all solvent under a vacuum for at least two hours.

Lipids were resuspended in KCl buffer (100mM KCl, 20mM HEPES, pH 7.5) to yield approximately 1 to 100 mM lipid. The solution was vortexed until the film has been completely removed from the sides of the tube, after which the lipid solution was subjected to five freeze-thaw cycles of -80 °C and approximately 50 °C. The resulting suspension was extruded to form vesicles 100 nm in diameter by twenty passages through two 100 nm pore size polycarbonate filters using a mini-extruder (Avanti Polar Lipids, Inc.) according to manufacturer's instructions. Resulting extruded vesicle solutions were stored at room temperature. The final concentration of phospholipid was determined by phosphate analysis as described above. Concentrations of vesicles in which DG was a component were calculated by dividing the phospholipid concentration by a factor of (1 minus the mole fraction of DG).

Preparation of *S*ucrose-*L*oaded Lipid *V*esicles (SLVs)

Vesicles containing an internal solution of sucrose were prepared in a manner similar to that outlined above and as described in (58). Trace tritium was introduced to the original lipid mixture in the form of tritiated 1,2-dipalmitoyl-sn-glycero-3-phosphocholine (typically 1 to 3 μl per 100 μl final volume of lipid). Dried lipid films were rehydrated in sucrose buffer containing 170 mM sucrose, 20 mM HEPES, pH 7.4 prior to freeze-thaw cycling. Resulting extruded vesicle solutions were washed by bringing the total volume to 1 ml in KCl Buffer (150 mM KCl, 20 mM HEPES, pH 7.5). The washed vesicle solutions were spun at 50,000 x g for 30 minutes at 25 C to

pellet the vesicles. After spinning, enough volume was removed to yield a solution of approximate desired lipid concentration. (This is typically the same volume of KCl Buffer that was used to bring the solution to 1 ml during washing.) Washed vesicle solutions were stored at room temperature. The final concentration of phospholipid was determined by phosphate analysis as described above. Concentrations of vesicles in which DG was a component were calculated by dividing the phospholipid concentration by a factor of (1 minus the mole fraction of DG).

Incorporation of PMA into Vesicles

PMA stock solutions were prepared by dissolution in dimethylsulfoxide. PMA was incorporated into lipid vesicles by addition of a PMA stock solution to a vesicle solution, followed by 30 seconds of rapid vortexing. The vesicle solutions were then incubated for at least 30 minutes at room temperature prior to use to ensure incorporation of all PMA.

Steady-State Fluorimetry

Steady-state tryptophan fluorescence data were collected using a Jobin (Edison, NJ) Yvon-SPEX FluoroMax-2 fluorescent spectrometer using constant wavelength analysis. Data were collected in triplicate at 25 °C by excitation at 280 nm and monitoring emission at 340 nm (monochrometer band pass widths set at 5 nm) with a 1 second integration time and 1% error (maximum of 5 trials). Solutions were successively added to a 10 mm rectangular quartz cuvette (Starna Cells, Inc.) and were allowed to equilibrate for at least 2 minutes before recording fluorescence. A circular

magnetic stir bar at the bottom of the quartz cuvette was used to mix solutions. The cuvette and stir bar were prepared by washing for at least 10 minutes in 10 mM EDTA, followed by rinsing with methanol. These were then rinsed with distilled water and dried in a 50 °C oven before use. Experiments were conducted in triplicate, from which the mean emission intensity and standard error were calculated. The mean emission intensity was corrected for differences in volume before plotting data.

Sucrose-Loaded Vesicle (SLV) Assay

The binding of the C1b domain to sucrose-loaded large unilamellar vesicles was measured as described previously (58) with modification. After vesicles were incubated with PMA as described above, 45 μl of 10X lipid solutions were prepared in polycarbonate centrifuge tubes (Beckman Coulter, Inc.). Lipid concentrations were chosen so as to span from about 20% to 95% bound. Wherever possible, typical concentrations represented ¼, ⅓, ½, 1, 2, 4, and 10 times the apparent K_d (K_d^{app}). A control tube was run in parallel, in which lipid solution was replaced by 45 μl KCl buffer alone. 375 μl of 1.2X standard buffer and 30 μl of 15X protein cocktail were then added to each tube and rapidly vortexed for 2 seconds. Standard buffer consisted of 300 μg/ml BSA, 150 mM KCl, 2 mM $CaCl_2$, 1 mM DTT, and 20 mM HEPES, pH 7.5. Protein cocktail consisted of 300 μg/ml BSA, 100 mM DTT, 20 mM HEPES, pH 7.5, and a 15X concentration of the desired protein, the final concentration of which was at least 10-fold less than the lowest concentration of lipid used.

Samples were incubated for 30 minutes at room temperature, after which they

were spun at 50,000 x g for 30 minutes at 25 °C. Free C1 domain (supernatant) was removed from bound C1 domain (pellet) by removing 337.5 µl of the supernatant. The pellet was rapidly vortexed for at least 15 seconds until no vesicles, as indicated by a change in refractive index, could be seen. 10% of the supernatant (33.75 µl) and the pellet (11.25 µl) were counted for tritium in 2 ml of scintillation fluid. ⅓ of the supernatant (112.5 µl) and pellet (37.5 µl) were run pairwise on 10% Tris-Tricine gels. Gels were silver-stained, and the amount of "bound" and "unbound" domain was quantified by densitometry using a GS-800 Calibrated Densitometer and Quantity One software (Bio-Rad Laboratories, Inc.).

Silver Staining of SDS-PAGE Gels

Stacking gel was excised from SDS-PAGE gels, and the separating gel was fixed for at least 30 minutes in 3:2:5 acetic acid:methanol:water. Gels were washed with gentle shaking with five exchanges of 1:1 ethanol:water for 5 minutes per exchange, with a wash volume no larger than was necessary to cover the gel (typically 100 ml for a gel in a 190 mm crystallization dish). Gels were then washed for 1 minute in water before washing for 90 seconds with Solution I (0.12% sodium thiosulfate). Gels were washed again for 1 minute with water before shaking for 15 minutes in Solution II (0.2% w/v silver nitrate, 0.1% v/v formaldehyde in water, prepared fresh). Gels were then rinsed with two washes of copious amounts (typically 200 ml) distilled water for no more than a total of 60 seconds prior to development. Development was achieved by shaking in Solution III (6% w/v anhydrous sodium bicarbonate, 3% v/v Solution I, and 0.1% v/v formaldehyde). Development was

quenched by exchange with 200 ml 10% acetic acid for at least 20 minutes.

Data Analysis for Sucrose-Loaded Vesicle Assay

The fraction of bound domain was calculated as in (58) and was plotted against the concentration of vesicles. Curves were fitted to the equation

$$\text{fraction bound} = (n * [L]^H)/([L]^H + K_d{}^H) + \text{int} \qquad \text{(Eq. 1)}$$

where K_d is the apparent equilibrium constant, *[L]* is the lipid concentration, *H* is the Hill coefficient, *n* is the range of apparent % bound, and *int* is the *y*-intercept. This equation allowed normalization of the data to encompass 0 to 100% bound by subtracting *int* from the calculated fraction bound and dividing the result by *n*. This curve was then fitted to the equation

$$\text{fraction bound} = [L]^H/([L]^H + K_d{}^H) \qquad \text{(Eq. 2)}$$

where terms represent the same parameters as in *Eq. 1*. Experiments were performed in triplicate. Measurements at each lipid concentration were averaged, and one master weighted plot of the form of *Eq. 2* was fitted to these data points with their associated standard errors (*S.E.*). All curve fitting was performed with KaleidaGraph v5.32.

Stopped-Flow Fluorescence Spectroscopy

Kinetic measurements were measured using an Applied Photophysics Π*-180 stopped-flow fluorescence spectrometer (Leatherhead, U.K.) as described previously (65,113). Lipid concentrations were chosen to be similar to those used in the equivalent sucrose-loaded vesicle assay (see above). Final protein concentrations for association experiments were chosen to be at least 10-fold below the lowest lipid

concentration tested. All experiments were temperature-controlled through the use of a 25 °C circulating water bath. All solutions were prepared in Chelex-treated buffer containing 20 mM HEPES, pH 7.5, 150 mM NaCl, 200 μM $CaCl_2$, and 1 mM DTT prior to mixing. Treatment of buffer with Chelex was critical for the acquisition of monoexponential fits for all traces, as untreated buffer often gave irreproducible fits deviating significantly from monoexponential decay. All curve fitting was done using KaleidaGraph v5.32.

Dissociation experiments were conducted in two ways: competition with the non-fluorescent wild-type protein and dilution with buffer. Dilution experiments were performed with lipid vesicles in the following manner: 0.5 μM C1bβ-Y123W was mixed with either 400 μM 5PMA:95PC lipid or 25 μM 5PMA:40PS:55PC lipid (~80% bound in both cases) and allowed to reach equilibrium for 10 minutes at room temperature, after which the mixture was rapidly diluted tenfold in the stopped-flow fluorescence spectrometer with Chelex-treated 20 mM HEPES, pH 7.5, 150 mM NaCl, 200 μM $CaCl_2$, and 1 mM DTT. Lower initial concentrations of C1bβ-Y123W showed qualitatively similar traces, albeit with less signal and more noise.

Competition experiments with lipid vesicles were conducted as follows: 0.1 μM C1bβ-Y123W was mixed with 100 μM lipid containing 5 mol% PMA and 95 mol% PC (~50% bound). Mutant C1 domain was then allowed to equilibrate with lipid vesicles for at least 10 minutes at room temperature before rapid mixing with a solution of a given molar excess wild-type C1bβ in the above buffer in the stopped-flow fluorescence spectrometer. Experiments using 10-, 20-, 50-, and 100-fold molar

excess wild-type C1bβ showed no further change in k_{obs} above 50-fold molar excess (Table 9).

Table 9. Dependence of k_{off} on the ratio of [C1bβ-WT] : [C1bβ-Y123W]. Data are from competition experiments as described in "Materials and Methods." Also shown are residence times, which describe the half-life for the dissociation of C1bb-Y123W from lipid vesicles. Experiments used vesicles composed of 5 mol% PMA and 95 mol% PC (i.e., 0 mol% PS). Values are presented as the average of three experiments ± *S.E.*

[WT] : [Y123W]	k_{off} (s^{-1})	τ (s)
10	0.057 ± 0.005	12 ± 1
20	0.063 ± 0.006	11 ± 1
50	0.0873 ± 0.0009	7.94 ± 0.08
100	0.095 ± 0.007	7.3 ± 0.5

Cell Culture

For imaging experiments, COS7 cells were plated and maintained in Dulbecco's modified Eagle's medium (Cellgro) containing 10% fetal bovine serum and 1% penicillin/streptomycin at 37 °C in 5% CO_2. Cells were plated in sterilized 35-mm imaging dishes at 60% confluency and transfected using FuGENE 6 (Roche Diagnostics). For C1b translocation imaging experiments, cells were cotransfected with PM-CFP and C1b-YFP constructs. For localization experiments, the YFP-tagged constructs were transfected alone. Cells were allowed to grow for 12-24 h post-transfection before imaging. For kinase activity assays, cells were transfected with PKCβII, PKCβII-Y123W, or PKCδ and allowed to grow for 48 h post-transfection before harvesting. All full-length PKC constructs were tagged with YFP on the C-terminus, so that expression could be confirmed by YFP fluorescence.

Protein Kinase C Activity Assay:

Untransfected COS7 cells or COS7 cells transfected with PKCβII, PKCβII-Y123W or PKCδ were lysed on ice for 20 min in 20 mM HEPES (pH 7.5), 0.1% Triton X-100, 1 mM DTT, 1 mM PMSF, 2 mM benzamidine, and 10 μM leupeptin. The lysate was cleared by centrifugation (16,000 x g, 5 min, 25°C). PKC activity in the detergent-soluble supernatant was assayed in a reaction volume of 80 μl by monitoring the rate of phosphorylation of a synthetic peptide substrate in the presence or absence of PS, DG, and Ca^{2+} as described elsewhere (23). The reaction mixture contained 10 μg total soluble protein from cleared lysates, 500 μg/ml PKC-selective peptide, 20 mM HEPES (pH 7.5), 1 mM dithiothreitol, 500 μM ATP (γ-^{32}P-ATP, 100 μCi per reaction), and 25 mM $MgCl_2$. Non-activating conditions contained 20 mM HEPES (pH 7.5) and 2 mM EGTA. Activating conditions contained 140 μM PS, 3.8 μM DG, and either 2 mM $CaCl_2$ (total PKC activity) or 2 mM EGTA (Ca^{2+}-independent PKC activity).

Cell Imaging

Cells were rinsed once with, and imaged in, HBSS (Sigma) containing 1 mM Ca^{2+}. Images were acquired on a Zeiss Axiovert microscope (Carl Zeiss Microimaging, Inc.) using a MicroMax digital camera (Roper-Princeton Instruments) controlled by MetaFluor software (Universal Imaging, Corp.). Optical filters were obtained from Chroma Technologies. Using a 10% neutral density filter, CFP and FRET images were obtained every 10-15 s through a 420/20-nm excitation filter, a

450-nm dichroic mirror, and a 475/40-nm emission filter (CFP) or 535/25-nm emission filter (FRET). YFP emission was also monitored as a control for photobleaching through a 495/10-nm excitation filter, a 505-nm dichroic mirror, and a 535/25-nm emission filter. Excitation and emission filters were switched in filter wheels (Lambda 10–2, Sutter). Integration times were 200 ms for CFP and FRET and 50–100 ms for YFP. Because of cell-to-cell variability in the amount of CFP and YFP expressed, the dynamic range of responses varied from cell to cell. However, treatment with 100 nM phorbol esters caused maximal membrane binding of each domain (Figure 22). Therefore, the responses to DG generation via UTP were calibrated to the dynamic range of the cell by dividing each point by the maximal response elicited by PDBu. Thus, the data are presented in relative translocation units.

Phospholipid Dot Blot

Proteins and membranes were prepared as described previously (114). Briefly, constructs for YFP-tagged C1ζ or CKAR were *in vitro* transcribed and translated with [^{35}S]methionine (Promega TNT coupled transcription/translation system). The ^{35}S-labeled proteins were incubated in 3% (wt/vol) fatty acid–free BSA (Sigma-Aldrich), 0.05% (vol/vol) Tween 20, 150 mM NaCl, 50 mM Tris, pH 7.5, with PVDF membranes spotted with phospholipids. Controls included the PH domain of PLCδ, the *Drosophila* homologs for Akt and ATG18, and a PX-domain containing protein from *Drosophila* with PI-3-phosphate specificity (SWISSPROT ID: Q9VK31). The synthetic diC16:0 phosphoinositides were from Cell Signals, Inc. and were spotted at 180, 60, and 20 pmoles per 100 nl spot. Phosphatidic acid was spotted at 180 and 60

pmoles. Ceramide, PI, sphingosine-1-phosphate, phosphatidylcholine, and phosphatidylethanolamine were each spotted at 180 pmoles. After incubation with ^{35}S-labeled proteins for 2 h at 4°C, the membranes were washed with 0.05% Tween 20, 150 mM NaCl, 50 mM Tris, pH 7.5. Proteins binding to lipid spots were detected by phosphorimaging.

Sequence Alignment and Phylogenetic Analysis

The sequences of the C1 domains of PKC isoforms were aligned using CLUSTALW in the Megalign program from the LaserGene 6 software package (DNASTAR, Inc.). Sequences were taken from Ref. (33) and from Entrez at the National Center for Biotechnology Information (http://www.ncbi.nlm.nih.gov/). Residues that contact ligand in the structure of C1bδ with phorbol were taken from the LIGPLOT file provided through the PDB repository (PDB ID: 1PTR). A phylogenetic tree was also constructed in Megalign.

Modeling

The structure of the C1 domain was visualized and manipulated using Swiss-PdbViewer, v3.7. Coordinates for C1b-PKCγ (1TBN), C1b-PKCδ (1PTQ), and C1-Raf (1FAR) were taken from the PDB repository (PDB IDs in parentheses). The C1 domain of human PKCζ was modeled by homology on the C1 domains of PKCδ (1PTQ), PKCγ (1TBN), DGKδ (1R79), Raf (1FAR), Ksr (1KBE), β2-chimaerin (1XA6), and munc-13 (1Y8F) using Swiss-PdbViewer (115-117). Molecular surfaces were calculated on the ~50 amino acids that comprise the C1 domain as depicted in

Figure 20.

Calculation of pI was performed using the San Diego Supercomputer Center's Biology Workbench (http://workbench.sdsc.edu). Electrostatic potential maps were generated by Adaptive Poisson-Boltzmann Solver (APBS) (118,119). PDB files were converted to .pqr format using the PDB2PQR Service at http://nbcr.sdsc.edu/pdb2pqr/ before being read into APBS. Potential maps were calculated using the following parameters: dime 65x65x65Å; glen 50x50x50; lpbe; $\varepsilon^{solute} = 78.54$, $\varepsilon^{solv} = 1.00$; ions of –1 and +1 charge, each 150mM with 2.0Å radius; surface tension 0.105 kJ/mol/Å^2; temp 298.15 K; solv radius 1.4Å. Potential maps were visualized with OpenDX (http://www.opendx.org).

REFERENCES

1. Newton, A. C. (1995) *J Biol Chem* **270**, 28495-28498

2. Nishizuka, Y. (1986) *Science* **233**, 305-312

3. Takai, Y., Kishimoto, A., Inoue, M., and Nishizuka, Y. (1977) *J Biol Chem* **252**, 7603-7609

4. Mellor, H., and Parker, P. J. (1998) *Biochem J* **332 (Pt 2)**, 281-292

5. Adams, R. A., Liu, X., Williams, D. S., and Newton, A. C. (2003) *Biochem J* **374**, 537-543

6. Koivunen, J., Aaltonen, V., and Peltonen, J. (2005) *Cancer Lett*

7. Newton, A. C. (2004) *Trends Pharmacol Sci* **25**, 175-177

8. Codazzi, F., Teruel, M. N., and Meyer, T. (2001) *Curr Biol* **11**, 1089-1097

9. Inoue, M., Kishimoto, A., Takai, Y., and Nishizuka, Y. (1977) *J Biol Chem* **252**, 7610-7616

10. Takai, Y., Kishimoto, A., Iwasa, Y., Kawahara, Y., Mori, T., and Nishizuka, Y. (1979) *J Biol Chem* **254**, 3692-3695

11. Takai, Y., Kishimoto, A., Iwasa, Y., Kawahara, Y., Mori, T., Nishizuka, Y., Tamura, A., and Fujii, T. (1979) *J Biochem (Tokyo)* **86**, 575-578

12. Kishimoto, A., Takai, Y., Mori, T., Kikkawa, U., and Nishizuka, Y. (1980) *J Biol Chem* **255**, 2273-2276

13. Castagna, M., Takai, Y., Kaibuchi, K., Sano, K., Kikkawa, U., and Nishizuka, Y. (1982) *J Biol Chem* **257**, 7847-7851

14. Creba, J. A., Downes, C. P., Hawkins, P. T., Brewster, G., Michell, R. H., and Kirk, C. J. (1983) *Biochem J* **212**, 733-747

15. Streb, H., Irvine, R. F., Berridge, M. J., and Schulz, I. (1983) *Nature* **306**, 67-69

16. Parker, P. J., Coussens, L., Totty, N., Rhee, L., Young, S., Chen, E., Stabel, S., Waterfield, M. D., and Ullrich, A. (1986) *Science* **233**, 853-859

17. Lee, M. H., and Bell, R. M. (1986) *J Biol Chem* **261**, 14867-14870

18. Knopf, J. L., Lee, M. H., Sultzman, L. A., Kriz, R. W., Loomis, C. R., Hewick, R. M., and Bell, R. M. (1986) *Cell* **46**, 491-502

19. Coussens, L., Parker, P. J., Rhee, L., Yang-Feng, T. L., Chen, E., Waterfield, M. D., Francke, U., and Ullrich, A. (1986) *Science* **233**, 859-866

20. Newton, A. C. (2001) *Chem Rev* **101**, 2353-2364

21. Newton, A. C. (2003) *Biochem J* **370**, 361-371

22. House, C., and Kemp, B. E. (1987) *Science* **238**, 1726-1728

23. Orr, J. W., Keranen, L. M., and Newton, A. C. (1992) *J Biol Chem* **267**, 15263-15266

24. Johnson, J. E., Giorgione, J., and Newton, A. C. (2000) *Biochemistry* **39**, 11360-11369

25. Cho, W., and Stahelin, R. V. (2005) *Annu Rev Biophys Biomol Struct* **34**, 119-151

26. Moscat, J., and Diaz-Meco, M. T. (2000) *EMBO Rep* **1**, 399-403

27. Hirai, T., and Chida, K. (2003) *J Biochem (Tokyo)* **133**, 1-7

28. Kraft, A. S., and Anderson, W. B. (1983) *Nature* **301**, 621-623

29. Kraft, A. S., Anderson, W. B., Cooper, H. L., and Sando, J. J. (1982) *J Biol Chem* **257**, 13193-13196

30. Bittova, L., Stahelin, R. V., and Cho, W. (2001) *J Biol Chem* **276**, 4218-4226

31. Stahelin, R. V., Digman, M. A., Medkova, M., Ananthanarayanan, B., Rafter, J. D., Melowic, H. R., and Cho, W. (2004) *J Biol Chem* **279**, 29501-29512

32. Colon-Gonzalez, F., and Kazanietz, M. G. (2006) *Biochim Biophys Acta*

33. Hurley, J. H., Newton, A. C., Parker, P. J., Blumberg, P. M., and Nishizuka, Y. (1997) *Protein Sci* **6**, 477-480

34. Zhang, G., Kazanietz, M. G., Blumberg, P. M., and Hurley, J. H. (1995) *Cell* **81**, 917-924

35. Hurley, J. H., and Misra, S. (2000) *Annu Rev Biophys Biomol Struct* **29**, 49-79

36. Canagarajah, B., Leskow, F. C., Ho, J. Y., Mischak, H., Saidi, L. F., Kazanietz, M. G., and Hurley, J. H. (2004) *Cell* **119**, 407-418

37. Oancea, E., and Meyer, T. (1998) *Cell* **95**, 307-318

38. Newton, A. C. (1993) *Annu Rev Biophys Biomol Struct* **22**, 1-25

39. Bazzi, M. D., and Nelsestuen, G. L. (1987) *Biochemistry* **26**, 1974-1982

40. Bazzi, M. D., and Nelsestuen, G. L. (1987) *Biochemistry* **26**, 5002-5008

41. Bazzi, M. D., and Nelsestuen, G. L. (1987) *Biochem Biophys Res Commun* **147**, 248-253

42. Newton, A. C., and Koshland, D. E., Jr. (1989) *J Biol Chem* **264**, 14909-14915

43. Orr, J. W., and Newton, A. C. (1992) *Biochemistry* **31**, 4661-4667

44. Orr, J. W., and Newton, A. C. (1992) *Biochemistry* **31**, 4667-4673

45. Lee, M. H., and Bell, R. M. (1989) *J Biol Chem* **264**, 14797-14805

46. Lee, M. H., and Bell, R. M. (1992) *Biochemistry* **31**, 5176-5182

47. Mosior, M., and Newton, A. C. (1998) *Biochemistry* **37**, 17271-17279

48. Johnson, J. E., Zimmerman, M. L., Daleke, D. L., Newton, A. C. (1998) *Biochemistry* **37**, 12020-12025

49. Corbalan-Garcia, S., and Gomez-Fernandez, J. C. (2006) *Biochim Biophys Acta* **1761**, 633-654

50. Dibble, A. R., Hinderliter, A. K., Sando, J. J., and Biltonen, R. L. (1996) *Biophys J* **71**, 1877-1890

51. Sharkey, N. A., Leach, K. L., and Blumberg, P. M. (1984) *Proc Natl Acad Sci U S A* **81**, 607-610

52. Burns, D. J., and Bell, R. M. (1991) *J Biol Chem* **266**, 18330-18338

53. Giorgione, J., Hysell, M., Harvey, D. F., and Newton, A. C. (2003) *Biochemistry* **42**, 11194-11202

54. Pu, Y., Peach, M. L., Garfield, S. H., Wincovitch, S., Marquez, V. E., and Blumberg, P. M. (2006) *J Biol Chem* **In Press**

55. Dries, D. R., Gallegos, L. L., and Newton, A. C. (2007) *J Biol Chem* **282**, 826-830

56. Mott, H. R., Carpenter, J. W., Zhong, S., Ghosh, S., Bell, R. M., and Campbell, S. L. (1996) *Proc Natl Acad Sci U S A* **93**, 8312-8317

57. Zhou, M., Horita, D. A., Waugh, D. S., Byrd, R. A., and Morrison, D. K. (2002) *J Mol Biol* **315**, 435-446

58. Mosior, M., and Newton, A. C. (1995) *J Biol Chem* **270**, 25526-25533

59. Xu, R. X., Pawelczyk, T., Xia, T. H., and Brown, S. C. (1997) *Biochemistry* **36**, 10709-10717

60. Giorgione, J. R., Lin, J. H., McCammon, J. A., and Newton, A. C. (2006) *J Biol Chem* **281**, 1660-1669

61. Hurley, J. H., and Meyer, T. (2001) *Curr Opin Cell Biol* **13**, 146-152

62. Keranen, L. M., Dutil, E. M., and Newton, A. C. (1995) *Curr Biol* **5**, 1394-1403

63. Newton, A. C., and Keranen, L. M. (1994) *Biochemistry* **33**, 6651-6658

64. Dutil, E. M., Toker, A., and Newton, A. C. (1998) *Curr Biol* **8**, 1366-1375

65. Nalefski, E. A., and Newton, A. C. (2001) *Biochemistry* **40**, 13216-13229

66. Ananthanarayanan, B., Stahelin, R. V., Digman, M. A., and Cho, W. (2003) *J Biol Chem* **278**, 46886-46894

67. Medkova, M., and Cho, W. (1999) *J Biol Chem* **274**, 19852-19861

68. Radic, Z., Kirchhoff, P. D., Quinn, D. M., McCammon, J. A., and Taylor, P. (1997) *J Biol Chem* **272**, 23265-23277

69. Gore, M. G. (2000) *Spectrophotometry and spectrofluorimetry : a practical approach*. Practical approach series ; 225., Oxford University Press, Oxford ; New York

70. Murray, D., and Honig, B. (2002) *Mol Cell* **9**, 145-154

71. Carman, G. M., Deems, R. A., and Dennis, E. A. (1995) *J Biol Chem* **270**, 18711-18714

72. Kazanietz, M. G., Krausz, K. W., and Blumberg, P. M. (1992) *J Biol Chem* **267**, 20878-20886

73. Nelsestuen, G. L., and Bazzi, M. D. (1991) *J Bioenerg Biomembr* **23**, 43-61

74. Bazzi, M. D., and Nelsestuen, G. L. (1989) *Biochemistry* **28**, 3577-3585

75. Nishizuka, Y. (1995) *Faseb J* **9**, 484-496

76. Shen, N., Guryev, O., and Rizo, J. (2005) *Biochemistry* **44**, 1089-1096

77. Gallegos, L. L., Kunkel, M. T., and Newton, A. C. (2006) *J Biol Chem*

78. Insel, P. A., Ostrom, R. S., Zambon, A. C., Hughes, R. J., Balboa, M. A., Shehnaz, D., Gregorian, C., Torres, B., Firestein, B. L., Xing, M., and Post, S. R. (2001) *Clin Exp Pharmacol Physiol* **28**, 351-354

79. Saito, N. (2003) *Methods Mol Biol* **233**, 93-103

80. Brodie, C., and Blumberg, P. M. (2003) *Apoptosis* **8**, 19-27

81. Carrasco, S., and Merida, I. (2004) *Mol Biol Cell* **15**, 2932-2942

82. Rodriguez-Alfaro, J. A., Gomez-Fernandez, J. C., and Corbalan-Garcia, S. (2004) *J Mol Biol* **335**, 1117-1129

83. Feng, X., Becker, K. P., Stribling, S. D., Peters, K. G., and Hannun, Y. A. (2000) *J Biol Chem* **275**, 17024-17034

84. Wang, Q. J., Fang, T. W., Nacro, K., Marquez, V. E., Wang, S., and Blumberg, P. M. (2001) *J Biol Chem* **276**, 19580-19587

85. Kazanietz, M. G., Wang, S., Milne, G. W., Lewin, N. E., Liu, H. L., and Blumberg, P. M. (1995) *J Biol Chem* **270**, 21852-21859

86. Killian, J. A., and von Heijne, G. (2000) *Trends Biochem Sci* **25**, 429-434

87. Khandwala, A. S., and Kasper, C. B. (1971) *Biochim Biophys Acta* **233**, 348-357

88. Pak, Y., Enyedy, I. J., Varady, J., Kung, J. W., Lorenzo, P. S., Blumberg, P. M., and Wang, S. (2001) *J Med Chem* **44**, 1690-1701

89. Marquez, V. E., and Blumberg, P. M. (2003) *Acc Chem Res* **36**, 434-443

90. Ono, Y., Fujii, T., Ogita, K., Kikkawa, U., Igarashi, K., and Nishizuka, Y. (1989) *Proc Natl Acad Sci U S A* **86**, 3099-3103

91. Limatola, C., Schaap, D., Moolenaar, W. H., and van Blitterswijk, W. J. (1994) *Biochem J* **304 (Pt 3)**, 1001-1008

92. Nakanishi, H., Brewer, K. A., and Exton, J. H. (1993) *J Biol Chem* **268**, 13-16

93. Neri, L. M., Martelli, A. M., Borgatti, P., Colamussi, M. L., Marchisio, M., and Capitani, S. (1999) *Faseb J* **13**, 2299-2310

94. Lozano, J., Berra, E., Municio, M. M., Diaz-Meco, M. T., Dominguez, I., Sanz, L., and Moscat, J. (1994) *J Biol Chem* **269**, 19200-19202

95. Bourbon, N. A., Yun, J., and Kester, M. (2000) *J Biol Chem* **275**, 35617-35623

96. Calcerrada, M. C., Miguel, B. G., Martin, L., Catalan, R. E., and Martinez, A. M. (2002) *FEBS Lett* **514**, 361-365

97. Standaert, M. L., Bandyopadhyay, G., Kanoh, Y., Sajan, M. P., and Farese, R. V. (2001) *Biochemistry* **40**, 249-255

98. Toker, A., Meyer, M., Reddy, K. K., Falck, J. R., Aneja, R., Aneja, S., Parra, A., Burns, D. J., Ballas, L. M., and Cantley, L. C. (1994) *J Biol Chem* **269**, 32358-32367

99. Nakanishi, H., and Exton, J. H. (1992) *J Biol Chem* **267**, 16347-16354

100. James, S. R., Downes, C. P., Gigg, R., Grove, S. J., Holmes, A. B., and Alessi, D. R. (1996) *Biochem J* **315 (Pt 3)**, 709-713

101. Frech, M., Andjelkovic, M., Ingley, E., Reddy, K. K., Falck, J. R., and Hemmings, B. A. (1997) *J Biol Chem* **272**, 8474-8481

102. Yu, J. W., and Lemmon, M. A. (2001) *J Biol Chem* **276**, 44179-44184

103. Lemmon, M. A., and Ferguson, K. M. (2000) *Biochem J* **350 Pt 1**, 1-18

104. Dove, S. K., Piper, R. C., McEwen, R. K., Yu, J. W., King, M. C., Hughes, D. C., Thuring, J., Holmes, A. B., Cooke, F. T., Michell, R. H., Parker, P. J., and Lemmon, M. A. (2004) *Embo J* **23**, 1922-1933

105. Yao, L., Suzuki, H., Ozawa, K., Deng, J., Lehel, C., Fukamachi, H., Anderson, W. B., Kawakami, Y., and Kawakami, T. (1997) *J Biol Chem* **272**, 13033-13039

106. Daub, M., Jockel, J., Quack, T., Weber, C. K., Schmitz, F., Rapp, U. R., Wittinghofer, A., and Block, C. (1998) *Mol Cell Biol* **18**, 6698-6710

107. Cutler, R. E., Jr., Stephens, R. M., Saracino, M. R., and Morrison, D. K. (1998) *Proc Natl Acad Sci U S A* **95**, 9214-9219

108. Ghosh, S., Xie, W. Q., Quest, A. F., Mabrouk, G. M., Strum, J. C., and Bell, R. M. (1994) *J Biol Chem* **269**, 10000-10007

109. Perander, M., Bjorkoy, G., and Johansen, T. (2001) *J Biol Chem* **276**, 13015-13024

110. Violin, J. D., Zhang, J., Tsien, R. Y., and Newton, A. C. (2003) *J Cell Biol* **161**, 899-909

111. Bartlett, G. R. (1959) *J Biol Chem* **234**, 466-468

112. Arbuzova, A., Wang, J., Murray, D., Jacob, J., Cafiso, D. S., and McLaughlin, S. (1997) *J Biol Chem* **272**, 27167-27177

113. Nalefski, E. A., and Newton, A. C. (2003) *Methods Mol Biol* **233**, 115-128

114. Mitra, P., Zhang, Y., Rameh, L. E., Ivshina, M. P., McCollum, D., Nunnari, J. J., Hendricks, G. M., Kerr, M. L., Field, S. J., Cantley, L. C., and Ross, A. H. (2004) *J Cell Biol* **166**, 205-211

115. Schwede, T., Kopp, J., Guex, N., and Peitsch, M. C. (2003) *Nucleic Acids Res* **31**, 3381-3385

116. Guex, N., and Peitsch, M. C. (1997) *Electrophoresis* **18**, 2714-2723

117. Peitsch, M. (1995) *Bio/Technology* **13**, 658-660

118. Baker, N. A., Sept, D., Joseph, S., Holst, M. J., and McCammon, J. A. (2001) *Proc Natl Acad Sci U S A* **98**, 10037-10041

119. Nielsen, J. E., Andersen, K. V., Honig, B., Hooft, R. W., Klebe, G., Vriend, G., and Wade, R. C. (1999) *Protein Eng* **12**, 657-662